



HAL
open science

Classification of Convergent OPE Channels for Lorentzian CFT Four-Point Functions

Jiixin Qiao

► **To cite this version:**

Jiixin Qiao. Classification of Convergent OPE Channels for Lorentzian CFT Four-Point Functions. SciPost Physics, 2022, 13 (4), pp.093. 10.21468/SciPostPhys.13.4.093 . hal-02863095

HAL Id: hal-02863095

<https://hal.science/hal-02863095v1>

Submitted on 23 Aug 2024

HAL is a multi-disciplinary open access archive for the deposit and dissemination of scientific research documents, whether they are published or not. The documents may come from teaching and research institutions in France or abroad, or from public or private research centers.

L'archive ouverte pluridisciplinaire **HAL**, est destinée au dépôt et à la diffusion de documents scientifiques de niveau recherche, publiés ou non, émanant des établissements d'enseignement et de recherche français ou étrangers, des laboratoires publics ou privés.



Distributed under a Creative Commons Attribution 4.0 International License

Classification of convergent OPE channels for Lorentzian CFT four-point functions

Jiaxin Qiao^{1,2}

¹ Laboratoire de Physique de l'École normale supérieure, ENS,
Université PSL, CNRS, Sorbonne Université, Université de Paris, F-75005 Paris, France

² Institut des Hautes Études Scientifiques, 91440 Bures-sur-Yvette, France

Abstract

We analyze the convergence properties of operator product expansions (OPE) for Lorentzian CFT four-point functions of scalar operators. We give a complete classification of Lorentzian four-point configurations. All configurations in each class have the same OPE convergence properties in s-, t- and u-channels. We give tables including the information of OPE convergence for all classes. Our work justifies that in a subset of the configuration space, Lorentzian CFT four-point functions are genuine analytic functions. Our results are valid for unitary CFTs in $d \geq 2$. Our work also provides some Lorentzian regions where one can do bootstrap analysis in the sense of functions.



Copyright J. Qiao

This work is licensed under the Creative Commons

[Attribution 4.0 International License](https://creativecommons.org/licenses/by/4.0/).

Published by the SciPost Foundation.

Received 15-03-2022

Accepted 01-09-2022

Published 12-10-2022

doi:[10.21468/SciPostPhys.13.4.093](https://doi.org/10.21468/SciPostPhys.13.4.093)



Check for updates

Contents

1	Introduction	3
2	Main problem and summary of results	5
2.1	Main problem	5
2.2	Summary of results	6
3	Euclidean CFT four-point function and its analytic continuation	7
3.1	Euclidean CFT four-point function	7
3.2	Expansion in z, \bar{z}	8
3.2.1	Definition of the coordinates	8
3.2.2	Conformal frame	8
3.2.3	Series expansion	9
3.3	Expansion in $\rho, \bar{\rho}$	10
3.3.1	Definition of the coordinates	10
3.3.2	Series expansion	10
3.4	Analytic continuation: case $d \geq 3$	11
3.4.1	Main idea	11
3.4.2	Path independent quantities	12
3.4.3	The end of the proof that $g(\tau_k, \mathbf{x}_k)$ is analytic in \mathcal{D}	14
3.5	Analytic continuation: case $d = 2$	14

4	Lorentzian CFT four-point function	15
4.1	Some preparations	15
4.2	Excluding light-cone singularities	16
4.3	Criteria of OPE convergence	16
4.3.1	s-channel	17
4.3.2	t-channel and u-channel	17
4.4	What happens if there is no convergent OPE channel?	22
4.4.1	s-channel condition	23
4.4.2	t- and u-channel conditions	23
5	Classifying the Lorentzian configurations	24
5.1	z, \bar{z} of Lorentzian configurations	24
5.2	Causal orderings	26
5.3	Classifying convergent OPE channels	27
5.3.1	Case $d \geq 3$	27
5.3.2	Comments on the 2d case	29
5.4	Time reversals	29
5.5	The table of four-point causal orderings	31
5.6	Examples	31
5.6.1	General time-ordered correlation functions	32
5.6.2	Conformally equivalent causal orderings	35
5.6.3	Regge kinematics	35
5.6.4	Causal ordering of bulk-point singularities	36
5.6.5	Digression	38
6	Wightman functions: a brief review	38
6.1	Wightman axioms for Lorentzian correlators	38
6.2	Wightman functions and their domains	39
6.2.1	Forward tube	39
6.2.2	Bargmann-Hall-Wightman theorem, extended tube	40
6.2.3	Jost points	41
6.2.4	Microscopic causality, envelope of holomorphy	41
6.3	Comparison with CFT	43
6.3.1	Justifying the definition of Wick rotation	43
6.3.2	Osterwalder-Schrader theorem	43
6.3.3	Domain of analyticity: Wightman axioms + conformal invariance	44
6.3.4	Domain of analyticity: unitarity + conformal invariance + OPE	45
7	Four-point functions of non-identical scalar or spinning operators	46
7.1	Generalization to the case of non-identical scalar operators	46
7.2	Comments on the case of spinning operators	47
8	Conclusions and outlooks	48
A	Why $z(\tau_k, \mathbf{x}_k), \bar{z}(\tau_k, \mathbf{x}_k)$ are not well defined on \mathcal{D} in $d \geq 3$?	50
A.1	Main idea	50
A.2	Proof	50
B	Connectedness of \mathcal{D}_L^α in $d \geq 3$	52
B.1	Step 1	53
B.2	Step 2	55

C	Tables of OPE convergence	56
	C.0.1 S_4 -action	56
	C.0.2 Lorentzian conformal frame	57
	C.0.3 Symmetry of the graph	61
	C.1 Type 1	61
	C.2 Type 2	63
	C.3 Type 3	63
	C.4 Type 4	64
	C.5 Type 5	64
	C.6 Type 6	65
	C.7 Type 7	66
	C.8 Type 8	67
	C.9 Type 9	67
	C.10 Type 10	67
	C.11 Type 11	69
	C.12 Type 12	69
	References	70

1 Introduction

In this paper we study the convergence properties of operator product expansion (OPE) for Lorentzian four-point functions in conformal field theories (CFT).

Historically, analyticity of correlation functions is an important bridge connecting Lorentzian quantum field theories (QFT) and Euclidean QFTs. Starting from a Lorentzian correlator, we can get a Euclidean correlator by analytically continuing the time variables onto the imaginary axis [1]. Under certain conditions we can also do the reverse [2–4]. This procedure of analytic continuation, called Wick rotation, allows us to explore the Lorentzian nature of QFTs which may originate from statistical models in the Euclidean signature.

The Lorentzian correlators are not always genuine functions, instead they belong to a class of tempered distributions which are called Wightman distributions [5]. It is interesting to know at which Lorentzian configurations (x_1, \dots, x_n) the correlators $G_n(x_1, \dots, x_n)$ are indeed functions. The Wightman distributions are known to be analytic functions in some regions \mathcal{J}_n which are the sets of “Jost points” [6] (G_n are called Wightman functions in their domains of analyticity).¹ \mathcal{J}_n corresponds to some (not all) Lorentzian configurations with totally space-like separations. By using the microscopic causality constraints, one can extend G_n to a larger domain, including all configurations with totally space-like separations [7]. In Minkowski space $\mathbb{R}^{d-1,1}$,² two points can also have time-like or light-like separation. The Lorentzian correlators usually diverge at configurations with light-like separations, and these configurations are called light-cone singularities [8]. Except for some exactly solvable models, the Lorentzian correlators at configurations which contain time-like separations are not fully studied.

There are more constraints in CFTs. In general QFTs, the domains of Wightman functions

¹It does not mean that the Lorentzian correlators cannot be functions in other regions. For example, the correlators of generalized free fields are functions aside from light-cone singularities. Here we are talking about the minimal domain of Lorentzian correlators which can be derived from general principles of QFT.

²Often one uses Minkowski space to denote $\mathbb{R}^{3,1}$ only. While in this paper, we use this terminology for $\mathbb{R}^{d-1,1}$ and general d .

are Poincaré invariant, while in CFTs this Poincaré invariant domain can be further extended by using conformal symmetry. Furthermore, in CFTs we have better control on correlators with the help of OPE [9]. A successful example is the four-point functions in 2d local unitary CFTs, where the conformal algebra is infinite dimensional [10]. In this case, by using Al. Zamolodchikov's uniformizing variables q, \bar{q} [11], one can show that the four-point function is regular analytic at all possible Lorentzian configurations aside from light-cone singularities [12]. We are going to study a similar problem in $d \geq 3$, for which the conformal group is finite dimensional and the radial coordinates $\rho, \bar{\rho}$ [13] are used in our analysis.³ In addition, in 2d there exists non-local unitary CFTs, which have only the global conformal symmetry. The analysis in this work also applies to 2d non-local unitary CFTs.

Recently the conformal bootstrap approach has become a powerful tool in the study of strongly coupled systems [15]. On the numerical side, it gives precise predictions of experimentally measurable quantities, such as the critical exponents of the 3d Ising model [16–20], $O(N)$ model [20–23] and other critical systems. The functional methods, which are used in the numerical approach, can be realized analytically in low dimensions, and lead to insights into low dimensional CFTs and S-matrices [24–27]. While the basic CFT assumptions are made in the Euclidean signature, many attempts have been made to study the bootstrap equations in the Lorentzian signature [28–34]. In the conformal bootstrap approach, for crossing equations to be valid in the sense of functions, there should be at least two convergent OPE channels. To play the bootstrap game for four-point functions in the Lorentzian signature, it is important to know the convergent domains of various OPE channels. This provides an additional motivation for our work.

The main goal of this work is to give complete tables of Lorentzian four-point configurations with the information about convergence in the sense of analytic functions in various OPE channels. In this paper we will mostly focus on four-point functions of identical scalar operators. Our techniques can be immediately generalized to the case of non-identical scalar operators (see section 7). The four-point functions of spinning operators require extra work because of tensor structures. In this paper, we will only make some comments on the case of spinning operators. One may also be interested in the convergence of OPE in the sense of distributions [35]. We leave the discussions of distributional properties to the series of papers [36–38].

The outline of this paper is as follows. In section 2 we introduce the main problem and provide a quick summary of the main results in this paper. In section 3 we justify the analytic continuation of the CFT four-point function to the domain \mathcal{D} (which will be defined in section 2.1), and the Lorentzian configurations live on the boundary of $\bar{\mathcal{D}}$. In section 4 we give criteria of OPE convergence in s-, u- and t-channels. In section 5, we make a classification of the Lorentzian four-point configurations. All configurations in the same class have the same convergent OPE channels. All information on the OPE convergence properties can be looked up in appendix C. In section 6 we review some classical results from Wightman QFT, and compare them with CFT four-point functions. In section 7 we generalize our results to the case of non-identical scalar operators and make some comments on the case of spinning operators. In section 8 we make conclusions and point out some open questions related to this work.

³The set of four-point configurations (x_1, x_2, x_3, x_4) with $|\rho|, |\bar{\rho}| < 1$ is a subset of (x_1, x_2, x_3, x_4) with $|q|, |\bar{q}| < 1$. Since the q -variable argument is based on the Virasoro symmetry which is only true in 2d [14], we cannot apply it to the case of $d \geq 3$.

2 Main problem and summary of results

2.1 Main problem

We start from CFT in the Euclidean signature. Let $x_k = (\tau_k, \mathbf{x}_k)$ denote the k -th point in the Euclidean space ($k = 1, 2, 3, 4$), where $\tau_k = x_k^0$ is the temporal variable and $\mathbf{x}_k = (x_k^1, x_k^2, \dots, x_k^{d-1}) \in \mathbb{R}^{d-1}$ represents the vector of spatial variables. Lorentzian points are given by Wick rotating the temporal variables: $\tau = it$ where t is a real number. To get Lorentzian four-point functions we need to analytically continue the Euclidean four-point functions with respect to temporal variables. We define the Wick rotation of the four-point function as follows:

Step 1.

We construct a function $G_4(x_1, x_2, x_3, x_4)$ such that:

- G_4 has domain \mathcal{D} of complex τ_k and real \mathbf{x}_k . The temporal variables $(\tau_1, \tau_2, \tau_3, \tau_4)$ are in the set

$$\mathbb{C}_{>}^4 := \left\{ (\tau_1, \tau_2, \tau_3, \tau_4) \in \mathbb{C}^4 \mid \text{Re}(\tau_1) > \text{Re}(\tau_2) > \text{Re}(\tau_3) > \text{Re}(\tau_4) \right\}. \quad (1)$$

In other words, $\mathcal{D} = \mathbb{C}_{>}^4 \times \mathbb{R}^{4(d-1)}$.⁴

- G_4 is analytic in the temporal variables τ_k and continuous in the spatial variables \mathbf{x}_k .
- G_4 agrees with the Euclidean four-point function G_4^E when all the temporal variables are real.

Step 2.

The Wick rotation to Lorentzian CFT four-point function is defined by

$$G_4^L(t_k, \mathbf{x}_k) := \lim_{\substack{\epsilon_k \rightarrow 0 \\ \epsilon_1 > \epsilon_2 > \epsilon_3 > \epsilon_4}} G_4(\epsilon_k + it_k, \mathbf{x}_k), \quad (2)$$

when such a limit exists.

The reason we define Wick rotation in the above way is that we expect the Lorentzian CFT four-point function to be a Wightman four-point distribution, which is the boundary value of the Wightman four-point function from its domain of complex coordinates [1]. The domain of the four-point Wightman function includes \mathcal{D} , so the limit (2) gives the Wightman four-point distribution when such a limit exists. We will discuss this in section 6.

The main problem we want to discuss in this paper is:

- In which Lorentzian regions does the Lorentzian CFT four-point function, defined by (2), have a convergent operator product expansion in the sense of functions?

The goal of this paper is to give tables which contain OPE convergence properties of four-point functions at all possible Lorentzian configurations.

⁴The analytic continuation can be done in a larger domain, e.g. the forward tube \mathcal{T}_4 defined by

$$\mathcal{T}_4 := \left\{ (x_1, x_2, x_3, x_4) \in \mathbb{C}^{4d} \mid \text{Re}(x_k^0 - x_{k+1}^0) > |\text{Im}(\mathbf{x}_k - \mathbf{x}_{k+1})|, \quad k = 1, 2, 3 \right\}.$$

See [37] for the discussion about the analytic continuation of G_4 to \mathcal{T}_4 . In this paper, we are only interested in the analyticity of G_4 in the Lorentzian regime. Since the whole Lorentzian regime is already contained in the closure of \mathcal{D} (see step 2), it suffices to consider the analytic continuation to \mathcal{D} .

2.2 Summary of results

In this subsection, we provide a quick summary of the main results for readers who wish to know the general ideas of this paper before going into the technical details.

- We prove that the Euclidean CFT four-point function G_4^E has analytic continuation to the domain \mathcal{D} (i.e. $\text{Re}(\tau_1) > \text{Re}(\tau_2) > \text{Re}(\tau_3) > \text{Re}(\tau_4)$) (section 3). The analytic continuation will be performed by using the s-channel OPE, which means taking the OPE $\phi(x_1) \times \phi(x_2)$ in the four-point function

$$G_4^E(x_1, x_2, x_3, x_4) = \langle \phi(x_1)\phi(x_2)\phi(x_3)\phi(x_4) \rangle. \quad (3)$$

The key observation is that for any four-point configuration in \mathcal{D} , the radial variables ρ and $\bar{\rho}$ belong to the open unit disk, i.e. $|\rho|, |\bar{\rho}| < 1$. This observation, together with the series expansion of G_4^E in ρ and $\bar{\rho}$, implies that the s-channel OPE is convergent for any configuration in \mathcal{D} .

One technical subtlety in $d \geq 3$ is that the radial variables ρ and $\bar{\rho}$ are not individually globally well-defined analytic functions (appendix A). We treat this subtlety carefully when performing the analytic continuation, and show that G_4 (constructed in terms of ρ and $\bar{\rho}$) is single valued and analytic everywhere in \mathcal{D} (section 3.4).

- We derive the criteria of OPE convergence of the Lorentzian CFT four-point function G_4^L in s-, t- and u-channels (section 4). G_4^L is defined to be the boundary value of analytically continued Euclidean four-point function (see eq. (2)). One can imagine that the OPE convergence properties of G_4^L rely on the behavior of cross-ratio variables along the analytic continuation path. In the end we will see that for any fixed Lorentzian four-point configuration, one can check the criteria using any analytic continuation path in \mathcal{D} (starting from a Euclidean four-point configuration), and the conclusion does not depend on the choice of the path.
- We classify all the Lorentzian four-point configurations aside from the light-cone singularities (section 5). The Lorentzian configurations are classified into a finite number of groups according to the range of cross-ratio variables (z, \bar{z}) (section 5.1) and the causal orderings (section 5.2). We conclude that in each group, all configurations have the same OPE convergence properties (section 5.3).

Then the problem is reduced to checking convergence properties in a finite number of cases. The conclusion of OPE convergence properties is lengthy because in our classification there are many groups (although finite) to check, so we leave this part to appendix C. We share the Mathematica code for readers who wish to check our results (see the ancillary file “/anc/OPE_check.nb” on arXiv).

- We review the classic results on the domain of analyticity of correlation functions in the framework of Wightman QFT (section 6). It was showed in the classic literature that the Wightman function is regular analytic in the totally space-like kinematic region. The domain of the CFT four-point function contains this region, and furthermore it contains much more regions including time-like separation of points.
- We generalize our results to non-identical scalar four-point functions (section 7). We show that the OPE convergence properties of non-identical scalar four-point functions are the same as the identical scalar case, using Cauchy-Schwarz argument. We also make a comment on the main technical difficulty that arises in the case of spinning operators.

3 Euclidean CFT four-point function and its analytic continuation

In this section justify the first step of Wick rotation: analytically continuing the Euclidean CFT four-point function G_4^E to the domain \mathcal{D} .

3.1 Euclidean CFT four-point function

Consider a Euclidean CFT four-point function of identical scalar primary operators ϕ with scaling dimension Δ . By conformal symmetry we write it as

$$G_4^E(x_1, x_2, x_3, x_4) := \langle \phi(x_1)\phi(x_2)\phi(x_3)\phi(x_4) \rangle = \frac{g(u, v)}{(x_{12}^2)^\Delta (x_{34}^2)^\Delta}, \tag{4}$$

where x_{ij}^2 are defined by

$$x_{ij}^2 := \sum_{\mu=0}^{d-1} (x_i^\mu - x_j^\mu)^2 = (\tau_i - \tau_j)^2 + (\mathbf{x}_i - \mathbf{x}_j)^2, \tag{5}$$

and $g(u, v)$ is a function of cross-ratios

$$u = \frac{x_{12}^2 x_{34}^2}{x_{13}^2 x_{24}^2}, \quad v = \frac{x_{14}^2 x_{23}^2}{x_{13}^2 x_{24}^2}. \tag{6}$$

G_4^E is originally defined in the Euclidean signature. To extend G_4^E to the domain of complex temporal variables,⁵ we first analytically continue x_{ij}^2 by eq. (5). Since the functions x_{ij}^2 do not vanish when the configurations are in \mathcal{D} ,⁶ the cross-ratios do not diverge. As a result, cross-ratios have analytic continuation to \mathcal{D} . Since $x_{ij}^2 \neq 0$ and \mathcal{D} is simply connected, the prefactor $(x_{12}^2 x_{34}^2)^{-\Delta}$ in (4) also has analytic continuation to \mathcal{D} .

Therefore, to show that $G_4^E(\tau_k, \mathbf{x}_k)$ has analytic continuation to the domain \mathcal{D} , it remains to show that $g(\tau_k, \mathbf{x}_k)$ has analytic continuation to the domain \mathcal{D} .⁷

In general, we do not know the exact expression of $g(\tau_k, \mathbf{x}_k)$. We want to extend its domain according to the basic properties of Euclidean unitary CFT [39, 40]:

- Conformal invariance (which has already been used in (4)).
- Reflection positivity (which is the Euclidean version of unitarity [2]).
- Convergence of operator product expansions in the Euclidean space.

Our main idea is to use the above properties via radial variables $\rho, \bar{\rho}$ [13], which we will introduce below. Roughly speaking, we want to first analytically continue the function $g(\rho, \bar{\rho})$ by a good series expansion. Then we want to stick the analytic functions $\rho(\tau_k, \mathbf{x}_k)$ and $\bar{\rho}(\tau_k, \mathbf{x}_k)$ into $g(\rho, \bar{\rho})$ to get analytic continuation of $g(\tau_k, \mathbf{x}_k)$.

⁵We want to remark here that in principle one can also consider analytically continuing the above functions to the domain of complex spatial variables. But since in this work we only want to discuss about the four-point functions in the Lorentzian signature, where \mathbf{x}_k are always real, we will not consider the analytic continuation problem with respect to spatial variables. By analytically continuing some function $f(\tau_k, \mathbf{x}_k)$ to \mathcal{D} , we mean extending the domain of f to \mathcal{D} , on which f is analytic in τ_k and continuous in \mathbf{x}_k .

⁶Let $\tau_k = \epsilon_k + it_k$ ($k = 1, 2, 3, 4$). For $i \neq j$, since $x_{ij}^2 = (\epsilon_i - \epsilon_j + it_i - it_j)^2 + (\mathbf{x}_i - \mathbf{x}_j)^2$ and $\epsilon_i \neq \epsilon_j$, x_{ij}^2 is real only when $t_i = t_j$, but then $x_{ij}^2 > 0$.

⁷In this paper we will abuse the notation by writing $g(u, v)$, $g(z, \bar{z})$, $g(\rho, \bar{\rho})$ and $g(\tau_k, \mathbf{x}_k)$ for four-point function in different coordinates. For example, $g(\tau_k, \mathbf{x}_k) := g(u(\tau_k, \mathbf{x}_k), v(\tau_k, \mathbf{x}_k))$.

3.2 Expansion in z, \bar{z}

3.2.1 Definition of the coordinates

We pass from u, v to z, \bar{z} by

$$u = z\bar{z}, \quad v = (1-z)(1-\bar{z}). \tag{7}$$

The above definition has an ambiguity of interchanging z and \bar{z} . We choose z, \bar{z} to be one particular solution of (7):

$$\begin{aligned} z(u, v) &= \frac{1}{2} \left(1 + u - v + i\sqrt{4u - (1 + u - v)^2} \right), \\ \bar{z}(u, v) &= \frac{1}{2} \left(1 + u - v - i\sqrt{4u - (1 + u - v)^2} \right). \end{aligned} \tag{8}$$

Since we are interested in the four-point configurations in \mathcal{D} , where the temporal variables τ_k are complex numbers, the cross-ratios $u(\tau_k, \mathbf{x}_k)$ and $v(\tau_k, \mathbf{x}_k)$ are also complex numbers. So we consider $z(u, v), \bar{z}(u, v)$ for $(u, v) \in \mathbb{C}^2$. For complex (u, v) , the expressions of $z(u, v), \bar{z}(u, v)$ have the same set of square-root branch points

$$\Gamma_{uv} := \left\{ (u, v) \in \mathbb{C}^2 \mid 4u - (1 + u - v)^2 = 0 \right\}, \tag{9}$$

and (8) is not single-valued when $(u, v) \in \mathbb{C}^2 \setminus \Gamma_{uv}$. We define the variables w, y by

$$w = 1 + u - v, \quad y^2 = 4u - (1 + u - v)^2, \tag{10}$$

and write (8) as

$$z = \frac{w}{2} + \frac{iy}{2}, \quad \bar{z} = \frac{w}{2} - \frac{iy}{2}. \tag{11}$$

As we discuss in appendix A, $y(\tau_k, \mathbf{x}_k)$, and hence $z(\tau_k, \mathbf{x}_k), \bar{z}(\tau_k, \mathbf{x}_k)$, are single-valued in \mathcal{D} for $d = 2$ but not for $d \geq 3$. This leads to some complication in constructing the analytic continuation of $g(\tau_k, \mathbf{x}_k)$, which will be overcome below (see section 3.4).

3.2.2 Conformal frame

We would like to introduce a proper conformal frame configuration to understand the geometrical meaning of z, \bar{z} . Let $(\mu\nu)$ -plane denote the 2d subspace of \mathbb{R}^d which only has non-vanishing coordinates x^μ, x^ν (recall that $x = (x^0, x^1, x^2, \dots, x^{d-1})$). In Euclidean space, there exists a conformal transformation which maps the configuration $C = (x_1, x_2, x_3, x_4)$ onto the (01)-plane:

$$\begin{aligned} x'_1 &= 0, \\ x'_2 &= (a, b, 0, \dots, 0), \\ x'_3 &= (1, 0, \dots, 0), \\ x'_4 &= \infty. \end{aligned} \tag{12}$$

Then $z = a+ib, \bar{z} = a-ib$. We call (12) a conformal frame configuration of C . Noticing that the reflection $(x^0, x^1, x^2, \dots, x^{d-1}) \mapsto (x^0, -x^1, x^2, \dots, x^{d-1})$ is a conformal transformation which preserves (01)-plane and keeps x'_1, x'_3, x'_4 in (12) fixed, the conformal frame configuration is not unique: it is allowed to replace b with $-b$ in (12). We see that changing b to $-b$ is the same as interchanging z and \bar{z} .

Let \mathcal{D}_E be the Euclidean subset of \mathcal{D} :

$$\mathcal{D}_E := \left\{ (x_1, x_2, x_3, x_4) \in \mathcal{D} \mid \tau_k \in \mathbb{R}, \quad k = 1, 2, 3, 4 \right\}, \quad (x_k = (\tau_k, \mathbf{x}_k)). \quad (13)$$

By using the conformal frame, one can show that

- All configurations in \mathcal{D}_E have the following property:

$$z, \bar{z} \in \mathbb{C} \setminus [1, +\infty). \quad (14)$$

This follows from the fact that conformal transformations map circles to circles or lines, preserving cyclic order.⁸ Suppose we have a configuration C with $z = \bar{z} \in [1, +\infty)$, then the conformal frame configuration (12) of C satisfies $x'_2 = (a, 0, \dots, 0)$ with $a > 1$, which means (x'_1, x'_2, x'_3, x'_4) have cyclic order [1324]. However, the cyclic order [1324] does not exist in \mathcal{D}_E because of the constraint $\tau_1 > \tau_2 > \tau_3 > \tau_4$.

3.2.3 Series expansion

By (7), we can think of $g(u(z, \bar{z}), v(z, \bar{z}))$ as a function of z, \bar{z} . Since u, v are symmetric polynomials of z, \bar{z} , we have

$$g(z, \bar{z}) = g(\bar{z}, z), \quad (z^* = \bar{z}). \quad (15)$$

The constraint $z^* = \bar{z}$ in (15) is because our assumptions of conformal invariance are made in the Euclidean signature, where z, \bar{z} are complex conjugate to each other. If $g(z, \bar{z})$ has analytic continuation to independent complex z, \bar{z} , then it is easy to remove this constraint by the Cauchy-Riemann equation, so that (15) will hold for any z, \bar{z} .

In the unitary CFT, the function $g(z, \bar{z})$ is known to have a series expansion in z, \bar{z} :

$$g(z, \bar{z}) = \sum_{h, \bar{h} \geq 0} a_{h, \bar{h}} z^h \bar{z}^{\bar{h}}, \quad (16)$$

where $a_{h, \bar{h}}$ are real non-negative coefficients. This expansion can be understood as follows. In the radial quantization picture, we insert a complete basis $\{|h, \bar{h}\rangle\}$ into the four-point function in the conformal frame (12):

$$\sum_{h, \bar{h}} \langle \phi(x'_1) \phi(x'_2) | h, \bar{h} \rangle \langle h, \bar{h} | \phi(x'_3) \phi(x'_4) \rangle = \frac{1}{(x'_{12} x'_{34})^\Delta} \sum_{h, \bar{h} \geq 0} a_{h, \bar{h}} z^h \bar{z}^{\bar{h}}, \quad (17)$$

where h, \bar{h} are the eigenvalues of Virasoro generators L_0, \bar{L}_0 [14] (L_0, \bar{L}_0 also belong to $so(1, d + 1)$, the Lie algebra of the global conformal group). Here $h, \bar{h} \geq 0$ are the consequences of unitarity [14].

The expansion (16) is absolutely convergent when $|z|, |\bar{z}| < 1$, so $g(z, \bar{z})$ has analytic continuation from its Euclidean domain $\{z^* = \bar{z}\}$ to the universal covering of $\{0 < |z|, |\bar{z}| < 1\}$. Our purpose is to extend the domain of $g(\tau_k, \mathbf{x}_k)$ from \mathcal{D}_E to \mathcal{D} by composing $g(z, \bar{z})$ with $z(\tau_k, \mathbf{x}_k)$ and $\bar{z}(\tau_k, \mathbf{x}_k)$. However, the set of (x_1, x_2, x_3, x_4) with $|z(\tau_k, \mathbf{x}_k)|, |\bar{z}(\tau_k, \mathbf{x}_k)| < 1$ does not cover \mathcal{D} (it does not even cover \mathcal{D}_E). To solve this issue, we will introduce a pair of radial coordinates $\rho, \bar{\rho}$ and expand the function g in $\rho, \bar{\rho}$ (see the next subsection).

⁸Given four Euclidean points x_1, x_2, x_3, x_4 , we say that they have the cyclic order $[i_1 i_2 i_3 i_4]$ if these four points lie on a circle or a line in the order $x_{i_1} x_{i_2} x_{i_3} x_{i_4}$.

3.3 Expansion in $\rho, \bar{\rho}$

3.3.1 Definition of the coordinates

We define the radial coordinates $\rho, \bar{\rho}$ by

$$\rho(z) = \frac{(1 - \sqrt{1-z})^2}{z}, \quad \bar{\rho}(\bar{z}) = \frac{(1 - \sqrt{1-\bar{z}})^2}{\bar{z}}. \tag{18}$$

Eq. (18) defines a one-to-one holomorphic map $\rho(z)$ from $z \in \mathbb{C} \setminus [1, +\infty)$ to the open unit disc $|\rho| < 1$. The same is true for \bar{z} and $\bar{\rho}$. By composing (18) with $z(\tau_k, \mathbf{x}_k)$ and $\bar{z}(\tau_k, \mathbf{x}_k)$, we get functions $\rho(\tau_k, \mathbf{x}_k)$ and $\bar{\rho}(\tau_k, \mathbf{x}_k)$. For configurations in \mathcal{D}_E , by the property (14) of z, \bar{z} , we have:

- In the Euclidean region \mathcal{D}_E , we have $|\rho(\tau_k, \mathbf{x}_k)|, |\bar{\rho}(\tau_k, \mathbf{x}_k)| < 1$.

Analogously to the conformal frame for z, \bar{z} , for $\rho, \bar{\rho}$ there exists a conformal transformation which maps C onto the (01)-plane:

$$\begin{aligned} x''_1 &= (\alpha, \beta, 0, \dots, 0), \\ x''_2 &= (-\alpha, -\beta, 0, \dots, 0), \\ x''_3 &= (-1, 0, \dots, 0), \\ x''_4 &= (1, 0, \dots, 0), \end{aligned} \tag{19}$$

with $\alpha^2 + \beta^2 < 1$. Then $\rho = \alpha + i\beta, \bar{\rho} = \alpha - i\beta$.

3.3.2 Series expansion

By (18), the maps from $\rho, \bar{\rho}$ to z, \bar{z} are given by

$$z = \frac{4\rho}{(1+\rho)^2}, \quad \bar{z} = \frac{4\bar{\rho}}{(1+\bar{\rho})^2}. \tag{20}$$

We get $g(\rho, \bar{\rho})$ by composing (20) with $g(z, \bar{z})$. By (15) and (20), we have

$$g(\rho, \bar{\rho}) = g(\bar{\rho}, \rho), \quad (\rho^* = \bar{\rho}). \tag{21}$$

In the Euclidean unitary CFT, the function $g(\tau_k, \mathbf{x}_k)$ is known to have an expansion in radial coordinates [9]:

$$g(\rho, \bar{\rho}) = \sum_{h, \bar{h} \geq 0} b_{h, \bar{h}} \rho^h \bar{\rho}^{\bar{h}}, \tag{22}$$

where $b_{h, \bar{h}}$ are positive coefficients. This expansion can be obtained by inserting a complete basis $\{|h, \bar{h}\rangle\}$ into the four-point function at the configuration (19):

$$\sum_{h, \bar{h}} \langle \phi(x''_1) \phi(x''_2) | h, \bar{h} \rangle \langle h, \bar{h} | \phi(x''_3) \phi(x''_4) \rangle = \frac{1}{(16\rho\bar{\rho})^\Delta} \sum_{h, \bar{h} \geq 0} b_{h, \bar{h}} \rho^h \bar{\rho}^{\bar{h}}. \tag{23}$$

Furthermore, the ρ -expansion (22) can be rearranged in the following way:

$$\begin{aligned} g(\rho, \bar{\rho}) &= \sum_{\Delta \geq 0} \sum_{l \in \mathbb{N}} c_{\Delta, l} (\rho\bar{\rho})^{\Delta/2} P^l(\rho, \bar{\rho}), \\ P^l(\rho, \bar{\rho}) &= \sum_{k=0}^l P_k^l \left(\frac{\rho}{\bar{\rho}} \right)^{l/2-k}, \quad P_k^l = P_{l-k}^l, \end{aligned} \tag{24}$$

where the function $P^l(\rho, \bar{\rho})$ in (24) is another form of the Gegenbauer polynomial $C_l^{d/2-1}$ [13]:

$$P^l(\rho, \bar{\rho}) = C_l^{d/2-1}(\cos \theta), \quad (\rho = r e^{i\theta}, \bar{\rho} = r e^{-i\theta}). \tag{25}$$

The function $g(\rho, \bar{\rho})$ is originally defined in the Euclidean region $\rho^* = \bar{\rho}$. Considering now $\rho, \bar{\rho}$ to be independent complex variables, since the expansion (22) is absolutely convergent when $|\rho|, |\bar{\rho}| < 1$, it defines an analytic function on the universal covering of the domain

$$R := \left\{ (\rho, \bar{\rho}) \in \mathbb{C}^2 \mid 0 < |\rho|, |\bar{\rho}| < 1 \right\}. \tag{26}$$

We write radial coordinates as

$$\rho = e^{i\chi}, \bar{\rho} = e^{i\bar{\chi}}. \tag{27}$$

The universal covering of R is characterized by a product of upper half planes

$$X := \left\{ (\chi, \bar{\chi}) \in \mathbb{C}^2 \mid \text{Im}(\chi), \text{Im}(\bar{\chi}) > 0 \right\}, \tag{28}$$

and the covering map is (27). The Euclidean region of X corresponds to $\chi^* = -\bar{\chi}$. By (24), the function $g(\chi, \bar{\chi})$ on X has the following properties:

$$\begin{aligned} g(\chi, \bar{\chi}) &= g(\bar{\chi}, \chi), \\ g(\chi, \bar{\chi}) &= g(\chi + 2\pi, \bar{\chi} - 2\pi). \end{aligned} \tag{29}$$

3.4 Analytic continuation: case $d \geq 3$

3.4.1 Main idea

In this section we will study the analytic continuation of $g(\tau_k, \mathbf{x}_k)$ in $d \geq 3$. Our goal is to analytically continue $g(\tau_k, \mathbf{x}_k)$ to \mathcal{D} . Naively, one may want to construct this analytic continuation by the following compositions:

$$(\tau_k, \mathbf{x}_k) \mapsto (u, v) \mapsto (z, \bar{z}) \mapsto (\rho, \bar{\rho}) \mapsto (\chi, \bar{\chi}) \mapsto g(\chi, \bar{\chi}). \tag{30}$$

This construction requires two conditions:

1. The step $(\tau_k, \mathbf{x}_k) \mapsto (z, \bar{z})$ in (30) should be well defined.
2. All configurations in \mathcal{D} satisfy $|\rho|, |\bar{\rho}| < 1$, or equivalently, $z, \bar{z} \notin [1, +\infty)$.

The first condition holds if we have well-defined analytic functions $z(\tau_k, \mathbf{x}_k)$ and $\bar{z}(\tau_k, \mathbf{x}_k)$ on \mathcal{D} . However, as already mentioned in section 3.2.1, such analytic functions do not exist in $d \geq 3$ (they exist in 2d). We will discuss the 2d case in section 3.5. For the $d \geq 3$ case, we discuss the non-existence of $z(\tau_k, \mathbf{x}_k), \bar{z}(\tau_k, \mathbf{x}_k)$ in appendix A.

Concerning the second condition, we have a crucial observation:

Theorem 3.1. [37] The above condition 2 holds in any $d \geq 2$.

This theorem is one of the results in [37], where the proof is given (see [37], lemma 6.1 and the proof in its section 6.4). In this paper we will accept it as a fact. For readers who wish to get some intuition on why $|\rho|, |\bar{\rho}| < 1$ in \mathcal{D} , we will give a proof of the 2d case in section 3.5.

Since it is impossible to construct analytic functions $z(\tau_k, \mathbf{x}_k), \bar{z}(\tau_k, \mathbf{x}_k)$ on \mathcal{D} in $d \geq 3$, we cannot naively do the composition like (30). We will construct analytic continuation of $g(\tau_k, \mathbf{x}_k)$ as follows.

Let Γ be the preimage of Γ_{uv} in \mathcal{D} (see eq. (9)).⁹ Given a four-point configuration $C = (x_1, x_2, x_3, x_4) \in \mathcal{D}$, we choose a path

$$\begin{aligned} \gamma &: [0, 1] \longrightarrow \mathcal{D}, \\ \gamma(0) &\in \mathcal{D}_E \setminus \Gamma, \\ \gamma(1) &= C, \\ \gamma(s) &\in \mathcal{D} \setminus \Gamma, \quad s < 1. \end{aligned} \tag{31}$$

The values of $u(s), v(s)$ along γ are uniquely computable via (6). We would like to also define $z, \bar{z}, \rho, \bar{\rho}, \chi, \bar{\chi}$ along the path γ . For this we make some conventions: at the start point of γ we choose

$$\begin{aligned} \text{Im}(z) &\geq 0, \quad \text{Im}(\bar{z}) \leq 0, \\ 0 \leq \text{Re}(\chi) &\leq \pi, \quad -\pi \leq \text{Re}(\bar{\chi}) \leq 0. \end{aligned} \tag{32}$$

This uniquely determines $z, \bar{z}, \rho, \bar{\rho}, \chi, \bar{\chi}$ at $s = 0$. Since we chose γ such that $\gamma(s) \notin \Gamma$ before the final point, the subsequent paths of $z, \bar{z}, \rho, \bar{\rho}, \chi, \bar{\chi}$ at $s > 0$ are then uniquely determined by continuity. We define path-dependent variables

$$z(C, \gamma), \bar{z}(C, \gamma), \rho(C, \gamma), \bar{\rho}(C, \gamma), \chi(C, \gamma), \bar{\chi}(C, \gamma), \tag{33}$$

to be the variables at the final point $\gamma(1) = C$. Our goal is to show that

- The function $g(\chi(\tau_k, \mathbf{x}_k, \gamma), \bar{\chi}(\tau_k, \mathbf{x}_k, \gamma))$ is actually independent of the path γ , so we write it as $g(\tau_k, \mathbf{x}_k)$.
- The function $g(\tau_k, \mathbf{x}_k)$ is analytic in τ_k .

This, then, is how we will analytically continue $g(\tau_k, \mathbf{x}_k)$ to the whole \mathcal{D} .

3.4.2 Path independent quantities

In the previous subsection we defined path dependent variables (33). Changing the path may change the values of these variables. In this subsection we are going to show that the following quantities are analytic functions on \mathcal{D} :

1. $(\rho \bar{\rho})^\Delta$ for any Δ .
2. $\left(\frac{\rho}{\bar{\rho}}\right)^{k/2} + \left(\frac{\bar{\rho}}{\rho}\right)^{k/2}$, where $k \in \mathbb{Z}$.

⁹We claim that $\mathcal{D} \setminus \Gamma$ is connected, so such a path γ exists. The reason is as follows. First we notice that the defining property of Γ (see eq. (9)) is equivalent to $z = \bar{z}$. According to section 3.2.2, any configuration $C = (x_1, x_2, x_3, x_4)$ can be written as $C = g \cdot C'$, where g is a conformal transformation and C' is the conformal-frame configuration in eq. (12). If C belongs to Γ , we have $b = 0$ in eq. (12) (which is equivalent to $z = \bar{z}$). Then we keep the conformal transformation g fixed and vary C' . One can show that at such a configuration, $\frac{\partial(z-\bar{z})}{\partial x_i^\mu} = \pm 2i \neq 0$ for $\mu = 1, 2, \dots, d-1$. Since the conformal transformation g is invertible, there exists at least one nonzero (complex) derivative of $z - \bar{z}$ in x_i^μ 's. If $\frac{\partial(z-\bar{z})}{\partial \tau_k} \neq 0$ for some k , then Γ is locally complex-codimension-1 (i.e. real-codimension-2) in \mathcal{D} near this configuration. This is the generic case for configurations in Γ . The "bad configurations", where $\frac{\partial(z-\bar{z})}{\partial \tau_k} = 0$ for all k , form a lower dimensional subspace than the subspace of generic configurations in Γ . We know that removing a subspace with real codimensions no less than 2 does not affect connectedness, therefore $\mathcal{D} \setminus \Gamma$ is connected.

We first need to show that the above quantities are path independent, then we need to show the analyticity.

For $(\rho\bar{\rho})^\Delta$, by (7) and (18), we write it as

$$(\rho\bar{\rho})^\Delta = \frac{u^\Delta}{I^{2\Delta}}, \quad I = (1 + \sqrt{1-z})(1 + \sqrt{1-\bar{z}}). \tag{34}$$

u^Δ is an analytic function on \mathcal{D} because (a) x_{ij}^2 's are non-zero analytic functions on \mathcal{D} and (b) \mathcal{D} is simply connected. Condition (a) guarantees that the path-dependent analytic continuation of $u^\Delta = \left(\frac{x_{12}^2 x_{34}^2}{x_{13}^2 x_{24}^2}\right)^\Delta$ can be performed, and condition (b) implies that the analytic continuation of u^Δ is path-independent (i.e. u^Δ , as a function of x_i^μ 's, has no monodromy issue).

Lemma 3.2. $I(\tau_k, \mathbf{x}_k)$ is an analytic function on \mathcal{D} .

Proof. By theorem 3.1, the variables z, \bar{z} are always in the same branch of the square-root functions $\sqrt{1-z}, \sqrt{1-\bar{z}}$. Together with the fact that changing the path at most interchanges z and \bar{z} (this follows from (7) and from u, v being functions of a point and not of a path), we conclude that I is a path independent quantity.

To show that $I(\tau_k, \mathbf{x}_k)$ is an analytic function on \mathcal{D} , we first show that $I(\tau_k, \mathbf{x}_k)$ is an analytic function on $\mathcal{D} \setminus \Gamma$. For a given configuration $C \in \mathcal{D} \setminus \Gamma$, we choose a path γ under conditions (31). Then the variables z, \bar{z} at C are determined by γ . By (8), we can find a neighbourhood $U \subset \mathcal{D} \setminus \Gamma$ of C such that the map $(u, v) \mapsto (z, \bar{z})$ is locally analytic. Thus $I(\tau_k, \mathbf{x}_k)$ is an analytic function on $\mathcal{D} \setminus \Gamma$.

It remains to show that $I(\tau_k, \mathbf{x}_k)$ is analytic near $C \in \Gamma$. For $C \in \Gamma$ we have $z = \bar{z} = z_*$. Because $I(z, \bar{z})$ is symmetric in z and \bar{z} , and because $I(z, \bar{z})$ is analytic in the variables z, \bar{z} in the domain $z, \bar{z} \notin [1, +\infty)$, $I(z, \bar{z})$ has the following Taylor expansion near (z_*, z_*) :

$$I(z, \bar{z}) = \sum_{m,n \in \mathbb{N}} a_{m,n} (z + \bar{z} - 2z_*)^m (z - \bar{z})^{2n}. \tag{35}$$

By (8) we have

$$\begin{aligned} z + \bar{z} &= 1 + u - v, \\ (z - \bar{z})^2 &= (1 + u - v)^2 - 4u. \end{aligned} \tag{36}$$

Although the map $(u, v) \mapsto (z, \bar{z})$ is not analytic near $(u, v) \in \Gamma_{uv}$, (35) and (36) imply that the function $I(u, v)$ is still locally analytic in the variables u, v . Thus $I(\tau_k, \mathbf{x}_k)$, which is the composition of analytic functions $I(u, v)$ and $(u(\tau_k, \mathbf{x}_k), v(\tau_k, \mathbf{x}_k))$, is analytic near $C \in \Gamma$. \square

To show $(\rho\bar{\rho})^\Delta$ is an analytic function on \mathcal{D} , it remains to show that $[I(\tau_k, \mathbf{x}_k)]^\Delta$ is an analytic function on \mathcal{D} . Since all configurations in \mathcal{D} have $z, \bar{z} \notin [1, +\infty)$, we have

$$-\frac{\pi}{2} < \text{Arg}(\sqrt{1-z}), \text{Arg}(\sqrt{1-\bar{z}}) < \frac{\pi}{2}, \tag{37}$$

which implies

$$I(\mathcal{D}) \subset \mathbb{C} \setminus (-\infty, 0]. \tag{38}$$

Thus $I(\mathcal{D})$ does not contain any curve which goes around zero. Together with lemma 3.2, we conclude that $[I(\tau_k, \mathbf{x}_k)]^\Delta$ is an analytic function on \mathcal{D} .

Recall definition (27) of $\chi, \bar{\chi}$, the fact that $(\rho\bar{\rho})^\Delta$ is analytic in \mathcal{D} is equivalent to the following lemma:

Lemma 3.3. $\chi + \bar{\chi}$ is an analytic function on \mathcal{D} .

Proof. We choose an arbitrary self-avoiding path to perform the analytic continuation of χ and $\bar{\chi}$.¹⁰ By (27), along the analytic continuation path we have

$$\chi + \bar{\chi} = -i \log(\rho \bar{\rho}). \tag{39}$$

The above discussion about analyticity of $(\rho \bar{\rho})^\Delta$ was actually proving that $\log(\rho \bar{\rho})$ is analytic in \mathcal{D} . In particular, the RHS of (39) does not depend on the choice of the analytic continuation path (although the analytic continuations of χ and $\bar{\chi}$ do). Thus $\chi + \bar{\chi}$ is also an analytic function on \mathcal{D} . \square

For $(\rho/\bar{\rho})^{k/2} + (\bar{\rho}/\rho)^{k/2}$, we write it as

$$\left(\frac{\rho}{\bar{\rho}}\right)^{k/2} + \left(\frac{\bar{\rho}}{\rho}\right)^{k/2} = (\rho \bar{\rho})^{-k/2} (\rho^k + \bar{\rho}^k). \tag{40}$$

The analyticity of $(\rho \bar{\rho})^{-k/2}$ has been proved. Changing the path at most interchanges ρ and $\bar{\rho}$, so $\rho^k + \bar{\rho}^k$ is path independent. The analyticity of $(\rho^k + \bar{\rho}^k)$ in \mathcal{D} follows from a similar argument as in the proof of lemma 3.2. Therefore, $(\rho/\bar{\rho})^{k/2} + (\bar{\rho}/\rho)^{k/2}$ is an analytic function on \mathcal{D} .

3.4.3 The end of the proof that $g(\tau_k, \mathbf{x}_k)$ is analytic in \mathcal{D}

In section 3.4.1 and 3.4.2, we introduced path dependent variables $z, \bar{z}, \rho, \bar{\rho}$ in \mathcal{D} and showed that $(\rho \bar{\rho})^\Delta$ and $(\rho/\bar{\rho})^{k/2} + (\bar{\rho}/\rho)^{k/2}$ are analytic functions on \mathcal{D} . Now sticking them into the expansion (24), we conclude that

- $g(\tau_k, \mathbf{x}_k) = \sum_{\Delta \geq 0} \sum_{l \in \mathbb{N}} c_{\Delta, l} (\rho \bar{\rho})^\Delta P^l(\rho, \bar{\rho})$ is a series of analytic functions on \mathcal{D} .

For any $C \in \mathcal{D}$, we can find a neighbourhood $U \subset \mathcal{D}$ of C such that the expansion (24) converges uniformly in U .¹¹ So we conclude that

- $g(\tau_k, \mathbf{x}_k)$ is an analytic function on \mathcal{D} .

3.5 Analytic continuation: case $d = 2$

In this section we would like to discuss separately the analytic continuation of $g(\tau_k, \mathbf{x}_k)$ in $2d$. Although this case is covered by section 3.4, in the 2d case a much simpler construction can be given. This is because the analytic functions $z(\tau_k, \mathbf{x}_k), \bar{z}(\tau_k, \mathbf{x}_k)$ exist. In 2d we use the complex coordinates [14]:

$$z_k = x_k^0 + ix_k^1, \quad \bar{z}_k = x_k^0 - ix_k^1, \quad k = 1, 2, 3, 4. \tag{41}$$

We choose z, \bar{z} to be

$$z = \frac{(z_1 - z_2)(z_3 - z_4)}{(z_1 - z_3)(z_2 - z_4)}, \quad \bar{z} = \frac{(\bar{z}_1 - \bar{z}_2)(\bar{z}_3 - \bar{z}_4)}{(\bar{z}_1 - \bar{z}_3)(\bar{z}_2 - \bar{z}_4)}. \tag{42}$$

¹⁰The self-avoiding condition is to make sure that there exists a simply connected neighbourhood of the path, so that the analytic continuation is always well-defined (no monodromy issue).

¹¹We can find a neighbourhood U of C such that $|\rho|, |\bar{\rho}| < R < 1$ in U . Then the uniform convergence follows from the fact that (24) is a rearrangement of the series expansion (22) which is absolutely convergent.

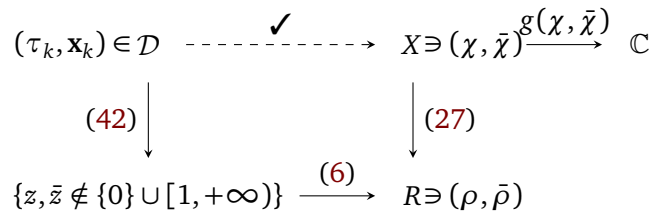


Figure 3.1: The diagram of maps in 2d.

One can check that (42) is consistent with (7). Furthermore, z, \bar{z} in (42) are analytic in all variables x_k^μ except for

$$(z_1 - z_3)(\bar{z}_1 - \bar{z}_3)(z_2 - z_4)(\bar{z}_2 - \bar{z}_4) = 0. \tag{43}$$

In particular, $z(\tau_k, \mathbf{x}_k), \bar{z}(\tau_k, \mathbf{x}_k)$ are analytic functions of x_k^μ on \mathcal{D} .

Let $x_k^0 = \epsilon_k + it_k$. We write down the complex coordinates defined in (41):

$$z_k = \epsilon_k + it_k + ix_k^1, \quad \bar{z}_k = \epsilon_k + it_k - ix_k^1, \quad k = 1, 2, 3, 4v. \tag{44}$$

Then z, \bar{z} are computed via (42). Notice that the Euclidean configuration $C' = (x'_1, x'_2, x'_3, x'_4)$,

$$(x'_k)^0 = \epsilon_k, \quad (x'_k)^1 = t_k + x_k^1 v, \tag{45}$$

gives the same z_k , and hence the same z . Applying eq. (14) to C' , we conclude that $z \neq [1, +\infty)$ ($\bar{z} \neq [1, +\infty)$ follows from the same argument). This proves the 2d case of theorem 3.1.

Furthermore, $z, \bar{z} \neq 0$ in \mathcal{D} because $z_i - z_j, \bar{z}_i - \bar{z}_j \neq 0$ for $i \neq j$. So we conclude that

$$z(\mathcal{D}), \bar{z}(\mathcal{D}) \subset \mathbb{C} \setminus (\{0\} \cup [1, +\infty)). \tag{46}$$

Based on (46), we safely map z, \bar{z} to $\rho, \bar{\rho}$ via (18), and we have $\rho, \bar{\rho} \neq 0$. Then consider the function $g(\chi, \bar{\chi})$ which is analytic in the domain $\text{Im}(\chi), \text{Im}(\bar{\chi}) > 0$ (see section 3.3.2). Figure 3.1 shows the procedure of analytic continuation.

Since \mathcal{D} is simply connected, by the lifting properties of the covering map [41], there exists a continuous map (dashed arrow in figure 3.1) from \mathcal{D} to X , which lifts the map from \mathcal{D} to R . Such a map is unique if we fix $\chi(\tau_k, \mathbf{x}_k)$ and $\bar{\chi}(\tau_k, \mathbf{x}_k)$ at one configuration in \mathcal{D}_E .¹² Because (42), (18), (27) are analytic functions, the map $\mathcal{D} \rightarrow X$ defines an analytic function $(\chi(\tau_k, \mathbf{x}_k), \bar{\chi}(\tau_k, \mathbf{x}_k))$. By composing $\chi(\tau_k, \mathbf{x}_k), \bar{\chi}(\tau_k, \mathbf{x}_k)$ with the function $g(\chi, \bar{\chi})$, we get a function $g(\tau_k, \mathbf{x}_k)$ which is analytic in the variables τ_k and $\mathbf{x}_k = x_k^1$.

4 Lorentzian CFT four-point function

4.1 Some preparations

In this section we are going to study the OPE convergence of Lorentzian CFT four-point functions. Since we have analytically continued the Euclidean CFT four-point function to the domain \mathcal{D} , the next step is to take the limit (2) to the Lorentzian configurations, which are at the boundary of \mathcal{D} (denoted by $\partial\mathcal{D}$).

The main differences between \mathcal{D} and $\partial\mathcal{D}$ are as follows:

¹²In \mathcal{D}_E , we choose $\chi(\tau_k, \mathbf{x}_k), \bar{\chi}(\tau_k, \mathbf{x}_k)$ with the constraint $\chi^* = -\bar{\chi}$ because $\rho^*(\tau_k, \mathbf{x}_k) = \bar{\rho}(\tau_k, \mathbf{x}_k)$ for configurations in the Euclidean region.

- (Position space) For any x_i, x_j pair in \mathcal{D} , x_{ij}^2 is always non-zero, while for x_i, x_j pairs in $\partial\mathcal{D}$, $x_{ij}^2 = 0$ when x_i and x_j are light-like separated:

$$\epsilon_i = \epsilon_j, \quad (t_i - t_j)^2 = (\mathbf{x}_i - \mathbf{x}_j)^2.$$

- (Cross-ratio space) For all configurations in \mathcal{D} , the variables z, \bar{z} never belong to $\{0\} \cup [1, +\infty)$, while the configurations in $\partial\mathcal{D}$ may have z or $\bar{z} \in \{0\} \cup [1, +\infty)$.

We call (4), (22) the s-channel expansion of the CFT four-point function. A priori we can also use the t- and u-channel expansions to construct the analytic continuation of the four-point function, starting from the t- and u-channel versions of (4):

$$\langle \phi(x_1)\phi(x_2)\phi(x_3)\phi(x_4) \rangle = \frac{g(u_t, v_t)}{(x_{14}^2)^\Delta (x_{23}^2)^\Delta} = \frac{g(u_u, v_u)}{(x_{13}^2)^\Delta (x_{24}^2)^\Delta}, \tag{47}$$

where

$$u_t = v, \quad v_t = u, \quad u_u = \frac{1}{u}, \quad v_u = \frac{v}{u}. \tag{48}$$

We want to remark that only the s-channel expansion could be used to extend $g(\tau_k, \mathbf{x}_k)$ to the whole \mathcal{D} , since theorem 3.1 holds only for the s-channel. We can use t- and u-channel expansion to analytically continue the four-point function to part of \mathcal{D} , but not to the whole \mathcal{D} . We will also consider t- and u-channel expansions because there are Lorentzian configurations where the s-channel expansion does not converge, but the t- or u-channel expansion converges (see section 4.3.2).

4.2 Excluding light-cone singularities

When $x_{ij}^2 = 0$ for some x_i, x_j pair, since at least one of the scaling factors in (4) and (47) is infinity, we expect the four-point function to be infinity. The configurations which contain at least one light-like x_i, x_j pair are called light-cone singularities.

One example, for which the correlation functions are divergent at light-cone singularities, is the generalized free field (GFF). Since we are interested in the Lorentzian configurations where the four-point functions are genuine functions for all unitary CFTs, we only consider the configurations which are not light-cone singularities. In other words, in this paper we will only consider the following set of Lorentzian configurations:

$$\mathcal{D}_L := \left\{ (x_1, x_2, x_3, x_4) \in \partial\mathcal{D} \mid x_k = (it_k, \mathbf{x}_k), \forall k; \quad x_{ij}^2 \neq 0, \forall i \neq j \right\}. \tag{49}$$

4.3 Criteria of OPE convergence

Now that $x_{ij}^2 \neq 0$ for all configurations in \mathcal{D}_L , all the cross-ratios defined in (6) and (48) are finite and non-zero, which implies

$$z, \bar{z} \neq 0, 1, \infty. \tag{50}$$

So the real axis in the z, \bar{z} -space is divided into three parts:

$$(-\infty, 0) \cup (0, 1) \cup (1, +\infty). \tag{51}$$

In this section, we are going to establish criteria of OPE convergence in s-, t- and u-channels. The three intervals in (51) will play important roles because each of them is the place where one OPE channel stops being convergent.

4.3.1 s-channel

We have analytically continued the four-point function G_4 to \mathcal{D} . So far, as already mentioned, we only used the s-channel expansion because of theorem 3.1. Actually by using the s-channel expansion, we are able to extend G_4 to a larger domain $\mathcal{D}^s \supset \mathcal{D}$ according the constraint $0 < |\rho|, |\bar{\rho}| < 1$ (or equivalently, $z, \bar{z} \neq \{0\} \cup [1, +\infty)$). \mathcal{D}^s contains some but not all Lorentzian configurations. In other words, the Lorentzian four-point function has convergent s-channel OPE on the set $\mathcal{D}^s \cap \mathcal{D}_L$.

By (18) and (50), $\rho, \bar{\rho} \neq 0, \pm 1$ for all configurations in \mathcal{D}_L . Because of theorem 3.1 and the continuity, all configurations in \mathcal{D}_L have $|\rho|, |\bar{\rho}| \leq 1$. To check the convergence of s-channel OPE, it suffices to check whether $|\rho|, |\bar{\rho}| \neq 1$ or not. Equivalently, it suffices to check whether $z, \bar{z} \notin (1, +\infty)$ or not.

Therefore, given a Lorentzian configuration $C_L \in \mathcal{D}_L$, we have the following criterion of s-channel OPE convergence:

Theorem 4.1. (*s-channel OPE convergence*) If neither z nor \bar{z} computed from C_L belong to $(1, +\infty)$, then the Lorentzian four-point function G_4 is analytic at C_L and is given by the formula

$$G_4(C_L) = \frac{g(\chi, \bar{\chi})}{[x_{12}^2 x_{34}^2]^\Delta}. \tag{52}$$

Here $g(\chi, \bar{\chi})$ is the same function as described in section 3.3.2, and the variables $\chi, \bar{\chi}$ are defined by the algorithm in section 3.4.1. The function $g(\chi, \bar{\chi})$ can be computed by the convergent series expansion (22).

4.3.2 t-channel and u-channel

We define the variables z_t, \bar{z}_t and z_u, \bar{z}_u by replacing u, v with u_t, v_t and u_u, v_u in (7). By (7) and (48), we choose proper solutions to the t- and u-channel versions of (7), and get the following relations¹³

$$z_t = 1 - z, \quad \bar{z}_t = 1 - \bar{z}, \quad z_u = 1/z, \quad \bar{z}_u = 1/\bar{z}. \tag{53}$$

Then we define the t- and u-channel versions of radial coordinates $\rho_t, \bar{\rho}_t, \rho_u, \bar{\rho}_u$ by replacing z, \bar{z} with z_t, \bar{z}_t and z_u, \bar{z}_u in (18). By (53) and the fact that z, \bar{z} are not real for configurations in $\mathcal{D}_E \setminus \Gamma$, $z_t, \bar{z}_t, z_u, \bar{z}_u$ are also not real for configurations in $\mathcal{D}_E \setminus \Gamma$. In particular, $z_t, \bar{z}_t, z_u, \bar{z}_u \notin [1, +\infty)$ for all configurations in $\mathcal{D}_E \setminus \Gamma$, which allows us to choose $|\rho_t| = |\bar{\rho}_t| < 1$ and $|\rho_u| = |\bar{\rho}_u| < 1$ to start with convergent t- and u-channel expansions. Analogously to the s-channel expansion, the t- and u-channel expansions are defined by replacing $\rho, \bar{\rho}$ with $\rho_t, \bar{\rho}_t$ and $\rho_u, \bar{\rho}_u$ in the series expansion (22).

For all configurations in $\mathcal{D}_E \setminus \Gamma$, the s-, t- and u-channel expansions converge to the same Euclidean CFT four-point function. This consistency condition is called the crossing symmetry [42, 43]. Now let us analytically continue the four-point function via the t-channel expansion. Suppose we have a path γ in $\mathcal{D} \setminus \Gamma$ such that $\gamma(0) \in \mathcal{D}_E \setminus \Gamma$, we can find a neighbourhood $U_\gamma \subset \mathcal{D} \setminus \Gamma$ of the set $\{\gamma(s) \mid 0 \leq s \leq 1\}$ and perform the analytic continuation of z, \bar{z} in U_γ via (6) and (8).¹⁴ Then we get the analytic continuation of z_t, \bar{z}_t in U_γ by the relation in (53). If $z_t, \bar{z}_t \notin (1, +\infty)$ in U_γ , or equivalently, $|\rho_t|, |\bar{\rho}_t| < 1$ in U_γ , then the t-channel expansion of G_4 is convergent in U_γ , and gives the analytic continuation to U_γ . Since the start point $\gamma(0)$ is a Euclidean configuration, $U_\gamma \cap \mathcal{D}_E$ is an open subset of \mathcal{D}_E , where the temporal variables τ_k are

¹³The other solutions of $z_t, \bar{z}_t, z_u, \bar{z}_u$ differ from (53) by interchanging z_t, \bar{z}_t or z_u, \bar{z}_u , which will give the same conclusions of convergence properties in t- and u-channel expansions.

¹⁴As long as $\gamma(s) \notin \mathcal{D} \setminus \Gamma$ along the path γ , such a neighbourhood U_γ always exists.

independent real numbers. According the crossing symmetry, the s- and t-channel expansions agree in $U_\gamma \cap \mathcal{D}_E$, so they also agree in U_γ , where τ_k are independent complex numbers. Furthermore, by taking the limit from $\mathcal{D} \setminus \Gamma$ to Γ , we can also use the t-channel expansion to compute the four-point function for configurations in Γ with the constraint $|\rho_t|, |\bar{\rho}_t| < 1$, and the result also agrees with the s-channel expansion by continuity. So we conclude that

- Given a configuration C in \mathcal{D} , the t-channel expansion gives the same analytic continuation of G_4 as the s-channel expansion if there exists a path γ in \mathcal{D} such that $\gamma(0) \in \mathcal{D}_E \setminus \Gamma$, $\gamma(1) = C$ and $z_t, \bar{z}_t \notin (1, +\infty)$ along γ .

Analogously, by replacing z_t, \bar{z}_t with z_u, \bar{z}_u , we have the same conclusion for the u-channel expansion.

While theorem 3.1 holds for z, \bar{z} , it does not hold for z_t, \bar{z}_t or z_u, \bar{z}_u , which means that the t- and u-channel expansions may diverge in \mathcal{D} . Unlike the s-channel, the convergence properties of t- and u-channel expansions require not only the values of $z_t, \bar{z}_t, z_u, \bar{z}_u$ of a configuration, but also the values of these variables along a path. For convenience we use the relation (53) to translate $z_t, \bar{z}_t, z_u, \bar{z}_u \notin (1, +\infty)$ to equivalent conditions in z, \bar{z} :

$$\begin{aligned} z_t, \bar{z}_t \notin (1, +\infty) &\Rightarrow z, \bar{z} \notin (-\infty, 0), \\ z_u, \bar{z}_u \notin (1, +\infty) &\Rightarrow z, \bar{z} \notin (0, 1). \end{aligned} \tag{54}$$

Then it suffices to compute and watch z, \bar{z} -curves along the path.

To give criteria of convergence properties in t- and u-channel expansions, we define some quantities which count how z, \bar{z} -curves cross the intervals $(-\infty, 0)$ and $(0, 1)$. Given a path γ defined as follows

$$\begin{aligned} \gamma : [0, 1] &\longrightarrow \bar{\mathcal{D}}, \\ \gamma(0) &\in \mathcal{D}_E \setminus \Gamma, \\ \gamma(s) &\in \mathcal{D} \setminus \Gamma, \quad s < 1, \end{aligned} \tag{55}$$

if the variables z, \bar{z} at the final point $\gamma(1)$ satisfy $z, \bar{z} \notin (-\infty, 0)$, we define

$$\begin{aligned} n_t(\gamma) &:= \text{number of times } z \text{ crosses } (-\infty, 0) \text{ from above} \\ &\quad - \text{number of times } z \text{ crosses } (-\infty, 0) \text{ from below,} \\ \bar{n}_t(\gamma) &:= \text{number of times } \bar{z} \text{ crosses } (-\infty, 0) \text{ from above} \\ &\quad - \text{number of times } \bar{z} \text{ crosses } (-\infty, 0) \text{ from below,} \end{aligned} \tag{56}$$

and

$$N_t(\gamma) := n_t(\gamma) + \bar{n}_t(\gamma). \tag{57}$$

Analogously, if the variables z, \bar{z} at the final point $\gamma(1)$ satisfy $z, \bar{z} \notin (0, 1)$, we define

$$\begin{aligned} n_u(\gamma) &:= \text{number of times } z \text{ crosses } (0, 1) \text{ from above} \\ &\quad - \text{number of times } z \text{ crosses } (0, 1) \text{ from below,} \\ \bar{n}_u(\gamma) &:= \text{number of times } \bar{z} \text{ crosses } (0, 1) \text{ from above} \\ &\quad - \text{number of times } \bar{z} \text{ crosses } (0, 1) \text{ from below,} \end{aligned} \tag{58}$$

and

$$N_u(\gamma) := n_u(\gamma) + \bar{n}_u(\gamma). \tag{59}$$

Let us consider the t-channel expansion. We claim that N_t is a path independent quantity:

Lemma 4.2. Given a configuration $C \in \overline{\mathcal{D}}$ with $z, \bar{z} \notin (-\infty, 0]$, N_t is independent of the choice of the path. Therefore, we can write N_t as $N_t(C)$.

Proof. Suppose we have a path γ under condition (55) and $\gamma(1) = C$. Under convention (32), the path γ uniquely determines the paths of $z, \bar{z}, \rho, \bar{\rho}, \chi, \bar{\chi}$. By (18) and (27), we have

$$\begin{aligned} z \in (-\infty, 0) &\iff \rho \in (-1, 0) \\ &\iff \operatorname{Re}(\chi) = (2k + 1)\pi \text{ for some } k \in \mathbb{Z}, \end{aligned} \tag{60}$$

which implies that the final point of $\chi(s)$ contains the information about n_t :

$$(2n_t - 1)\pi < \operatorname{Re}(\chi(1)) < (2n_t + 1)\pi. \tag{61}$$

Analogously we have

$$(2\bar{n}_t - 1)\pi < \operatorname{Re}(\bar{\chi}(1)) < (2\bar{n}_t + 1)\pi. \tag{62}$$

Now we pick another path γ' under condition (55) and $\gamma'(1) = C$. We let $\chi', \bar{\chi}', n'_t, \bar{n}'_t, N'_t$ denote the corresponding variables of the path γ' . By lemma 3.3, we have

$$\chi(1) + \bar{\chi}(1) = \chi'(1) + \bar{\chi}'(1). \tag{63}$$

Since $\rho, \bar{\rho}$ at C at most interchange with each other, the relation (63) implies that there only two possibilities:

1. $\chi(1) = \chi'(1) + 2k\pi, \bar{\chi}(1) = \bar{\chi}'(1) - 2k\pi$ for some $k \in \mathbb{Z}$,
2. $\chi(1) = \bar{\chi}'(1) + 2k\pi, \bar{\chi}(1) = \chi'(1) - 2k\pi$ for some $k \in \mathbb{Z}$,

which, by (61) and (62), are equivalent to

1. $n_t = n'_t + k, \bar{n}_t = \bar{n}'_t - k$ for some $k \in \mathbb{Z}$.
2. $n_t = \bar{n}'_t + k, \bar{n}_t = n'_t - k$ for some $k \in \mathbb{Z}$.

Thus we have $N_t(\gamma) = N_t(\gamma')$. □

Suppose C is a configuration in $\mathcal{D} \cup \mathcal{D}_L$ with $z, \bar{z} \notin (-\infty, 0)$ and $N_t = 0$. By choosing an arbitrary path γ with conditions (55) and $\gamma(1) = C$, we get the paths $\chi(s), \bar{\chi}(s)$ along γ . We define a pair of new variables $\tilde{\chi}, \tilde{\bar{\chi}}$ by

$$\tilde{\chi} = \chi(1) - 2n_t\pi, \quad \tilde{\bar{\chi}} = \bar{\chi}(1) + 2n_t\pi. \tag{64}$$

Since $N_t = 0$ (which implies $n_t = -\bar{n}_t$), by (61) and (62), the construction (64) gives

$$-\pi < \operatorname{Re}(\tilde{\chi}) < \pi, \quad -\pi < \operatorname{Re}(\tilde{\bar{\chi}}) < \pi. \tag{65}$$

We have the following lemma.

Lemma 4.3. The following maps

$$\chi \mapsto \rho = e^{i\chi} \mapsto z = \frac{4\rho}{(1 + \rho)^2} = \frac{1}{\cos^2 \frac{\chi}{2}}, \tag{66}$$

are biholomorphic maps from $\{\chi \in \mathbb{C} \mid -\pi < \operatorname{Re}(\chi) < \pi, \operatorname{Im}\chi > 0\}$ to $\{\rho \in \mathbb{C} \mid |\rho| < 1, \rho \neq (-1, 0]\}$, then to the double-cut plane $\{z \in \mathbb{C} \mid z \notin (-\infty, 0] \cup [1, +\infty)\}$.

Proof. For the map $\chi \mapsto \rho$, since $-\pi < \text{Re}(\chi) < \pi$, its image in the ρ -space does not contain $(-\infty, 0)$, hence does not contain curves which go around 0. So the inverse $\chi = -i \ln \rho$ exists. The constraint $\text{Im}\chi > 0$ is equivalent to $0 < |\rho| < 1$.

The map $\rho \mapsto z$ is known to be a biholomorphic map from the open unit disc to $\mathbb{C} \setminus [1, +\infty)$ [13]. One can show by direct computation that $\rho \in (-1, 0]$ is equivalent to $z \in (-\infty, 0]$. \square

Since the double-cut plane is preserved under the map $z \rightarrow 1 - z$, by lemma 4.3 we define a pair of t-channel variables $\tilde{\chi}_t, \tilde{\tilde{\chi}}_t$ by

$$\begin{aligned} \tilde{\chi} &\mapsto \tilde{z} \mapsto \tilde{z}_t = 1 - \tilde{z} \mapsto \tilde{\chi}_t, \\ \tilde{\tilde{\chi}} &\mapsto \tilde{\tilde{z}} \mapsto \tilde{\tilde{z}}_t = 1 - \tilde{\tilde{z}} \mapsto \tilde{\tilde{\chi}}_t, \end{aligned} \tag{67}$$

where the maps $\tilde{\chi} \mapsto \tilde{z}, \tilde{\tilde{\chi}} \mapsto \tilde{\tilde{z}}$ are the same as (66), and the maps $\tilde{z}_t \mapsto \tilde{\chi}_t, \tilde{\tilde{z}}_t \mapsto \tilde{\tilde{\chi}}_t$ are the inverse of (66).

Since $\text{Im}\tilde{\chi}, \text{Im}\tilde{\tilde{\chi}} > 0$ for all configurations in \mathcal{D} , above we defined the (path dependent) variables $\tilde{\chi}_t, \tilde{\tilde{\chi}}_t$ for configurations in \mathcal{D} with the constraints $z, \bar{z} \notin (-\infty, 0)$ and $N_t = 0$. In fact such definition can be extended to Lorentzian configurations in \mathcal{D}_L with the same constraints. This is because any configuration C_L with $z, \bar{z} \notin (-\infty, 0)$ and $N_t = 0$ can be approached by configurations in \mathcal{D} with the same constraints, and then $\tilde{\chi}_t, \tilde{\tilde{\chi}}_t$ at C_L are defined by continuity.

Note that if z nor \bar{z} do not cross $(-\infty, 0)$ at all, then $|\rho_t|, |\bar{\rho}_t| < 1$ along the whole path, and the t-channel OPE is guaranteed to converge. The criterion we give is more general in that it allows some crossings. Let us prove that this more general criterion is indeed sufficient.

Theorem 4.4. (*t-channel OPE convergence*) Given a Lorentzian configuration $C_L \in \mathcal{D}_L$. If the variables z, \bar{z} of C_L do not belong to $(-\infty, 0)$, and furthermore if $N_t(C_L) = 0$, then the Lorentzian four-point function G_4 is analytic at C_L and is given by the formula

$$G_4(C_L) = \frac{g(\tilde{\chi}_t, \tilde{\tilde{\chi}}_t)}{[x_{23}^2 x_{14}^2]^\Delta}. \tag{68}$$

Here g is the same function as described in section 3.3.2, and the variables $\tilde{\chi}_t, \tilde{\tilde{\chi}}_t$ are defined by the algorithm in (64) and (67). The function $g(\tilde{\chi}_t, \tilde{\tilde{\chi}}_t)$ can be computed by the convergent series expansion (22).

Before the proof of theorem 4.4, we introduce the following lemma:

Lemma 4.5. Given a configuration $C \in \mathcal{D}$. If the variables z, \bar{z} of C do not belong to $(-\infty, 0)$, and furthermore if $N_t(C) = 0$, then we have

$$\frac{g(\chi, \bar{\chi})}{[x_{12}^2 x_{34}^2]^\Delta} = \frac{g(\tilde{\chi}_t, \tilde{\tilde{\chi}}_t)}{[x_{23}^2 x_{14}^2]^\Delta}. \tag{69}$$

We would like to postpone the proof of lemma 4.5. Let us first see how lemma 4.5 implies theorem 4.4.

Suppose we have a Lorentzian configuration C_L which satisfies the conditions of theorem 4.4. Since $C_L \in \overline{\mathcal{D}}$, we can approach C_L by a sequence of configurations $\{C_n\}$ in \mathcal{D} such that C_n satisfies $z, \bar{z} \notin (-\infty, 0)$ and $N_t(C_n) = 0$. By construction $\text{Im}\tilde{\chi}_t, \text{Im}\tilde{\tilde{\chi}}_t > 0$ for C_L and all C_n in the sequence, so $g(\tilde{\chi}_t, \tilde{\tilde{\chi}}_t)$ can be computed by the convergent series expansion (22). We choose $\tilde{\chi}_t(C_n), \tilde{\tilde{\chi}}_t(C_n)$ such that they form two sequences which approach $\tilde{\chi}_t(C_L), \tilde{\tilde{\chi}}_t(C_L)$, then by continuity, the limit of $g(\tilde{\chi}_t(C_n), \tilde{\tilde{\chi}}_t(C_n))$ is exactly $g(\tilde{\chi}_t(C_L), \tilde{\tilde{\chi}}_t(C_L))$.¹⁵ By lemma 4.5, we

¹⁵For this claim we choose a path $\gamma(s)$ with $\gamma(1) = C_L$ and let the sequence $\{C_n\}$ be along the path γ . Let the sequences of $\chi(C_n), \bar{\chi}(C_n)$ also be along the path, then it is natural to see that the sequences of $\tilde{\chi}_t(C_n), \tilde{\tilde{\chi}}_t(C_n)$ have the limits $\tilde{\chi}_t(C_L), \tilde{\tilde{\chi}}_t(C_L)$.

have eq. (69) for C_n . Note that the LHS of (69) is the four-point function in the s-channel expansion, thus we have

$$G_4(C_L) = \lim_{n \rightarrow \infty} G_4(C_n) = \lim_{n \rightarrow \infty} \frac{g(\tilde{\chi}_t, \tilde{\tilde{\chi}}_t)}{[x_{23}^2 x_{14}^2]^\Delta} \Big|_{C_n} = \frac{g(\tilde{\chi}_t, \tilde{\tilde{\chi}}_t)}{[x_{23}^2 x_{14}^2]^\Delta} \Big|_{C_L}. \tag{70}$$

So we finish the proof of theorem 4.4. We would like to make two comments. First, theorem 4.4 covers the case when s-channel expansion is not convergent. For this case we have z or $\bar{z} \in (1, +\infty)$. To compute G_4 it is important to know whether $\text{Arg}(1-\bar{z})$ or $\text{Arg}(1-\tilde{\tilde{z}})$ is equal to π or $-\pi$. A crucial point is that the information about these phases are contained in $\tilde{\chi}_t$ and $\tilde{\tilde{\chi}}_t$.¹⁶ Second, eq. (68) indeed corresponds to the t-channel expansion because each term in the series expansion (22) of $g(\tilde{\chi}_t, \tilde{\tilde{\chi}}_t)$ corresponds to a state which appears in the $\phi(x_2)\phi(x_3)$ OPE.

It remains to prove lemma 4.5.

Proof. We have

$$\begin{aligned} \frac{g(\chi, \bar{\chi})}{[x_{12}^2 x_{34}^2]^\Delta} &= \frac{g(\tilde{\chi}, \tilde{\tilde{\chi}})}{[x_{12}^2 x_{34}^2]^\Delta} \\ &= \frac{1}{[x_{12}^2 x_{34}^2]^\Delta} \times \left[\frac{\tilde{\tilde{z}}\tilde{z}}{(1-\tilde{z})(1-\tilde{\tilde{z}})} \right]^\Delta g(\tilde{\chi}_t, \tilde{\tilde{\chi}}_t) \\ &= \frac{1}{[x_{12}^2 x_{34}^2]^\Delta} \times \left[\frac{z\bar{z}}{(1-z)(1-\bar{z})} \right]^\Delta g(\tilde{\chi}_t, \tilde{\tilde{\chi}}_t) \\ &= \frac{1}{[x_{12}^2 x_{34}^2]^\Delta} \times \left[\frac{u}{v} \right]^\Delta g(\tilde{\chi}_t, \tilde{\tilde{\chi}}_t) \\ &= \frac{g(\tilde{\chi}_t, \tilde{\tilde{\chi}}_t)}{[x_{23}^2 x_{14}^2]^\Delta}. \end{aligned} \tag{71}$$

The first equality is a consequence of eq. (29). The second equality follows from the crossing symmetry

$$g(z, \bar{z}) = \left[\frac{z\bar{z}}{(1-z)(1-\bar{z})} \right]^\Delta g(1-z, 1-\bar{z}), \quad z, \bar{z} \in \mathbb{C} \setminus (-\infty, 0] \cup [0, +\infty). \tag{72}$$

Here we also use the fact that both s- and t-channel expansions are convergent if z, \bar{z} are in the double-cut plane, and in the same branch as the Euclidean case.

For the third equality, we recall our definition of $\tilde{\chi}, \tilde{\tilde{\chi}}$ in (64): the variables z, \bar{z} acquire extra phases and $1-z, 1-\bar{z}$ do not go around 0. In other words, we have

$$\begin{aligned} \tilde{z} &= e^{-2n_t \pi i} z, & \tilde{\tilde{z}} &= e^{2n_t \pi i} \bar{z}, \\ 1-\tilde{z} &= 1-z, & 1-\tilde{\tilde{z}} &= 1-\bar{z}. \end{aligned} \tag{73}$$

The remaining steps in (71) are trivial. □

The criterion of u-channel convergence is similar to t-channel. Given a configuration C_L with $z, \bar{z} \notin (0, 1)$ and $N_u = 0$. We choose a path γ to get $\chi(1), \bar{\chi}(1)$, then the u-channel versions of (61) and (62) are given by

$$\begin{aligned} -2n_u \pi &< \text{Re}(\chi(1)) < -2n_u \pi + 2\pi, \\ -2\bar{n}_u \pi - 2\pi &< \text{Re}(\bar{\chi}(1)) < -2\bar{n}_u \pi. \end{aligned} \tag{74}$$

¹⁶Since $\tilde{\rho}_t = e^{i\tilde{\chi}_t}$, we have $\text{Arg}(\tilde{\rho}_t) = \text{Re}\tilde{\chi}_t$. If $z = \tilde{z} \in (1, +\infty)$, then we have $\text{Arg}(1-\tilde{z}) = \text{Re}\tilde{\chi}_t$. The argument is similar for \bar{z} .

The u-channel variables $\tilde{\chi}_u, \tilde{\bar{\chi}}_u$ are defined by following algorithm, which is analogous to (67):

$$\begin{aligned} \tilde{\chi} &= \chi(1) + 2n_u\pi \mapsto \tilde{z} \mapsto \tilde{z}_u = \frac{1}{\tilde{z}} \mapsto \tilde{\chi}_u, \\ \tilde{\bar{\chi}} &= \bar{\chi}(1) - 2n_u\pi \mapsto \tilde{\bar{z}} \mapsto \tilde{\bar{z}}_u = \frac{1}{\tilde{\bar{z}}} \mapsto \tilde{\bar{\chi}}_u. \end{aligned} \tag{75}$$

We give the u-channel criterion without proof.

Theorem 4.6. (*u-channel OPE convergence*) Given a Lorentzian configuration $C_L \in \mathcal{D}_L$. If the variables z, \bar{z} of C_L do not belong to $(0, 1)$, and furthermore if $N_u(C_L) = 0$, then the Lorentzian four-point function G_4 is analytic at C_L and is given by the formula

$$G_4(C_L) = \frac{g(\tilde{\chi}_u, \tilde{\bar{\chi}}_u)}{[x_{13}^2 x_{24}^2]^\Delta}. \tag{76}$$

Here g is the same function as described in section 3.3.2, and the variables $\tilde{\chi}_u, \tilde{\bar{\chi}}_u$ are defined by the algorithm (75). The function $g(\tilde{\chi}_u, \tilde{\bar{\chi}}_u)$ can be computed by the convergent series expansion (22).

Unlike the s-channel case, even if we only want to check the convergence properties of t- and u-channel expansions, we have to choose a path to compute N_t and N_u .

Before finishing this subsection, we want to remark that actually the condition (55) of the path γ can be relaxed in the way that γ is allowed to touch Γ :

$$\begin{aligned} \gamma &: [0, 1] \longrightarrow \overline{\mathcal{D}}, \\ \gamma(0) &\in \mathcal{D}_E \setminus \Gamma, \\ \gamma(1) &\in \mathcal{D}_L. \end{aligned} \tag{77}$$

Suppose we have a path γ which intersects with Γ . Let $\gamma(s_*) \in \Gamma$ be the first intersection point. At s_* we have $z(s_*) = \bar{z}(s_*)$, then $z(s), \bar{z}(s)$ become indistinguishable for $s > s_*$, so the quantities $n_t, \bar{n}_t, n_u, \bar{n}_u, \chi, \bar{\chi}$ are not well defined for γ . However, by manually choosing z, \bar{z} after each intersection, we still get two curves $z(s), \bar{z}(s)$: they may not be smooth at intersection points, but they are still continuous. By this trick we get $n_t, \bar{n}_t, n_u, \bar{n}_u, \chi, \bar{\chi}$, so that we are able to compute N_t, N_u and the four-point function. On the other hand, we can always deform γ to a path γ' , such that γ' has the same start and final points as γ but γ' does not intersect with Γ . By doing proper deformation, we can make γ' have the same $n_t, \bar{n}_t, n_u, \bar{n}_u, \chi, \bar{\chi}$ as selected on γ . Therefore, our manual selection will give the correct OPE convergence properties and the correct value of the four-point function.

4.4 What happens if there is no convergent OPE channel?

We want to make a comment that theorem 4.1, 4.4 and 4.6 give sufficient conditions for OPE convergence. For a Lorentzian configuration C_L which is not a light-cone singularity and which does not satisfy the conditions in these theorems, it does not mean that G_4 cannot be a function at C_L . It just means that for general CFT, we are not able to use the radial coordinates $\rho, \bar{\rho}$ ($\rho_t, \bar{\rho}_t, \rho_u, \bar{\rho}_u$) and the expansion (22) to prove the analyticity of G_4 at C_L . The four-point function still has a chance to be analytic at C_L . For example, the four-point function of generalized free fields has analytic continuation to the whole Lorentzian region except for the light-cone singularities.

An interesting related open question is: can we relax the conditions in theorem 4.1, 4.4 and 4.6?

4.4.1 s-channel condition

In theorem 4.1, we only assume the condition $z, \bar{z} \notin (1, +\infty)$ (equivalently, $|\rho|, |\bar{\rho}| < 1$). The Lorentzian configurations which violate this condition has $|\rho| = 1$ or $|\bar{\rho}| = 1$, then the proof of theorem 4.1 fails because in the proof we used the fact that the series expansion (22) is absolutely convergent when $|\rho|, |\bar{\rho}| < 1$.

We are interested in the Lorentzian configurations where the s-channel expansion is convergent for all unitary CFTs. For configurations with $|\rho| = 1$ or $|\bar{\rho}| = 1$, we may exhibit an explicit CFT four-point function, for which the s-channel expansion is divergent (then such configurations are ruled out). The generalized free field (GFF) theory is such an example. The GFF four-point function of identical scalar operators (with scaling dimension Δ) is defined by

$$(G_4)_{GFF}(x_1, x_2, x_3, x_4) = \frac{1}{[x_{12}^2 x_{34}^2]^\Delta} + \frac{1}{[x_{23}^2 x_{14}^2]^\Delta} + \frac{1}{[x_{13}^2 x_{24}^2]^\Delta}. \tag{78}$$

By (4), the conformal invariant part of $(G_4)_{GFF}$ is given by

$$g_{GFF}(\rho, \bar{\rho}) = 1 + \left(\frac{16\rho\bar{\rho}}{(1+\rho)^2(1+\bar{\rho})^2} \right)^\Delta + \left(\frac{16\rho\bar{\rho}}{(1-\rho)^2(1-\bar{\rho})^2} \right)^\Delta. \tag{79}$$

It has the series expansion

$$g_{GFF}(\rho, \bar{\rho}) = 1 + (16\rho\bar{\rho})^\Delta \sum_{m,n=0}^{\infty} \frac{(1+(-1)^{m+n})\Gamma(\Delta+m)\Gamma(\Delta+n)}{m!n!\Gamma(\Delta)^2} \rho^m \bar{\rho}^n, \tag{80}$$

which diverges when $|\rho| = 1$ or $|\bar{\rho}| = 1$. It follows that theorem 4.1 cannot be extended to configurations with $|\rho| = 1$ or $|\bar{\rho}| = 1$ without extra assumptions on the theory. One such extra assumption will be mentioned in section 5.3.2 (locality of 2d CFT).

4.4.2 t- and u-channel conditions

In theorem 4.4, we assumed two conditions: $z, \bar{z} \notin (-\infty, 0)$ and $N_t = 0$. For Lorentzian configurations which violate the first condition, (analogously to the s-channel case) we can use GFF to conclude that these configurations do not have convergent t-channel expansion for some unitary CFTs.

Let us explain more about our motivation for assuming $N_t = 0$. By the s-channel series expansion (22) and crossing symmetry (72), the function $g(\chi_t, \bar{\chi}_t)$ has analytic continuation to the universal covering of the domain

$$\begin{aligned} -\pi < \text{Re}(\chi_t) < \pi, \quad \chi_t \neq 0, \\ -\pi < \text{Re}(\bar{\chi}_t) < \pi, \quad \bar{\chi}_t \neq 0. \end{aligned} \tag{81}$$

The series expansion of $g(\chi_t, \bar{\chi}_t)$ is absolutely convergent in the region where

$$\begin{aligned} -\pi < \text{Re}(\chi_t) < \pi, \quad 0 < \text{Arg}(\chi_t) < \pi, \\ -\pi < \text{Re}(\bar{\chi}_t) < \pi, \quad 0 < \text{Arg}(\bar{\chi}_t) < \pi. \end{aligned} \tag{82}$$

Suppose we have a configuration C_L with $N_t \neq 0$. By choosing a path γ , we compute the paths $\chi_t(s), \bar{\chi}_t(s)$, and then determine the final points $\chi_t(1), \bar{\chi}_t(1)$. When the path $z(s)$ crosses $(-\infty, 0)$ from above, $\chi_t(s)$ either crosses $(-\pi, 0)$ from above, or crosses $(0, \pi)$ from below. Since the start points $\chi_t(0), \bar{\chi}_t(0)$ are in the region (82), we have

$$n_t \pi < \text{Arg}(\chi_t) < (n_t + 1)\pi, \quad \bar{n}_t \pi < \text{Arg}(\bar{\chi}_t) < (\bar{n}_t + 1)\pi, \tag{83}$$

which are the t-channel versions of (61) and (62). We see that $\chi_t(1)e^{-n_t\pi i}, \bar{\chi}_t(1)e^{-\bar{n}_t\pi i}$ are in the region (82). The property (29) says that we have¹⁷

$$g(\chi_t(1), \bar{\chi}_t(1)) = g(\chi_t(1)e^{\pi i}, \bar{\chi}_t(1)e^{-\pi i}). \tag{84}$$

However, if $N_t \neq 0$, then $n_t \neq -\bar{n}_t$ for any path γ . So in this case we cannot use (84) to move $\chi_t(1), \bar{\chi}_t(1)$ to the region (82). This is where the proof of theorem 4.4 fails for $N_t \neq 0$.

The arguments for theorem 4.6 are similar.

5 Classifying the Lorentzian configurations

In the previous section we gave the criteria of convergence properties of OPE in various channels for Lorentzian CFT four-point functions. These criteria say that given a Lorentzian configuration C_L , one can just start with an arbitrary Euclidean configuration in $\mathcal{D}_E \setminus \Gamma$ and choose an arbitrary path towards C_L , then decide if the conditions in theorem 4.1, 4.4 and 4.6 hold or not by watching the z, \bar{z} -curves (in theorem 4.1 one does not even have to choose a path).

However, it would be frustrating if we have to check the analytic continuation curves for all Lorentzian configurations in \mathcal{D}_L (recall definition (49)). We expect that these Lorentzian configurations can be classified such that for each class it suffices to choose one representative configuration to see if various OPE channels converge or not. There are two natural classification methods, one according to the range of z and \bar{z} , the other according to the causal orderings. We will show that combining these two methods leads to a complete classification for the convergence properties of Lorentzian CFT four-point functions.

5.1 z, \bar{z} of Lorentzian configurations

For all Lorentzian configurations, since x_{ij}^2 are real, the cross-ratios u, v are also real. By (8), there are only two possibilities for z, \bar{z} :

1. z, \bar{z} are independent real variables.
2. z, \bar{z} are complex conjugate to each other.

In addition, we have already excluded light-cone singularities in \mathcal{D}_L (recall definition (49)), so the configurations in \mathcal{D}_L have $z, \bar{z} \neq 0, 1, \infty$. According to the range of the z, \bar{z} variables, we divide \mathcal{D}_L into four classes:

$$\mathcal{D}_L = S \sqcup T \sqcup U \sqcup E, \tag{85}$$

where the classes are defined as follows.

- Class S: configurations with $0 < z < 1, \bar{z} < 0$ or $z < 0, 0 < \bar{z} < 1$.
- Class T: configurations with $z > 1, 0 < \bar{z} < 1$ or $0 < z < 1, \bar{z} > 1$.
- Class U: configurations with $z > 1, \bar{z} < 0$ or $z < 0, \bar{z} > 1$.
- Class E: configurations with $z, \bar{z} < 0$ or $0 < z, \bar{z} < 1$ or $z, \bar{z} > 1$ or $z^* = \bar{z}$.

¹⁷Recall the map $\chi \mapsto \chi_t$ in (67), the transformation $\chi \rightarrow \chi + 2\pi$ corresponds to $\chi_t \rightarrow \chi_t e^{i\pi}$.

We use the name “S” (resp. “T”, “U”) because it corresponds to the configurations where only the s-channel (resp. t-channel, u-channel) expansion has a chance to converge. The name “E” means “Euclidean”, since the variables z, \bar{z} in class E can be realized by the configurations with totally space-like separation. In addition, we divide the class E into four subclasses:

$$E = E_{su} \sqcup E_{st} \sqcup E_{tu} \sqcup E_{stu}, \tag{86}$$

where the subclasses are defined as follows.

- Subclass E_{su} : configurations with $z, \bar{z} < 0$.
- Subclass E_{st} : configurations with $0 < z, \bar{z} < 1$.
- Subclass E_{tu} : configurations with $z, \bar{z} > 1$.
- Subclass E_{stu} : configurations with $z^* = \bar{z}$ not real.

The subscripts in above names indicate the possible convergent channels. Figure 5.1 shows the range of (z, \bar{z}) pair corresponding to each class/subclass. Let $P(C)$ denote the subset of (z, \bar{z}) pairs corresponding to class/subclass C . Under identification $(z, \bar{z}) \sim (\bar{z}, z)$, $P(C)$ are connected subsets of \mathbb{C}/\mathbb{Z}_2 . $P(S), P(T), P(U), P(E)$ are disconnected from each other, but $P(E_{su}), P(E_{st})$ and $P(E_{tu})$ are connected to $P(E_{stu})$ (also note that $P(E_{su}), P(E_{st})$ and $P(E_{tu})$ are disconnected from each other).

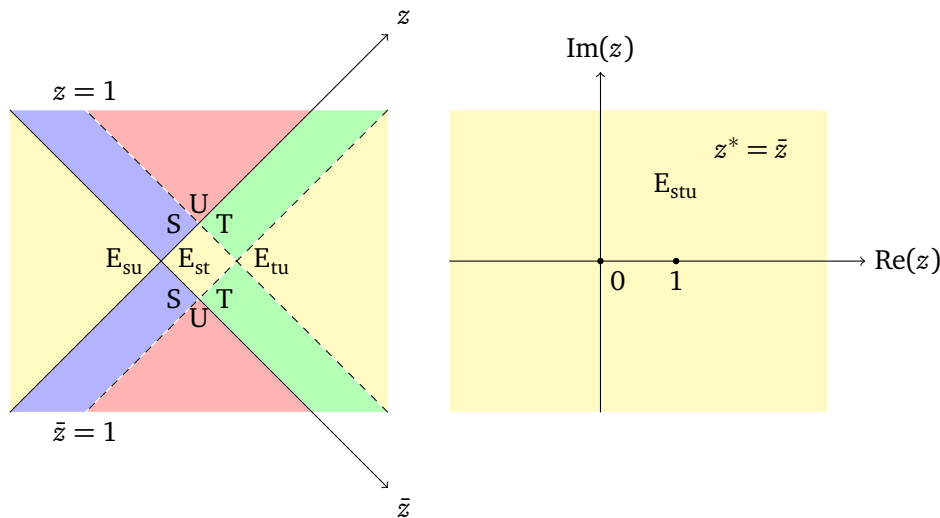


Figure 5.1: The corresponding range of (z, \bar{z}) pair of each class/subclass.

For each class/subclass, we immediately get some information about OPE convergence properties by theorem 4.1, 4.4 and 4.6 (see table 1). In table 1, the check mark means that the sufficient conditions in theorem 4.1 or 4.4 or 4.6 holds, hence the corresponding channel is convergent. The cross mark means that the sufficient conditions do not hold, we cannot conclude that the corresponding channel is convergent or not (basically because one or both $\rho, \bar{\rho}$ variables are on the unit circles). The blank means that there is room for convergence but we need to check N_t, N_u conditions.

Table 1: OPE convergence properties of classes/subclasses

class/subclass	s-channel	t-channel	u-channel
S	✓	✗	✗
T	✗		✗
U	✗	✗	
E_{st}	✓		✗
E_{su}	✓	✗	
E_{tu}	✗		
E_{stu}	✓		

5.2 Causal orderings

In Minkowski space $\mathbb{R}^{d-1,1}$, causal ordering is a binary relation between two arbitrary points. Let $x_1 = (it_1, \mathbf{x}_1)$ and $x_2 = (it_2, \mathbf{x}_2)$ be two points in $\mathbb{R}^{d-1,1}$,¹⁸ we say $x_1 \rightarrow x_2$ if x_2 is in the open forward light-cone of x_1 , or equivalently, $t_2 - t_1 > |\mathbf{x}_1 - \mathbf{x}_2|$.

By the triangle inequality, the causal ordering is transitive: if $x_1 \rightarrow x_2$ and $x_2 \rightarrow x_3$, then $x_1 \rightarrow x_3$.

Causal orderings are preserved by translations, Lorentz transformations and dilatations. But special conformal transformations may violate causal orderings.¹⁹ Given a pair of time-like separated points x_i, x_j in $\mathbb{R}^{d-1,1}$, there exists a special transformation such that the images x'_i, x'_j are space-like separated [44].

By “the causal ordering of a configuration $C = (x_1, x_2, x_3, x_4)$ ”, we will mean the directed graph (V, E) , where $V = \{1, 2, 3, 4\}$ is the set of indices and $E = \{(ij)\}$ is the set of arrows $i \rightarrow j$ encoding the causal orderings $x_i \rightarrow x_j$. For example, the causal ordering of the configuration

$$\begin{aligned}
 x_1 &= (0, 0, \dots, 0), \\
 x_2 &= (i, 0, \dots, 0), \\
 x_3 &= (2i, 0, \dots, 0), \\
 x_4 &= (3i, 0, \dots, 0),
 \end{aligned}
 \tag{87}$$

is given by

$$\begin{array}{ccc}
 1 & \longrightarrow & 2 \\
 \downarrow & \times & \downarrow \\
 4 & \longleftarrow & 3
 \end{array}
 \tag{88}$$

Since causal ordering is transitive, some arrows in the graph (88) are redundant and we will drop them. E.g. the graph

$$1 \rightarrow 2 \rightarrow 3 \rightarrow 4
 \tag{89}$$

¹⁸Since in this work our discussions start from the Euclidean signature, we use the Euclidean coordinates $x = (\epsilon + it, \mathbf{x})$. The Euclidean points correspond to $t = 0$ and the Lorentzian points correspond to $\epsilon = 0$.

¹⁹We will come back to this point in section 5.6.2.

represents the same causal ordering as (88). For simplicity, we will use the graphic notation with the least number of arrows like (89).

5.3 Classifying convergent OPE channels

We decompose the set \mathcal{D}_L according to the causal orderings of the configurations:

$$\mathcal{D}_L = \bigsqcup_{\alpha} \mathcal{D}_L^{\alpha}, \tag{90}$$

where each \mathcal{D}_L^{α} is the set of configurations with the same causal ordering, labelled by the index α .

5.3.1 Case $d \geq 3$

In $d \geq 3$, each \mathcal{D}_L^{α} in (90) is a connected component of \mathcal{D}_L . It is not hard to see that different \mathcal{D}_L^{α} are disconnected to each other. The proof that each \mathcal{D}_L^{α} is connected is given in appendix B.

Since \mathcal{D}_L^{α} is connected, with the identification $(z, \bar{z}) \sim (\bar{z}, z)$, the set of corresponding (z, \bar{z}) pairs is a connected subset of $\mathbb{C}^2/\mathbb{Z}_2$. Recalling our classification in section 5.1, we conclude that

Lemma 5.1. For $d \geq 3$, all configurations with the same causal ordering belong to the same class S, T, U, E (see section 5.1).

By the lemma, we can assign class S, T, U and E to each causal ordering of the configurations. In addition, if \mathcal{D}_L^{α} is in class E, we subdivide \mathcal{D}_L^{α} according to the subclasses of class E. We summarize these relations in figure 5.2.

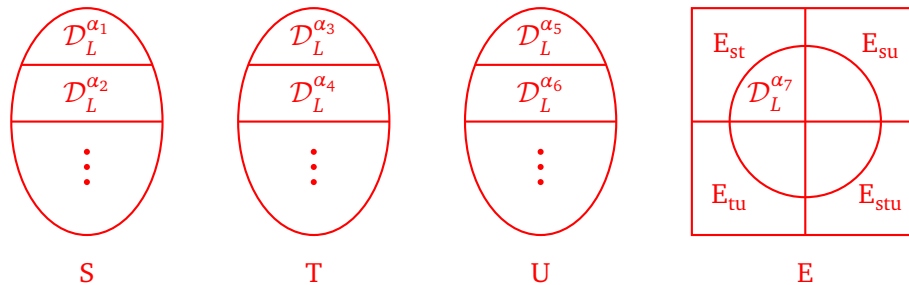


Figure 5.2: The class S, T, U and E are subdivided according causal orderings. For each \mathcal{D}_L^{α} in class E, \mathcal{D}_L^{α} is subdivided according to subclasses.

Now we are ready to state the classification of convergent OPE channels for Lorentzian CFT four-point functions.

Theorem 5.2. Let G_4^L be the Lorentzian four-point function which is defined by the Wick rotation (2) from a Euclidean unitary CFT in $d \geq 3$. Let α be a causal ordering and let \mathcal{D}_L^{α} be the set of all configurations with this causal ordering.

- If \mathcal{D}_L^{α} is in class S, then all configurations in \mathcal{D}_L^{α} only have convergent s-channel expansion for G_4^L .
- If \mathcal{D}_L^{α} is in class T, then all configurations in \mathcal{D}_L^{α} have the same N_t .
- If \mathcal{D}_L^{α} is in class U, then all configurations in \mathcal{D}_L^{α} have the same N_u .

- If \mathcal{D}_L^α is in class E, then
 - All configurations in $\mathcal{D}_L^\alpha \cap E_{st}$ have the convergent s-channel expansion and the same N_t .
 - All configurations in $\mathcal{D}_L^\alpha \cap E_{su}$ have the convergent s-channel expansion and the same N_u .
 - All configurations in $\mathcal{D}_L^\alpha \cap E_{tu}$ have the same N_t, N_u .
 - All configurations in $\mathcal{D}_L^\alpha \cap E_{stu}$ have the convergent s-channel expansion and the same N_t, N_u .

Proof. Let us check the conclusions case by case.

Case 1: \mathcal{D}_L^α is in class S.

The s-channel convergence follows from theorem 4.1. For other cases, the s-channel arguments are the same, and we will only focus on N_t and N_u .

Case 2: \mathcal{D}_L^α is in class T.

It remains to show that N_t is a constant in \mathcal{D}_L^α . For any $C_L, C'_L \in \mathcal{D}_L^\alpha$, since \mathcal{D}_L^α is connected, there exists a path γ_1 which connects C_L and C'_L :

$$\begin{aligned} \gamma_1 : [0, 1] &\longrightarrow \mathcal{D}_L^\alpha, \\ \gamma_1(0) &= C_L, \quad \gamma_1(1) = C'_L. \end{aligned} \tag{91}$$

Since $\gamma_1(s)$ are always configurations in class T, the corresponding z, \bar{z} never touch the interval $(-\infty, 0)$. So $n_t(\gamma_1) = \bar{n}_t(\gamma_1) = 0$, which implies $N_t(\gamma_1) = 0$. On the other hand, given a path γ_2 from $\mathcal{D}_E \setminus \Gamma$ to C_L , we get a path from $\mathcal{D}_E \setminus \Gamma$ to C'_L by connecting γ_1 and γ_2 . So we have

$$N_t(C'_L) = N_t(\gamma_1) + N_t(\gamma_2) = N_t(C_L). \tag{92}$$

In other words, N_t is a constant in \mathcal{D}_L^α .

Case 3: \mathcal{D}_L^α is in class U.

It remains to show that N_u is a constant in \mathcal{D}_L^α . The argument is similar to case 2.

Case 4: \mathcal{D}_L^α is in class E.

Suppose C_L, C'_L are two configurations in $\mathcal{D}_L^\alpha \cap E_{st}$. It remains to show that $N_t(C_L) = N_t(C'_L)$. Analogously to case 2, there exists a path γ_1 satisfying the condition (91), and it suffices to show that $N_t(\gamma_1) = 0$. Here it is different from case 2 because $\gamma_1(s)$ may go through the other subclasses of the class E, and the curves of z, \bar{z} may touch the interval $(-\infty, 0)$. In class E, the curves $z(s), \bar{z}(s)$ touch the interval $(-\infty, 0)$ only when $\gamma(s)$ enters the subclass E_{su} . However, $\gamma(s)$, which starts from E_{st} , must go through E_{stu} before entering E_{su} . When $\gamma(s)$ leaves E_{su} , it must go through E_{stu} again. Since in E_{stu} , the variables z, \bar{z} are complex conjugate to each other, the curves of z, \bar{z} must cross $(-\infty, 0)$ from opposite directions, see figure 5.3.

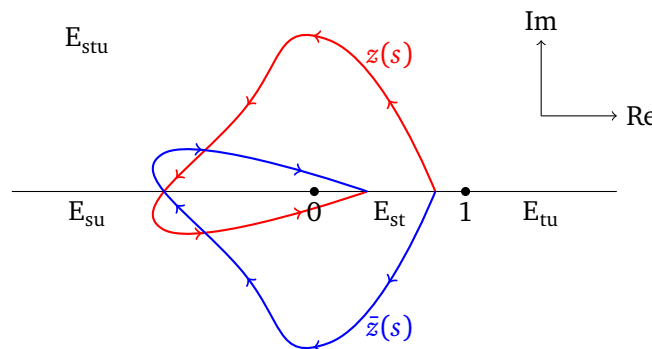


Figure 5.3: An example of $z(s), \bar{z}(s)$ along γ_1 in case 4.

So we get

$$n_t(\gamma_1) = -\bar{n}_t(\gamma_1), \tag{93}$$

which implies $N_t(\gamma_1) = 0$, hence $N_t(C_L) = N_t(C'_L)$.

The arguments for $\mathcal{D}_L^\alpha \cap E_{su}$, $\mathcal{D}_L^\alpha \cap E_{tu}$ and $\mathcal{D}_L^\alpha \cap E_{stu}$ are similar. □

An immediate consequence of theorem 5.2 is that for a fixed causal ordering (say \mathcal{D}_L^α), each blank space in table 1 satisfy the all-or-none law: either check mark for all configurations in \mathcal{D}_L^α or cross mark for all configurations in \mathcal{D}_L^α . Therefore, if \mathcal{D}_L^α is in class S or T or U, then all its configurations have the same OPE convergence properties; if \mathcal{D}_L^α is in class E, then all its configurations in the same subclass have the same OPE convergence properties.²⁰

5.3.2 Comments on the 2d case

In 2d unitary local CFTs, we have Al. Zamolodchikov’s uniformizing variables q, \bar{q} [11]. The function g in (4) has a convergent expansion in terms of Virasoro blocks, and Virasoro blocks have convergent series expansions in q, \bar{q} if $0 < |q|, |\bar{q}| < 1$, which includes the configurations with $0 \leq |\rho|, |\bar{\rho}| \leq 1$ except for ρ or $\bar{\rho} = \pm 1$. However, ρ or $\bar{\rho} = \pm 1$ only happens at light-cone singularities.²¹ So we conclude that in the Lorentzian signature, the s-channel OPE is always convergent aside from light-cone singularities [12].

The above CFT argument is valid only for 2d unitary local CFTs, where by local we mean there exists a stress tensor $T_{\mu\nu}(x)$, which has the mode expansion in Virasoro generators [14]. There are also non-local CFTs, e.g. the generalized free field theories. These non-local CFTs have only global conformal symmetry, for which we can only use $\rho, \bar{\rho}$ instead of q, \bar{q} .

We claim that the conclusions in theorem 5.2 are still true for 2d unitary CFT (here we only assume global conformal symmetry). Unlike the case $d \geq 3$, the sets \mathcal{D}_L^α are usually disconnected in 2d. This is because in 2d, there are two disconnected space-like separations. So we cannot copy the proof of theorem 5.2. However, any 2d configuration can be embedded into $d \geq 3$. Since our criteria of OPE convergence properties are based on counting how the analytic continuation curves of z, \bar{z} cross the intervals $(-\infty, 0)$, $(0, 1)$ and $(1, +\infty)$, which is dimension independent, the 2d path gives the same counting of N_t, N_u as in $d \geq 3$. Therefore, theorem 5.2 also covers the 2d case.

The only little difference is that in the 2d case, the Lorentzian four-point configurations only have real z, \bar{z} . This follows from (41) and (42). So the subclass E_{stu} , where z, \bar{z} are not real, does not exist in 2d.

5.4 Time reversals

In theorem 5.2, we have classified the Lorentzian configurations in \mathcal{D}_L into a finite number of cases. For each case, we will have to choose a representative configuration and a path from $\mathcal{D}_E \setminus \Gamma$, then check if conditions of theorem 4.1, 4.4 and 4.6 hold. Actually, there are some further simplifications which will reduce the number of checks to perform. We are going to show that different \mathcal{D}_L^α which are related by time reversals have the same convergent OPE channels.

We define two time reversals:

$$\begin{aligned} \theta_E : (\epsilon + it, \mathbf{x}) &\mapsto (-\epsilon + it, \mathbf{x}), \\ \theta_L : (\epsilon + it, \mathbf{x}) &\mapsto (\epsilon - it, \mathbf{x}). \end{aligned} \tag{94}$$

²⁰By configurations having the same OPE convergence properties, we mean that in each OPE channel, all or none of these configurations have the convergent expansion for the four-point function.

²¹If ρ or $\bar{\rho} = 1$, then $v = 0$. If ρ or $\bar{\rho} = -1$, then u or $v = \infty$. Thus, for any configuration with ρ or $\bar{\rho} = \pm 1$, there exists at least one x_i, x_j pair such that $(x_i - x_j)^2 = 0$.

They correspond to the time reversals in Euclidean and Minkowski space. Under time reversals, x_{ij}^2 takes its complex conjugate

$$(\theta_E x_i - \theta_E x_j)^2 = (\theta_L x_i - \theta_L x_j)^2 = [(x_i - x_j)^2]^* . \tag{95}$$

Given a configuration $C = (x_1, x_2, x_3, x_4)$, we define the time reversals of the configuration by (notice the change of order of points in $\theta_E C$)

$$\begin{aligned} \theta_E C &= (\theta_E x_4, \theta_E x_3, \theta_E x_2, \theta_E x_1), \\ \theta_L C &= (\theta_L x_1, \theta_L x_2, \theta_L x_3, \theta_L x_4). \end{aligned} \tag{96}$$

Then the following properties are easily checked:

- The sets \mathcal{D} , \mathcal{D}_E and \mathcal{D}_L are preserved by θ_E and θ_L .
- Under the transformation $C \mapsto \theta_E C$ or $C \mapsto \theta_L C$, the conformal invariants $u, v, z, \bar{z}, \rho, \bar{\rho}$ become their complex conjugates.

Suppose we have a path γ from $\mathcal{D}_E \setminus \Gamma$ to \mathcal{D}_L . Then $\theta_E \gamma$ and $\theta_L \gamma$ are still paths from $\mathcal{D}_E \setminus \Gamma$ to \mathcal{D}_L . The curves of z, \bar{z} are reflected with respect to the real axis, which implies

$$\begin{aligned} N_t(\theta_E \gamma), N_t(\theta_L \gamma) &= -N_t(\gamma), \\ N_u(\theta_E \gamma), N_u(\theta_L \gamma) &= -N_u(\gamma). \end{aligned} \tag{97}$$

By theorem 4.1, 4.4 and 4.6, we conclude that

- Different Lorentzian configurations which are related by θ_E, θ_L have the same convergent OPE channels.

By lemma 5.1 and theorem 5.2, we translate the above results to the level of causal orderings:

- If two different sets $\mathcal{D}_L^\alpha, \mathcal{D}_L^\beta$ are related by θ_E, θ_L , then they belong to the same class (S, T, U, E).
- If two different sets $\mathcal{D}_L^\alpha, \mathcal{D}_L^\beta$ are in class S or T or U and are related by θ_E, θ_L , then they have the same convergent OPE channels.
- If two different sets $\mathcal{D}_L^\alpha, \mathcal{D}_L^\beta$ are in class E and are related by θ_E, θ_L , then their intersections with each subclass have the same convergent OPE channels.

Given a Lorentzian configuration $C = (x_1, x_2, x_3, x_4)$, θ_E interchanges $x_1 \leftrightarrow x_4$ and $x_2 \leftrightarrow x_3$. At the level of causal orderings, θ_E is the permutation of indices

$$1 \leftrightarrow 4, \quad 2 \leftrightarrow 3, \tag{98}$$

with all the arrows kept fixed. For example, under θ_E we have

$$1 \longrightarrow 2 \begin{cases} \nearrow 3 \\ \searrow 4 \end{cases} \Rightarrow 4 \longrightarrow 3 \begin{cases} \nearrow 2 \\ \searrow 1 \end{cases} . \tag{99}$$

Under θ_L , the Lorentzian configuration $x_k = (it_k, \mathbf{x}_k)$ is mapped to $C' = (x'_1, x'_2, x'_3, x'_4)$ with

$$x'_k = \theta_L x_k = (-it_k, \mathbf{x}_k), \quad k = 1, 2, 3, 4. \tag{100}$$

So the operator ordering does not change but the causal ordering is reversed. For example, under θ_L we have

$$\begin{array}{c}
 & & 3 & & \\
 & \nearrow & & \nwarrow & \\
 1 & \longrightarrow & 2 & & 3 \\
 & \searrow & & \swarrow & \\
 & & 4 & &
 \end{array}
 \Rightarrow
 \begin{array}{c}
 & & 3 & & \\
 & \nwarrow & & \swarrow & \\
 1 & \longleftarrow & 2 & & 3 \\
 & \swarrow & & \nwarrow & \\
 & & 4 & &
 \end{array}
 . \tag{101}$$

By definitions (94) and (96), we have the following properties for θ_E, θ_L :

$$\theta_E^2 = id, \quad \theta_L^2 = id, \quad \theta_E \theta_L = \theta_L \theta_E. \tag{102}$$

So the group generated by θ_E, θ_L is $\mathbb{Z}_2 \times \mathbb{Z}_2$. Under the $\mathbb{Z}_2 \times \mathbb{Z}_2$ -actions, the orbit of a given causal ordering contains 1 or 2 or 4 causal orderings. In each orbit, it suffices to check the OPE convergence properties of only one causal ordering and make the same conclusions for other causal orderings. This simplifies our work.

5.5 The table of four-point causal orderings

Given two Lorentzian configurations (x_1, \dots, x_n) and (y_1, \dots, y_n) , we say that they are in the same causal type if there is a permutation $\sigma \in S_n$ such that $(x_{\sigma(1)}, \dots, x_{\sigma(n)})$ has the same causal ordering as (y_1, \dots, y_n) or $(\theta_L y_1, \dots, \theta_L y_n)$.

In table 2, we give a classification of four-point causal orderings according to the causal types. The vertices labelled by a, b, c, d can be any permutation of $1, 2, 3, 4$. In the end we will give a table about OPE convergence properties for each causal type in table 2. Each causal type thus represents at most $4! \times 2$ causal orderings ($4!$ for possible assignments of $1, 2, 3, 4 \rightarrow a, b, c, d$ and $\times 2$ for two columns). This maximal number is realized for type 3, while for other types it is smaller because often second column is equivalent to the first and because of little group (see appendix C.0.3).

It makes sense to do this grouping of causal orderings into causal types for two reasons:

- causal orderings related by θ_E and θ_L action (and which thus have same OPE convergence properties) belong to the same causal type.
- if we know class/subclass of \mathcal{D}_L^α for one α in a given causal type, it is easy to determine the class/subclass of any other \mathcal{D}_L^α in the same causal type (see appendix C.0.1).

5.6 Examples

The tables which classify the OPE convergence properties will be particularly large, we leave them in appendix C. Readers can pick the cases they are interested in. To make it easy for readers to check, we also share the Mathematica code which contain the OPE convergence results of all causal orderings, see the file “/anc/OPE_check.nb”. In this section we only give some examples.

The Lorentzian four-point correlation functions defined in (2) are either (maximally) time-ordered ($t_1 > t_2 > t_3 > t_4$) or out of time order (not $t_1 > t_2 > t_3 > t_4$). The time-ordered correlators have applications in scattering theories [45, 46], and the out-of-time-order correlation functions have applications in the study of many-body systems [47–54]. An example in [36] shows the existence of out-of-time-order correlators which do not have a convergent OPE channel (see appendix A in [36]).²² Our first example is the case of time-ordered correlator. We will see that time-ordered correlators at different causal orderings may have different OPE convergence properties.

²²By “a configuration do not have a convergent OPE channel” we mean the configuration do not satisfy the conditions of theorem 4.1, 4.4 and 4.6.

Table 2: Classification of four-point causal orderings

Type No.	causal ordering	θ_L time reversal
1	$a \rightarrow b \rightarrow c \rightarrow d$	same
2	$a \rightarrow b \begin{cases} \nearrow c \\ \searrow d \end{cases}$	$\begin{cases} c \searrow \\ d \nearrow \end{cases} b \rightarrow a$
3	$a \begin{cases} \rightarrow b \\ \searrow d \end{cases} \rightarrow c$	$c \rightarrow b \begin{cases} \rightarrow a \\ \nearrow d \end{cases}$
4	$a \begin{cases} \nearrow b \\ \searrow c \end{cases} \rightarrow d$	same
5	$a \begin{cases} \nearrow b \\ \rightarrow c \\ \searrow d \end{cases}$	$\begin{cases} b \searrow \\ c \rightarrow \\ d \nearrow \end{cases} a$
6	$a \rightarrow b \rightarrow c$ d	same
7	$a \begin{cases} \nearrow b \\ \searrow c \end{cases}$ d	$\begin{cases} b \searrow \\ c \nearrow \end{cases} a$ d
8	$a \begin{cases} \nearrow b \\ \searrow d \end{cases}$ $c \nearrow d$	same
9	$a \rightarrow b$ c d	same
10	$a \begin{cases} \nearrow c \\ \rightarrow d \end{cases}$ $b \begin{cases} \nearrow c \\ \rightarrow d \end{cases}$	same
11	$a \rightarrow b$ $c \rightarrow d$	same
12	$a \quad b \quad c \quad d$	same

The second example is to clarify that two conformally equivalent configurations/causal orderings may have different OPE convergence properties.

Then we will discuss two other examples from AdS/CFT. One is the Regge kinematics [55, 56], the other is related to the bulk-point singularities [12].

5.6.1 General time-ordered correlation functions

In this example, we would like to consider the general Lorentzian four-point functions with the maximal time ordering:

$$G_4^L(x_1, x_2, x_3, x_4) = \langle 0 | \phi(x_1) \phi(x_2) \phi(x_3) \phi(x_4) | 0 \rangle, \tag{103}$$

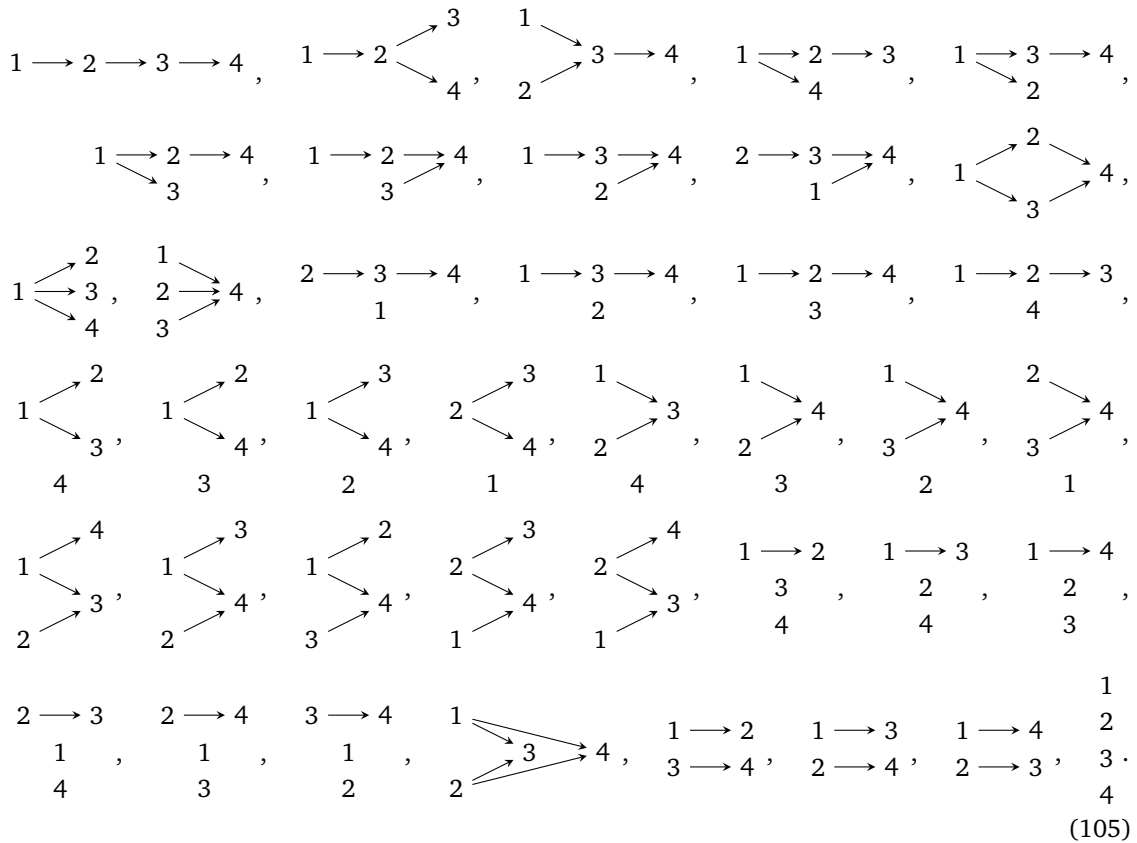
$$x_k = (t_k, \mathbf{x}_k), \quad t_1 > t_2 > t_3 > t_4,$$

where $G_4^L(x_1, x_2, x_3, x_4)$ is the same as in eq. (2). Since Lorentzian correlator is the boundary value of the analytic function on domain \mathcal{D} , it does not depend on our choice of the path (but we should keep the ordering of the Euclidean times until we reach the Lorentzian configuration). A simple way to obtain the Lorentzian correlator is by the so-called “ ϵ -prescription”:

$$x_1 = (t_1, \mathbf{x}_1), \quad x_2 = (t_2 - i\epsilon, \mathbf{x}_2), \quad x_3 = (t_3 - 2i\epsilon, \mathbf{x}_3), \quad x_4 = (t_4 - 3i\epsilon, \mathbf{x}_4), \quad \epsilon \rightarrow 0^+. \tag{104}$$

Here ϵ plays the role of the Euclidean time difference. Then one can check whether G_4^L exists in the sense of functions in such a limit.

According to theorem 5.2, the OPE convergence properties are determined by the causal ordering and (in a special case) the range of cross-ratios. For time-ordered four-point functions, we have 40 possible causal orderings compatible with the maximal time ordering. Here we list all of them according to table 2:



Reader can look up the OPE convergence properties of these causal orderings in the tables in appendix C. The way how to look up these tables is shown at the beginning of appendix C.

Here we pick two of the above causal orderings.

Example (a). The simplest example of the time-ordered configuration is the first case in (105):

$$1 \rightarrow 2 \rightarrow 3 \rightarrow 4. \tag{106}$$

This causal ordering belongs to causal type 1 in table 2. By comparing it with the template causal ordering (195), we see that it corresponds to the sequence “(1234)”. Then we look up the convergence properties of “(1234)” in table 5. We see that for this causal ordering, the s-channel and t-channel OPEs are convergent, while the u-channel OPE is not convergent.

Example (b). The second example is the following causal ordering (the second one in the fourth row of (105)):

$$\begin{array}{c}
 & & 3 \\
 & \nearrow & \\
 1 & & \\
 & \searrow & \\
 & & 4 \\
 & \nearrow & \\
 2 & &
 \end{array}
 \tag{107}$$

This causal ordering belongs to causal type 8 in table 2. By comparing it with the template causal ordering (210), we see that it corresponds to the sequence “(1324)” in table 12. Then by looking up table 12, we conclude that there is no convergent OPE channel for this causal ordering. As a consistency check, one can also pick a representative configuration of this causal ordering:

$$x_1 = (0, 0), \quad x_2 = (-0.1, 1), \quad x_3 = (-2, -1.5), \quad x_4 = (-2.1, 1.5). \tag{108}$$

We choose a start point in $\mathcal{D}_E \setminus \Gamma$ and a path to compute the z, \bar{z} -curves. Figure 5.4 shows the z, \bar{z} -curves along the path.²³

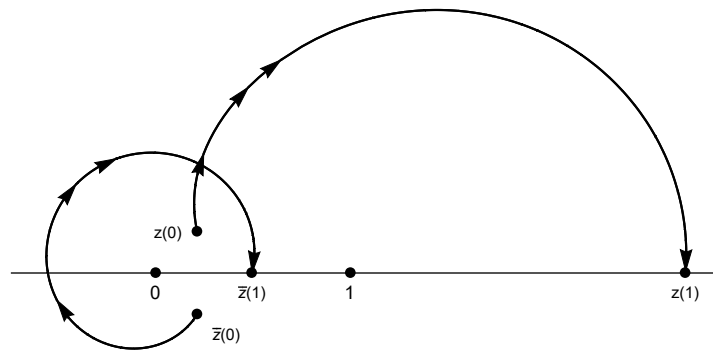


Figure 5.4: z, \bar{z} -curves of the configuration (108).

We see from figure 5.4 that $z > 1, 0 < \bar{z} < 1$ at the final point, which implies that the configuration (108) is in class T (i.e. only the t-channel OPE has a chance to converge). The curve of z variable crosses $(-\infty, 0)$ from below, which gives $N_t = -1$. So the t-channel OPE (the only undetermined case by table 1) is not convergent. Thus, as already mentioned, there is no convergent OPE channel for the four-point function at this causal ordering. This example shows that not all time-ordered correlation functions have a convergent OPE channel.

From the above two examples, we see that the OPE convergence properties depend not only on time ordering, but also on the causal ordering of the configuration. Actually, the time ordering is not crucial here.

Remark. Readers may find that some of the causal orderings above have the same OPE convergence properties in s-channel, t-channel and u-channel. This is just a coincidence because we only have $2^3 = 8$ possibilities for OPE convergence (3 channels, 2 possibilities for each channel) but 40 causal orderings!

Before finishing this subsection, we would like to comment on another extremal example, which is about the four-point correlators with the maximal out-of-time ordering.

$$\begin{aligned}
 G_4^L(x_1, x_2, x_3, x_4) &= \langle 0 | \phi(x_1) \phi(x_2) \phi(x_3) \phi(x_4) | 0 \rangle, \\
 x_k &= (t_k, \mathbf{x}_k), \quad t_1 < t_2 < t_3 < t_4.
 \end{aligned}
 \tag{109}$$

²³We choose the start point $x_1^E = (0, -0.8), x_2^E = (-1, -0.2), x_3^E = (-2, -0.6)$ and $x_4^E = (-3, -0.3)$. The path is given by the straight line.

As discussed in section 5.4, if two causal orderings are related by some time-reversal operation, their OPE convergence properties are the same. We know that the time-reversal operation θ_L (defined by $(t, \mathbf{x}) \mapsto (-t, \mathbf{x})$) gives a one-to-one correspondence between time-ordered configurations and maximally-out-of-time-order configurations. At the level of causal orderings, this operation reverses all the arrows in eq. (105). Once we know the OPE convergence properties of all the time-ordered correlators, we immediately make the same conclusion for all the maximally-out-of-time-order correlators.

5.6.2 Conformally equivalent causal orderings

As mentioned in section 5.2, causal orderings may be violated by special conformal transformations. As a consequence, there are different causal orderings which have the same range of cross-ratios z and \bar{z} . However, being in the same conformal equivalence class does not guarantee that they have the same OPE convergence properties.

To see a counter example, we consider the following two causal orderings:

$$1 \rightarrow 2 \rightarrow 3 \rightarrow 4 \quad \& \quad 2 \rightarrow 1 \rightarrow 4 \rightarrow 3. \tag{110}$$

One can check that any configuration with the second causal ordering can be mapped to a configuration with the first causal ordering via some Lorentzian conformal transformation, and vice versa. A simple consistency check is that $0 < z, \bar{z} < 1$ in both cases.

By looking up table 5, we see that the four-point function has convergent s-channel and t-channel OPEs at configurations with the first causal ordering, while it has only convergent s-channel OPE at configurations with the second causal ordering.

This example shows that two causal orderings may have different OPE convergence properties even if they are conformally equivalent to each other.

5.6.3 Regge kinematics

The second example is the Lorentzian four-point function in the Regge regime [55–57]. Let x_1, x_4 and x_2, x_3 pairs be time-like separated, while other pairs be space-like separated (see figure 5.5).

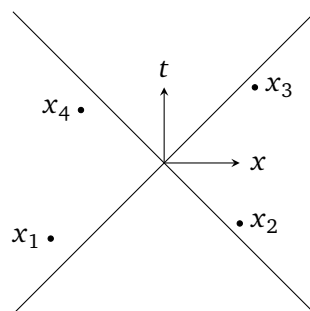


Figure 5.5: Regge kinematics.

It is well known that the four-point function at Regge kinematics only has convergent t-channel expansion [55]. Here we just review this result. The causal ordering of the Regge kinematics is given by

$$\begin{aligned} 1 &\rightarrow 4 \\ 2 &\rightarrow 3 \end{aligned} \tag{111}$$

The Regge kinematics belongs to causal type 11 in table 2. Let us look up this causal ordering in appendix C.11. The causal ordering (111) corresponds to the label “(1423)” in table 15. We see that only t-channel OPE is convergent.

We would like to also choose a representative configuration and a path to compute the curves of z, \bar{z} . The plot is given by figure 5.6.²⁴

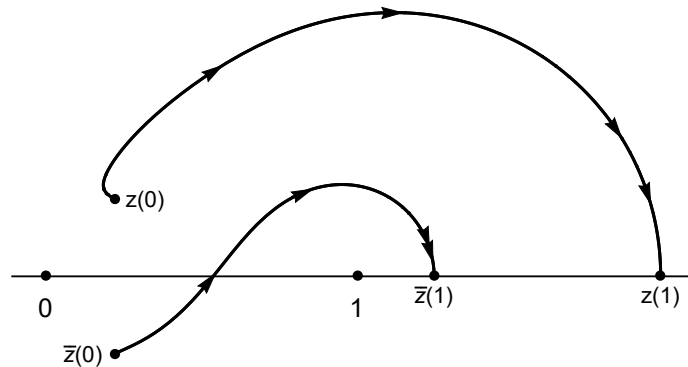


Figure 5.6: The plot of z, \bar{z} -curves of the Regge kinematics.

We see from figure 5.6 that $z, \bar{z} > 1$ at the final point,²⁵ which implies that the Regge kinematics is in class E. In fact the Regge kinematics can only be in the subclass E_{tu} , where $z, \bar{z} > 1$ [55], so only t- and u-channel expansions have a chance to converge. We see from figure 5.6 that the \bar{z} -curve crosses $(0, 1)$ from below, and z, \bar{z} -curves do not cross $(-\infty, 0)$. So we get

$$N_t = 0, \quad N_u = -1, \tag{112}$$

which implies that only the t-channel expansion is convergent.

5.6.4 Causal ordering of bulk-point singularities

The third example is as follows. Let x_1, x_2 and x_3, x_4 pairs be space-like separated. We put the x_1, x_2 pair in the open backward light-cone of some base point and x_3, x_4 pair in the open forward light-cone of the base point (see figure 5.7).

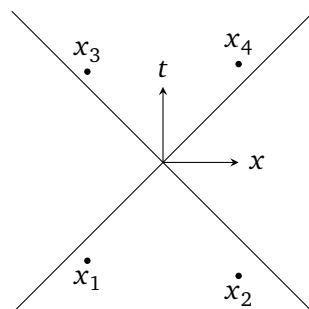


Figure 5.7: Configuration of example 3.

²⁴We choose the Euclidean configuration $x_1 = 0, x_2 = (-1, 0, 0, 0), x_3 = (-2, 0.9, 0, 0), x_4 = (-4, 0, 0, 0)$ and the representative Lorentzian configuration $y_1 = 0, y_2 = (0, 0, 0.6, 0), y_3 = (2i, 0, 0, 0.7), y_4 = (2i, -0.05, 0, -3)$. We choose the path to be the straight line between them.

²⁵The definition of z, \bar{z} in [55] is different from this paper. In their work, $0 < z, \bar{z} < 1$ at Regge kinematics, while in this paper, $z, \bar{z} > 1$. One can compare the definitions and get the relation of z, \bar{z} between [55] and our work: $z \rightarrow 1/z, \bar{z} \rightarrow 1/\bar{z}$.

Such configurations have the causal ordering

$$\begin{array}{c}
 1 \\
 \swarrow \searrow \\
 3 \\
 \swarrow \searrow \\
 2 4
 \end{array}
 . \tag{113}$$

The causal ordering (113) is of causal type 10 in table 2. We look up the OPE convergence properties in appendix C.10. The causal ordering (113) corresponds to the label “(1234)” in table 14. We see that this causal ordering is in class E, which has four subclasses. From table 14 we also see that the configurations with the causal ordering (113) exist in each subclass. We wish to consider the subclass E_{ut} , where $z, \bar{z} > 1$. In table 14, we see that the configurations with causal ordering (113) and in subclass E_{ut} have no convergent OPE channels.

Let us also choose a representative configuration to check this result. We want to remark that such case does not exist in 2d (see appendix C.10 for the proof). We choose the following three-dimensional configuration

$$x_1 = (0, 0, 0), \quad x_2 = (0, 1, 0), \quad x_3 = (i, 0.2, 0.5), \quad x_4 = (i, 0.5, 0.8). \tag{114}$$

Figure 5.8 shows the plot of z, \bar{z} -curves.

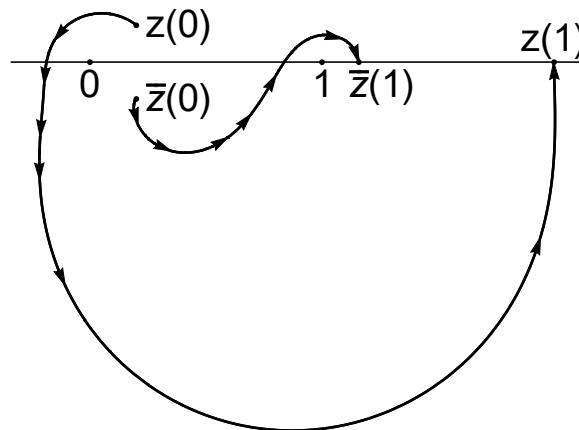


Figure 5.8: The plot of z, \bar{z} -curves of the configuration (114).

We see that along the path, z crosses the interval $(-\infty, 0)$ and \bar{z} crosses the interval $(0, 1)$. We get

$$N_t = 1, \quad N_u = -1, \tag{115}$$

which implies that the t- and u-channel expansions do not converge.

We conclude that there is no convergent OPE channel for the causal ordering (113) with $z, \bar{z} > 1$.

Here we give a hint why this example is related to the bulk-point singularities in AdS/CFT [12]. The bulk-point singularities are not exactly the configurations in Minkowski space $\mathbb{R}^{d-1,1}$, instead they are configurations on the Minkowski cylinder $\mathbb{R} \times S^{d-1}$ [58]. The Minkowski space can be embedded into a patch of the Minkowski cylinder in a Weyl equivalent way, this patch is called the Poincaré patch [59]. The Minkowski cylinder also admits a causal ordering which is equivalent to the causal ordering of the Minkowski space in the Poincaré patch [60, 61]. One can show the following facts:

- The bulk-point singularities have the causal ordering (113) and $z, \bar{z} > 1$.

- One can find a path from an arbitrary bulk-point singularity to a configuration in the Poincaré patch, such that the causal ordering (113) is preserved along the path.
- The CFT four-point function in the Poincaré patch is the same as the CFT four-point function in the Minkowski space up to a scaling factor.²⁶

Based on the above facts, the OPE convergence properties of the bulk-point singularities are exactly the same as this example: there is no convergent OPE channel. More details will be given in [38]. Our result does not contradict the two-dimensional result in [12] (see the beginning of section 5.3.2) because here we only use the global conformal symmetry instead of the Virasoro symmetry.

5.6.5 Digression

We can see from figure 5.4, 5.6 and 5.8 that the z, \bar{z} -curves do not touch the interval $(1, +\infty)$ until the end. One can also see this phenomenon by picking representative configurations of other causal orderings and compute the z, \bar{z} -curves. This numerical observation is consistent with theorem 3.1.

6 Wightman functions: a brief review

In this section we will review some classical results about regular points (points where Wightman distributions are genuine functions) in a general QFT [5, 6, 62]. For simplicity let us still consider a scalar theory in the Minkowski space, which is characterized by a collection of Lorentzian correlators:

$$\mathcal{W}_n(x_1, x_2, \dots, x_n) := \langle 0 | \phi(x_1)\phi(x_2)\dots\phi(x_n) | 0 \rangle, \tag{116}$$

where x_i are Lorentzian coordinates.²⁷ We will introduce the Wightman axioms for QFTs, and then review the domain of correlation functions which can be derived from Wightman axioms. In the end, we will compare these classical results with our results for CFT four-point functions.

This section is logically independent from the rest of the paper. Here we assume Wightman axioms while in the rest we did not. The only connection is to justify the definition of Wick rotation (steps 1 and 2 in section 2.1).

6.1 Wightman axioms for Lorentzian correlators

We assume the Wightman axioms for correlators $\{\mathcal{W}_n\}$:

(W1) Temperedness.

\mathcal{W}_n is a tempered distribution (called Wightman distribution). It becomes a complex number after being smeared with rapidly decreasing test functions f_n :

$$\mathcal{W}_n(f_n) = \int f(x_1, \dots, x_n) \mathcal{W}_n(x_1, \dots, x_n) dx_1 \dots dx_n. \tag{117}$$

The Fourier transform $\hat{\mathcal{W}}_n$ of \mathcal{W}_n is well defined since the space of rapidly decreasing test functions (Schwartz space) is closed under Fourier transform [63]. One has the definition $\hat{\mathcal{W}}_n(f_n) := \mathcal{W}_n(\hat{f}_n)$.

²⁶The definition of the CFT four-point function on the Minkowski cylinder is similar to Minkowski space. We replace the planar time variables τ_k by the cylindrical time variables. Then do Wick rotations.

²⁷In the rest of the paper we the Lorentzian points were denoted by (it_k, \mathbf{x}_k) . Only in this section we use the notation $x_k = (t_k, \mathbf{x}_k)$.

(W2) Poincaré invariance.

The correlators transform invariantly under action of the Poincaré group:

$$\mathcal{W}_n(g \cdot x_1, \dots, g \cdot x_n) = \mathcal{W}_n(x_1, \dots, x_n), \tag{118}$$

for all $n \geq 0$ and g in the Poincaré group.

(W3) Unitarity.

The vector space generated by the states of the form

$$\Psi(\underline{f}) = \sum_{n \geq 0} \int f_n(x_1, \dots, x_n) \phi(x_1) \dots \phi(x_n) |0\rangle dx_1 \dots dx_n, \tag{119}$$

has a non-negative inner product. Here f is an arbitrary finite sequence of complex valued Schwartz functions: $\underline{f} = (f_0, f_1, f_2, \dots)$ and \overline{f}_n denotes the Schwartz function with n Lorentzian points as variables. If we assume that $\phi(x)$ are Hermitian operators, i.e. $[\phi(x)]^\dagger = \phi(x)$, then the unitarity condition is written as

$$\sum_{n,m} \int \overline{f_n(x_1, \dots, x_n)} f_m(y_1, \dots, y_m) \mathcal{W}_{n+m}(x_n, \dots, x_1, y_1, \dots, y_m) dx dy \geq 0, \tag{120}$$

(W4) Spectral condition.

The open forward light-cone V_+ is defined by the collection of vectors $x \in \mathbb{R}^d$ such that

$$x^0 > \sqrt{\sum_{\mu \geq 1} (x^\mu)^2}. \tag{121}$$

In a general QFT we have self-adjoint momentum operators P^μ . The spectral condition says that the spectrum of $P = (P^0, P^1, \dots, P^{d-1})$ is inside the closed forward light-cone \overline{V}_+ , and the normalized eigenvector of $P = 0$ is unique (up to a phase factor), denoted by $|0\rangle$.

We define the reduced correlators W_{n-1} by

$$W_n(x_2 - x_1, \dots, x_{n+1} - x_n) = \mathcal{W}_{n+1}(x_1, \dots, x_{n+1}). \tag{122}$$

Since \mathcal{W}_{n+1} is a translational invariant tempered distribution, W_n is well defined and is also a tempered distribution. The spectral condition implies that the Fourier transforms \hat{W}_n of W_n is supported in the forward light-cone. That is to say, $\hat{W}_n(p_1, \dots, p_n) \neq 0$ only if all the momentum variables p_k are inside \overline{V}_+ .

(W5) Microscopic causality.

$\mathcal{W}_n(x_1, \dots, x_k, x_{k+1}, \dots, x_n) = \mathcal{W}_n(x_1, \dots, x_{k+1}, x_k, \dots, x_n)$ if x_k and x_{k+1} are space-like separated.

6.2 Wightman functions and their domains

6.2.1 Forward tube

Let us consider the “reduced correlator” W_n defined in eq. (122). W_n has Fourier transform

$$W_n(x_1, \dots, x_n) = \int \frac{dp_1}{(2\pi)^d} \dots \frac{dp_n}{(2\pi)^d} \hat{W}_n(p_1, \dots, p_n) e^{-i(p_1 \cdot x_1 + \dots + p_n \cdot x_n)}, \tag{123}$$

where \hat{W}_n is also a tempered distribution, and the Lorentzian inner product is defined by $p \cdot x = -p^0 x^0 + p^1 x^1 + \dots + p^{d-1} x^{d-1}$. In general, W_n is not a function if x_k are real. However,

if we replace x_k with complex coordinates $x_k \rightarrow z_k = x_k + iy_k$, because of the spectral condition (W4), $W_n(z_1, \dots, z_n)$ is indeed a function if the imaginary parts of z_k belong to V_+ . The argument is as follows. Suppose $y_k \in V_+$ for all $k = 1, 2, \dots, n$, then there exists a Schwartz function $f(p_1, \dots, p_n)$ in the momentum space such that $f(p_1, \dots, p_n) = e^{-i(p_1 \cdot z_1 + \dots + p_n \cdot z_n)}$ when all the momentum variables p_k are inside the closure of forward light-cone.²⁸ Since \hat{W}_n is supported in $\overline{V_+^n}$, $\hat{W}_n(f)$ is exactly in the form of (123) with x_k replaced by z_k . So $W_n(z_1, \dots, z_n)$ is a well-defined complex number when $Im(z_k) \in V_+$ for all k .

Furthermore, since $-i(p_k)_\mu f(p_1, \dots, p_n)$ is also a Schwartz test function, we have

$$\frac{\partial}{\partial z_k^\mu} W_n(z_1, \dots, z_n) = \hat{W}_n[-i(p_k)_\mu f], \tag{124}$$

$$k = 1, \dots, n \text{ and } \mu = 0, \dots, d-1.$$

As a result $W_n(z_1, \dots, z_n)$ is an analytic function inside the “forward tube”, denoted as I_n

$$I_n = \left\{ (z_1, \dots, z_n) \in \mathbb{C}^{nd} \mid Im(z_k) \in V_+, k = 1, 2, \dots, n \right\}. \tag{125}$$

The distribution $W_n(x_1, \dots, x_n)$ is the boundary value of the analytic function $W_n(z_1, \dots, z_n)$ on the forward tube I_n :

$$W_n(x_1, \dots, x_n) = \lim_{\substack{y \rightarrow 0 \\ y \in V_+^n}} W_n(x_1 + iy_1, \dots, x_n + iy_n). \tag{126}$$

6.2.2 Bargmann-Hall-Wightman theorem, extended tube

Now let us use the Lorentz invariance (W2) to analytically continue W_n to a larger domain. By (W2), W_n is invariant under the action of real Lorentz group $SO^+(1, d-1)$:²⁹

$$W_n(g \cdot x_1, \dots, g \cdot x_n) = W_n(x_1, \dots, x_n), \quad \forall g \in SO^+(1, d-1). \tag{127}$$

The Lorentz transformations preserve the inner product $p_k \cdot x_k$ and the measure dx_k , so the Fourier transform \hat{W}_n is also Lorentz invariant

$$W_n(g \cdot p_1, \dots, g \cdot p_n) = W_n(p_1, \dots, p_n), \quad \forall g \in SO^+(1, d-1). \tag{128}$$

Since $W_n(z_1, \dots, z_n)$ is defined by the Fourier transform (123) (replace x_k with z_k), we have

$$W_n(g \cdot z_1, \dots, g \cdot z_n) = W_n(z_1, \dots, z_n), \quad \forall g \in SO^+(1, d-1). \tag{129}$$

Here we remark that the real Lorentz group actions preserve the forward tube I_n .

An important observation is that (129) remains true if we replace the real Lorentz group $SO^+(1, d-1)$ by the proper complex Lorentz group $L_+(\mathbb{C})$.³⁰ Given an arbitrary $g \in L_+(\mathbb{C})$, we define

$$W_n^g(z_1, \dots, z_n) := W_n(g^{-1} \cdot z_n, \dots, g^{-1} \cdot z_1), \tag{130}$$

²⁸The crucial point is that if all y_k are inside the forward light-cone, then $f(p_1, \dots, p_n)$ decays exponentially fast when some p_k goes to infinity inside the forward light-cone.

²⁹By $SO^+(1, d-1)$ we mean the connected component of the identity element in $O(1, d-1)$.

³⁰Let d be the spacetime dimension. The complex Lorentz group $L(\mathbb{C})$ is defined by the set of all $d \times d$ complex matrices M such that $M^t \eta M = \eta$. Here $\eta = \text{diag}(-1, 1, \dots, 1)$ is the matrix of Lorentzian inner product, and M^t is the transpose of M . $L_+(\mathbb{C})$ is the subgroup of $L(\mathbb{C})$ with constraint $\det M = 1$. $L_+(\mathbb{C})$ is connected, unlike the real case where we need to introduce the constraints “proper”, “orthochronous” for connectedness.

for $(z_1, \dots, z_n) \in gI_n$. The Bargmann-Hall-Wightman theorem [64] tells us that if we choose different complex Lorentz group elements g_1, g_2 , the functions $W_n^{g_1}$ and $W_n^{g_2}$ coincide in the domain $g_1I_n \cap g_2I_n$. So $W_n(z_1, \dots, z_n)$ has analytic continuation to the “extended forward tube”, denoted by \tilde{I}_n :

$$\tilde{I}_n := \left\{ (z_1, \dots, z_n) \in \mathbb{C}^{nd} \mid (g \cdot z_1, \dots, g \cdot z_n) \in I_n \text{ for some } g \in L_+(\mathbb{C}) \right\}. \quad (131)$$

Here we only give the idea of the proof. It suffices to show that for any $g \in L_+(\mathbb{C})$, the function W_n^g coincides with W_n in the domain $gI_n \cap I_n$. Since I_n and gI_n are two convex sets, their intersection $gI_n \cap I_n$ is also convex, thus connected. So it suffices to show that W_n^g coincides with W_n in the neighbourhood of one point. This is obvious for g near the identity element, but the proof for an arbitrary g is based on the fact that the set $\{g \in L_+(\mathbb{C}) \mid gI_n \cap I_n \neq \emptyset\}$ is connected, which follows from the group structure of the complex Lorentz group $L_+(\mathbb{C})$ (for more details, see [1]).

6.2.3 Jost points

While I_n does not contain Lorentzian points (i.e. points with $\text{Im}(z_k) = 0$ for all k), \tilde{I}_n contains a region of Lorentzian points. These points are called Jost points [6], and they are defined by the configurations (x_1, \dots, x_n) such that the following cone

$$\left\{ \lambda_1 x_1 + \dots + \lambda_n x_n \mid \lambda_k \geq 0 \text{ for all } k, \sum_{k=1}^n \lambda_k > 0 \right\}, \quad (132)$$

contains only space-like points (see [1], the theorem on page 81 and the corollary on page 82).

6.2.4 Microscopic causality, envelope of holomorphy

Now let us go back to $\mathcal{W}_n(x_1, \dots, x_n)$ via (122). We define \mathcal{J}_n as the set of (x_1, \dots, x_n) such that $(x_2 - x_1, \dots, x_n - x_{n-1})$ are Jost points. The configurations in \mathcal{J}_n have totally space-like separations. To see this we rewrite $x_i - x_j$ ($i > j$) as

$$x_i - x_j = (x_i - x_{i-1}) + (x_{i-1} - x_{i-2}) + \dots + (x_{j+1} - x_j), \quad (133)$$

which is in the form of (132). By the definition of Jost points, we have $(x_i - x_j)^2 > 0$ for $i \neq j$. It is obvious that \mathcal{J}_2 contains all totally space-like configurations. For $n \geq 3$, \mathcal{J}_n does not contain all totally space-like configurations.

Since Jost points are the configurations with totally space-like separations, by the microscopic causality condition (W5), $\mathcal{W}_n(x_1, \dots, x_n)$ is also regular at (x_1, \dots, x_n) if there exists a permutation $\sigma \in S_n$ such that

$$(x_{\sigma(1)}, x_{\sigma(2)}, \dots, x_{\sigma(n)}) \in \mathcal{J}_n. \quad (134)$$

Then the equation $\mathcal{W}_n(x_1, \dots, x_n) = \mathcal{W}_n(x_{\sigma(1)}, \dots, x_{\sigma(n)})$ in \mathcal{J}_n can be analytically continued to

$$\mathcal{W}_n(z_1, \dots, z_n) = \mathcal{W}_n(z_{\sigma(1)}, \dots, z_{\sigma(n)}), \quad (z_2 - z_1, \dots, z_n - z_{n-1}) \in \tilde{I}_{n-1}. \quad (135)$$

Therefore, \mathcal{W}_n has analytic continuation to the following domain of complex coordinates (z_1, \dots, z_n) :

$$\mathcal{U}_n = \left\{ (z_1, \dots, z_n) \in \mathbb{C}^{nd} \mid \exists \sigma \in S_n \text{ s.t. } (z_{\sigma(2)} - z_{\sigma(1)}, \dots, z_{\sigma(n)} - z_{\sigma(n-1)}) \in \tilde{I}_{n-1} \right\}. \quad (136)$$

\mathcal{U}_n have the following properties:³¹

1. In 2d, \mathcal{U}_n contains all totally space-like configurations.
2. \mathcal{U}_3 contains all totally space-like configurations.
3. In $d \geq 3$ and $n \geq 4$, \mathcal{U}_n does not contain all totally space-like configurations [1].

To show the first property, we use an analogous version of the complex coordinates (44):

$$w_k = \mathbf{x}_k + t_k, \quad \bar{w}_k = \mathbf{x}_k - t_k. \tag{137}$$

Given an arbitrary totally space-like configuration, we have

$$(w_j - w_k)(\bar{w}_j - \bar{w}_k) > 0, \quad (j \neq k), \tag{138}$$

which implies $w_j > w_k, \bar{w}_j > \bar{w}_k$ or $w_j < w_k, \bar{w}_j < \bar{w}_k$. So we can find a permutation σ such that

$$w_{\sigma(k)} < w_{\sigma(k+1)}, \quad \bar{w}_{\sigma(k)} < \bar{w}_{\sigma(k+1)}, \quad k = 1, 2, \dots, n-1. \tag{139}$$

We see from (139) that $w_{\sigma(k+1)} - w_{\sigma(k)}, \bar{w}_{\sigma(k+1)} - \bar{w}_{\sigma(k)}$ are positive, so the cone (132) generated from these vectors only contain points with positive components. Thus the configuration $(x_{\sigma(1)}, \dots, x_{\sigma(n)})$ is in \mathcal{J}_n , or equivalently, (x_1, \dots, x_n) is in \mathcal{U}_n .

To show the second property, we consider the totally space-like three-point configurations in the following form:

$$x_1 = 0, \quad x_2 = (0, 1, 0), \quad x_3 = (a, b, c). \tag{140}$$

To check that all totally space-like configurations are in \mathcal{U}_3 , it suffices to check the totally space-like configurations in the form of (140) because \mathcal{U}_n is Poincaré invariant and scale invariant, and any totally space-like configuration can be mapped to a configuration in the form of (140) by Poincaré transformations and dilatation. If $(x_1, x_2, x_3) \in \mathcal{J}_3$ then we are done. Suppose $(x_1, x_2, x_3) \notin \mathcal{J}_3$, which means that there exists a positive λ such that $\lambda(x_2 - x_1) + (x_3 - x_2)$ is a null vector:

$$a^2 = (b - 1 + \lambda)^2 + c^2. \tag{141}$$

The above equation implies $a^2 \geq c^2$, so there exists a Lorentz transformation which maps the configuration (140) to

$$x'_1 = 0, \quad x'_2 = (0, 1, 0), \quad x'_3 = (a', b, 0). \tag{142}$$

We see that the problem is reduced to the 2d case. According second property, the configuration (142) is in \mathcal{U}_3 . So we conclude that all totally space-like configurations are in \mathcal{U}_3 .

To show the third property, it suffices to give a counterexample for $d = 3$ and $n = 4$:

$$\begin{aligned} x_1 &= (1 - \epsilon, 1, 1), & x_2 &= (1 - \epsilon, -1, -1), \\ x_3 &= (\epsilon - 1, 1, -1), & x_4 &= (\epsilon - 1, -1, 1), \end{aligned} \tag{143}$$

where $\epsilon > 0$ is small. (143) is a totally space-like configuration but it does not belong to \mathcal{U}_4 (see [1], p. 89).

\mathcal{W}_n has analytic continuation from \mathcal{U}_n to its envelope of holomorphy $H(\mathcal{U}_n)$ [65], which is defined by the following property:

- Any holomorphic function on \mathcal{U}_n has analytic continuation to $H(\mathcal{U}_n)$.

A theorem proved by Ruelle [7] shows that $H(\mathcal{U}_n)$ contains all totally space-like configurations.

We conclude that Wightman distributions $\mathcal{W}_n(x_1, \dots, x_n)$ are analytic functions at all totally space-like configurations.

³¹We were unable to track properties 1,2 in prior literatures. Readers are welcome to provide us with references.

6.3 Comparison with CFT

6.3.1 Justifying the definition of Wick rotation

In section 3 of this paper, we used CFT arguments (not using Wightman axioms) to show that the CFT four-point function is analytic in the domain \mathcal{D} , where only the temporal variables are complex numbers (see section 2.1). Consider the points $(x_2 - x_1, x_3 - x_2, x_4 - x_3)$ where $(x_1, \dots, x_4) \in \mathcal{D}$. The notation we use in the rest of the paper is $x_k = (\epsilon_k + it_k, \mathbf{x}_k)$, so we have

$$x_{k+1} - x_k = (\epsilon_{k+1} - \epsilon_k + it_{k+1} - it_k, \mathbf{x}_{k+1} - \mathbf{x}_k). \tag{144}$$

By translating (144) to the notation in this section (see footnote 27), we have

$$x_{k+1} - x_k = (t_{k+1} - t_k, \mathbf{x}_{k+1} - \mathbf{x}_k) + i(\epsilon_k - \epsilon_{k+1}, 0). \tag{145}$$

We see from (145) that the points $(x_2 - x_1, x_3 - x_2, x_4 - x_3)$ are in the forward tube I_3 if $(x_1, x_2, x_3, x_4) \in \mathcal{D}$ (because $\epsilon_1 > \epsilon_2 > \epsilon_3 > \epsilon_4$). Recalling that the Wightman distributions $\mathcal{W}_n(x_1, \dots, x_n)$ can be obtained by taking the limit of the analytic functions $\mathcal{W}_n(z_1, \dots, z_n)$ from the domain $\{(z_2 - z_1, \dots, z_n - z_{n-1}) \in I_{n-1}\}$, we see that our definition of Wick rotation (2) is consistent with Wightman QFT.

6.3.2 Osterwalder-Schrader theorem

In fact we use the same analytic continuation path as in the Osterwalder-Schrader (OS) theorem [2]. The OS theorem shows that under certain conditions, a Euclidean QFT can be Wick rotated to a Wightman QFT.

In this paper we focus on the domain of analyticity of the four-point function, and we do not explore the distributional properties of it. To show that the limit (2) of the CFT four-point functions defines a Wightman four-point distribution, one needs to deal with the four-point function not only at regular points (where $|\rho|, |\bar{\rho}| < 1$ in s- or t- or u-channel), but also at all the other Lorentzian configurations where ρ and/or $\bar{\rho}$ is 1 in absolute value (this needs a lot of extra work). Readers can go to [37], where we show that Wick rotating a Euclidean CFT four-point function indeed results in a Wightman four-point distribution.

Let us contrast our construction and the OS construction. Our construction extends G_4 in a CFT to domain \mathcal{D} using only information about the four-point function itself. The OS construction can extend G_4 (in fact any G_n) to domain \mathcal{D} in a general QFT. But the price to pay is that analytic continuation involves infinitely many steps and needs information about higher-point functions [3, 4].

We would also like to point out that the OS theorem requires an extra assumption, called the *linear growth condition*. The linear growth condition is introduced as a technical condition for showing that the analytically continued Euclidean correlator is a tempered distribution in the Lorentzian regime. Without this condition, the Euclidean correlator still has analytic continuation to the domain \mathcal{D} (i.e. step 1 in section 2 can still be done). However, since \mathcal{D} does not contain any Lorentzian configurations, one has to take a limit towards the Lorentzian regime from \mathcal{D} . To show such a limit exists in the sense of tempered distributions, one needs to derive some power-law upper bound on the correlator in \mathcal{D} (or \mathcal{T}_4 , the forward tube), and this is where the linear growth condition is used. So far, it is not understood whether the linear growth condition can be derived from basic CFT assumptions (conformal invariance, OPE convergence, unitarity) or not.

6.3.3 Domain of analyticity: Wightman axioms + conformal invariance

Let us summarize how the domains of Wightman functions are derived in Wightman QFT. We first use the temperedness property (W1), translational invariance (W2) and the spectral condition (W4) to show that the reduced Wightman distribution W_n is an analytic function in the forward tube I_n . Then we use the Lorentz invariance (W2) to show that W_n has analytic continuation to the “extended tube” \tilde{I}_n , which includes the set of Jost points. Finally we use the microscopic causality condition (W5) to show that \mathcal{W}_{n+1} has analytic continuation to all configurations with totally space-like separations.

The unitarity condition (W3) is not involved in the above argument, only the conditions (W1), (W2), (W4) and (W5) are used.

In the rest of the paper we explored the domain of CFT four-point functions by assuming unitarity, Euclidean conformal invariance and OPE (not assuming Wightman axioms). Here we would like to discuss a related but different situation:

- What is the domain of the four-point function if we only assume Wightman axioms and conformal invariance (not assuming OPE)?

We want to emphasize that global conformal invariance does not hold for general CFT in $\mathbb{R}^{d-1,1}$ because Lorentzian special conformal transformations may violate causal orderings. The precise meaning of conformal invariance here is the Euclidean global conformal invariance: we Wick rotate Wightman functions to the Euclidean signature, then the corresponding Euclidean correlation functions are invariant under Euclidean global conformal transformations. This assumption is called *weak conformal invariance* [58].

It is obvious that the Wightman function \mathcal{W}_4 is analytic in \mathcal{U}_4 (as discussed in section 6.2). In section 6.2, a crucial step is to extend the real Poincaré invariance to complex Poincaré invariance. Then the reduced Wightman function W_3 has analytic continuation from the forward tube I_3 to the extended forward tube \tilde{I}_3 . Now that we assume weak conformal invariance, given any Euclidean conformal transformation g and Euclidean configuration $C = (x_1, x_2, x_3, x_4)$, we have

$$\begin{aligned} \mathcal{W}_4(C) &= \Omega(x_1)^\Delta \Omega(x_2)^\Delta \Omega(x_3)^\Delta \Omega(x_4)^\Delta \mathcal{W}_4(g \cdot C), \\ g \cdot C &= (g \cdot x_1, g \cdot x_2, g \cdot x_3, g \cdot x_4), \end{aligned} \tag{146}$$

where $\Omega(x)$ is the scaling factor of the conformal transformation. It is not hard to show that given any configuration C (which can be non-Euclidean) in the domain of \mathcal{W}_4 , eq. (146) holds for g in a neighbourhood of the identity element in the Euclidean conformal group (this neighbourhood depends on configuration). Then we can show that for a fixed C , eq. (146) holds not only in a neighbourhood of identity element in the Euclidean conformal group, but also in a neighbourhood in the complex conformal group.³² Therefore, by using (146) with g in the complex conformal group, we can extend \mathcal{W}_4 to a bigger domain than \mathcal{U}_4 (recall definition (136)).³³ We say that configurations $C = (x_1, x_2, x_3, x_4)$, $C' = (x'_1, x'_2, x'_3, x'_4)$ are conformally equivalent if there exists a path $g(s)$ in the complex conformal group such that

- $g(0) = \text{id}$, and $g(1) \cdot C_1 = C_2$.
- The scaling factors $\Omega(x_1), \Omega(x_2), \Omega(x_3), \Omega(x_4)$ along $g(s)$ do not go to 0 or ∞ .

³²The complex conformal group is generated by translations $x \rightarrow x+a$, rotations $x \rightarrow \exp[\alpha^{\mu\nu} M_{\mu\nu}]x$, dilatations $x \rightarrow e^\tau x$, special conformal translations $x \rightarrow x'^\mu = \frac{x^\mu - x^2 b^\mu}{1 - 2b \cdot x + b^2 x^2}$ with complex parameters.

³³This can be called conformal extension of Bargmann-Hall-Wightman theory. We were unable to find this idea in prior literature.

We define

$$\mathcal{U}_4^c = \{C = (x_1, x_2, x_3, x_4) \in \mathbb{C}^{4d} \mid C \text{ is conformally equivalent to some } C' \in \mathcal{U}_4\}, \quad (147)$$

where the superscript “c” in \mathcal{U}_4^c means “conformal”. Naively, one may expect that \mathcal{W}_4 has analytic continuation to \mathcal{U}_4^c by (146).³⁴ However, for each conformally equivalent C, C' pair in \mathcal{U}_4^c , the path $g(s)$ in the complex conformal group is not unique, which means choosing different $g(s)$ may give different analytic continuation. In other words, \mathcal{W}_4 may not be a single-valued function on \mathcal{U}_4^c .

There is one very simple partial case which is guaranteed not to lead to multi-valuedness. It is the case when the whole curve $C(s) = g(s) \cdot C = (x_1(s), x_2(s), x_3(s), x_4(s))$ has point differences $(y_1(s), y_2(s), y_3(s))$ (where $y_k = x_{k+1} - x_k$) in the forward tube I_3 , except for the end point $g(1) \cdot C$.

In this paper we do not fully explore the Lorentzian domain of \mathcal{W}_4 by using the above method. We left it for future work. Here we only give a simple example which shows that by assuming weak conformal invariance in Wightman QFT, the domain of the Wightman function contains more Lorentzian configurations than totally space-like configurations.

We would like to show that the following Lorentzian configurations are in the domain of (conformally invariant) \mathcal{W}_4 :

$$x_k = (t_k, \mathbf{x}_k), \quad 1 \rightarrow 2 \rightarrow 3 \rightarrow 4. \quad (148)$$

We act with complex dilatation on (148):

$$x'_k = e^{i\alpha} x_k. \quad (149)$$

Then the point differences are given by $x'_{jk} = x_{jk} \cos \alpha + ix_{jk} \sin \alpha$. By the causal ordering in (148), we have $(x'_2 - x'_1, x'_3 - x'_2, x'_4 - x'_3) \in I_3$ when $0 < \alpha \leq 1$. On the other hand, the scaling factors of complex dilatations (149) are constants: $\Omega(x) = e^{i\alpha}$, which are finite and non-zero. Thus, we can use the above-mentioned simple partial case. We conclude that the Lorentzian configurations in the form of (148) are in the domain of (conformally invariant) \mathcal{W}_4 .

6.3.4 Domain of analyticity: unitarity + conformal invariance + OPE

Now back to our CFT construction in this paper. We assumed unitarity, conformal invariance and OPE, but did not assume Wightman axioms.

With the help of OPE, we are able to control the upper bound of the CFT four-point function more efficiently [9]. It seems to be rather difficult to apply the unitarity condition (120) in a general Wightman QFT because it is a non-linear constraint. While, in the expansion (22), we are able to use the unitarity condition for CFT four-point functions.

The domain of the Lorentzian CFT four-point function G_4 contains all configurations where there exists at least one convergent OPE channel. The results in appendix C show that the domain of G_4 contains much richer set of causal orderings than just the totally space-like causal ordering obtainable from Wightman axioms alone.

One interesting point is that if we act with conformal transformations on the configurations which have point differences in the forward tube I_3 (let us call this set \mathcal{I}_4), we can get at most Lorentzian configurations whose cross-ratios can be realized by configurations in \mathcal{I}_4 because conformal transformations do not change cross-ratios.³⁵ However, if we additionally assume

³⁴As a next step, one could consider the Lorentzian configurations in envelope of holomorphy $H(\mathcal{U}_4^c)$.

³⁵The similar idea has been used to look for the domain of analyticity of the Wightman functions in a general QFT. E.g. G. Källén explored the domain of the Wightman four-point function by studying configurations (x_1, x_2, x_3, x_4) such that the Poincaré invariants $x_{ij} \cdot x_{kl}$ can be realized by configurations in \mathcal{I}_4 [66].

OPE, then it is not necessary that the cross-ratios of the Lorentzian configurations can be realized by configurations in \mathcal{I}_4 (the only requirement is that $|\rho|, |\bar{\rho}| < 1$ in the corresponding OPE channel). It would be interesting to figure out:

- can we get more Lorentzian configurations by assuming unitarity + conformal invariance + OPE than by assuming Wightman axioms + conformal invariance?

We left it for future work.

7 Four-point functions of non-identical scalar or spinning operators

7.1 Generalization to the case of non-identical scalar operators

In this section we generalize our results of section 3, 4 and 5 to the CFT four-point functions of non-identical scalar operators. We start from a Euclidean CFT four-point function

$$G_{1234}(x_1, x_2, x_3, x_4) := \langle \mathcal{O}_1(x_1)\mathcal{O}_2(x_2)\mathcal{O}_3(x_3)\mathcal{O}_4(x_4) \rangle. \quad (150)$$

The scalar operators \mathcal{O}_i in (150) have scaling dimensions Δ_i . By conformal symmetry, (150) can be factorized as

$$G_{1234}(x_1, x_2, x_3, x_4) = \frac{1}{(x_{12}^2)^{\frac{\Delta_1+\Delta_2}{2}} (x_{34}^2)^{\frac{\Delta_3+\Delta_4}{2}}} \left(\frac{x_{24}^2}{x_{14}^2}\right)^{\frac{\Delta_1-\Delta_2}{2}} \left(\frac{x_{14}^2}{x_{13}^2}\right)^{\frac{\Delta_3-\Delta_4}{2}} g_{1234}(\rho, \bar{\rho}). \quad (151)$$

As we discussed in section 3.1, the prefactor multiplying $g_{1234}(\rho, \bar{\rho})$ has analytic continuation to the domain \mathcal{D} . It remains to show that $g_{1234}(\tau_k, \mathbf{x}_k)$ has analytic continuation to \mathcal{D} .

In the region $|\rho|, |\bar{\rho}| < 1$ in the Euclidean signature, g_{1234} has a convergent expansion in conformal blocks:

$$g_{1234}(\rho, \bar{\rho}) = \sum_{\mathcal{O}} C_{12\mathcal{O}} C_{34\mathcal{O}} g_{\mathcal{O}}^{12,34}(\rho, \bar{\rho}), \quad (152)$$

where $C_{ij\mathcal{O}}$ are OPE coefficients and \mathcal{O} are the primary operators which appear in the $\mathcal{O}_1 \times \mathcal{O}_2$ OPE. In the unitary CFTs, we can assume $C_{ij\mathcal{O}}$ to be real by choosing proper basis of operators.

Each conformal block $g_{\mathcal{O}}^{12,34}(\rho, \bar{\rho})$ has a series expansion

$$g_{\mathcal{O}}^{12,34}(\rho, \bar{\rho}) = \sum_{\psi \in [\mathcal{O}]} a_{12\psi} b_{34\psi} \rho^{h(\psi)} \bar{\rho}^{\bar{h}(\psi)}, \quad (153)$$

where $\psi \in [\mathcal{O}]$ form an orthonormal basis in the highest weight representation $[\mathcal{O}]$ of the conformal group $SO(1, d + 1)$. Here we choose ψ to be eigenstates of Virasoro generators $L_0, \bar{L}_0 \in so(1, d + 1)$ and $h(\psi), \bar{h}(\psi)$ are the corresponding eigenvalues. The real coefficients $a_{12\psi}, b_{34\psi}$ in (153) are totally fixed by conformal symmetry and $a_{12\mathcal{O}} = b_{34\mathcal{O}} = 1$, where \mathcal{O} is the primary state in $[\mathcal{O}]$.

We stick (153) into (152) and apply the Cauchy-Schwartz inequality:

$$\begin{aligned}
 |g^{12,34}(\rho, \bar{\rho})|^2 &= \left| \sum_{\mathcal{O}} C_{12\mathcal{O}} C_{34\mathcal{O}} \sum_{\psi \in [\mathcal{O}]} a_{12\psi} b_{34\psi} \rho^{h(\psi)} \bar{\rho}^{\bar{h}(\psi)} \right|^2 \\
 &\leq \left| \sum_{\mathcal{O}} \sum_{\psi \in [\mathcal{O}]} C_{12\mathcal{O}} C_{34\mathcal{O}} a_{12\psi} b_{34\psi} \rho^{h(\psi)} \bar{\rho}^{\bar{h}(\psi)} \right|^2 \\
 &\leq \left(\sum_{\mathcal{O}} \sum_{\psi \in [\mathcal{O}]} C_{12\mathcal{O}}^2 a_{12\psi}^2 |\rho|^{h(\psi)} |\bar{\rho}|^{\bar{h}(\psi)} \right) \\
 &\quad \times \left(\sum_{\mathcal{O}} \sum_{\psi \in [\mathcal{O}]} C_{34\mathcal{O}}^2 b_{34\psi}^2 |\rho|^{h(\psi)} |\bar{\rho}|^{\bar{h}(\psi)} \right).
 \end{aligned} \tag{154}$$

Since the primaries \mathcal{O} are in the intersection of $\mathcal{O}_1 \times \mathcal{O}_2$ and $\mathcal{O}_3 \times \mathcal{O}_4$ OPE, we have

$$\begin{aligned}
 \sum_{\mathcal{O}} \sum_{\psi \in [\mathcal{O}]} C_{12\mathcal{O}}^2 a_{12\psi}^2 |\rho|^{h(\psi)} |\bar{\rho}|^{\bar{h}(\psi)} &\leq g^{12,21}(r, r), \\
 \sum_{\mathcal{O}} \sum_{\psi \in [\mathcal{O}]} C_{34\mathcal{O}}^2 b_{34\psi}^2 |\rho|^{h(\psi)} |\bar{\rho}|^{\bar{h}(\psi)} &\leq g^{43,34}(r, r),
 \end{aligned} \tag{155}$$

where $r = \max\{|\rho|, |\bar{\rho}|\}$. The above inequalities show that the ρ -expansion of $g^{12,34}$ is absolutely convergent in the domain $|\rho|, |\bar{\rho}| < 1$. As a result we have an analytic function $g_{1234}(\chi, \bar{\chi})$ in the domain (28), where $\chi, \bar{\chi}$ are defined in (27).

On the other hand, for the case of non-identical scalar operators, we can still rearrange the series (153) in the same way as (24). This follows from the fact that only the operators in traceless totally-symmetric representations of $SO(d)$ can appear in the OPE of two scalar operators, which leads to ρ -expansion in the form of Gegenbauer polynomials (25) [13]. Therefore, by the results in section 3.4.2, the function $g_{1234}(\tau_k, \mathbf{x}_k)$ is analytic in \mathcal{D} .

The remaining steps are the same as the case of identical scalar operators. We conclude that for the case of four-point functions with non-identical scalar operators, the OPE convergence properties are the same as the case of identical scalar operators.

7.2 Comments on the case of spinning operators

Before finishing this section we want to make some comments on the case of four-point functions with spinning operators:

$$G_{1234}^{a_1 a_2 a_3 a_4}(x_1, x_2, x_3, x_4) := \langle \mathcal{O}_1^{a_1}(x_1) \mathcal{O}_2^{a_2}(x_2) \mathcal{O}_3^{a_3}(x_3) \mathcal{O}_4^{a_4}(x_4) \rangle, \tag{156}$$

where $\mathcal{O}_i^{a_i}$ are primary operators with scaling dimensions Δ_i and $SO(d)$ -representation ρ_i . a_i are the indices for the spin representations ρ_i . In the Euclidean signature, the Jacobian of any conformal transformation f in $SO(1, d + 1)$ can be factorized as

$$J_v^\mu(x) := \frac{\partial f^\mu(x)}{\partial x^\nu} = \Omega(x) \mathcal{R}_v^\mu(x), \tag{157}$$

where $\Omega(x) > 0$ is a scaling factor and \mathcal{R} is a rotation matrix. The four-point function $G_{1234}^{a_1 a_2 a_3 a_4}$ is invariant if we replace all $\mathcal{O}_i^{a_i}(x)$ in (156) with

$$\mathcal{O}_i^{a_i}(x) \rightarrow \Omega(x)^{\Delta_i} [\rho_i(\mathcal{R}(x))^{-1}]_{b_i}^{a_i} \mathcal{O}_i^{b_i}(f(x)). \tag{158}$$

If we choose the conformal transformation f to be the one which maps (x_1, x_2, x_3, x_4) to its $\rho, \bar{\rho}$ -configuration (19), then we get

$$G_{1234}^{a_1 a_2 a_3 a_4}(x_1, x_2, x_3, x_4) = \frac{1}{(x_{12}^2)^{\frac{\Delta_1 + \Delta_2}{2}} (x_{34}^2)^{\frac{\Delta_3 + \Delta_4}{2}}} \left(\frac{x_{24}^2}{x_{14}^2}\right)^{\frac{\Delta_1 - \Delta_2}{2}} \left(\frac{x_{14}^2}{x_{13}^2}\right)^{\frac{\Delta_3 - \Delta_4}{2}} \times T_{b_1 b_2 b_3 b_4}^{a_1 a_2 a_3 a_4}(\mathcal{R}_1, \mathcal{R}_2, \mathcal{R}_3, \mathcal{R}_4) g_{1234}^{b_1 b_2 b_3 b_4}(\rho, \bar{\rho}), \tag{159}$$

where \mathcal{R}_k is the rotation matrix of f at x_k , and T is a function of rotation matrices, which is determined by the representations ρ_i of the spinning operators \mathcal{O}_i .

Analogously to the scalar case, the function $g_{1234}^{b_1 b_2 b_3 b_4}(\rho, \bar{\rho})$ can be bounded by Cauchy-Schwarz inequality. We can still write $g_{1234}^{b_1 b_2 b_3 b_4}(\rho, \bar{\rho})$ in the form of (24), but in general the functions $P^l(\rho, \bar{\rho})$ are not Gegenbauer polynomials of $\cos \theta$ (recall that $\frac{\rho}{\bar{\rho}} = e^{2i\theta}$). The difficulty is that there is the function $T(\mathcal{R}_k)$ in (159) because of the non-trivial representations of the spinning operators. If we think of the above conformal transformation f as a conformal-group-valued function of (x_1, x_2, x_3, x_4) ,³⁶ then \mathcal{R}_k are also functions of (x_1, x_2, x_3, x_4) . In general, the entries of \mathcal{R}_k have singularities in the domain \mathcal{D} , e.g. at Γ [67, 68]. In a word, it is not obvious that $T(\mathcal{R}_k)$ in (159) is under control. Some extra work is required for a good estimate on the object

$$T_{b_1 b_2 b_3 b_4}^{a_1 a_2 a_3 a_4}(\mathcal{R}_1, \mathcal{R}_2, \mathcal{R}_3, \mathcal{R}_4) g_{1234}^{b_1 b_2 b_3 b_4}(\rho, \bar{\rho}).$$

In this paper we do not study the correlators of spinning operators. We leave these for future work.

8 Conclusions and outlooks

In this work we studied the convergence properties of various OPE channels for Lorentzian CFT four-point functions of scalar operators in $d \geq 2$, assuming global conformal symmetry. Our analysis is based on the convergence properties of OPE in the Euclidean unitary CFTs. We classified the Lorentzian four-point configurations according to their causal orderings and the range of the variables z, \bar{z} . The Lorentzian correlators are analytic functions in a neighbourhood of some Lorentzian configuration as long as there exists at least one convergent OPE channel in the sense of functions. We showed that the convergence properties of various OPE channels are determined by the causal orderings and the range of z, \bar{z} of the four-point configurations. The CFT four-point functions are analytic in a very big domain, including configurations with totally space-like separations and configurations with some other causal orderings. All the results of OPE convergence properties are given in Appendix C.

Before ending, we would like to point out some related open questions. We list these questions in the order of difficulty (based on personal perspective):

1. (Easy) CFTs can also live on the Minkowski cylinder [58]. We start from CFT four-point function defined on the Euclidean cylinder and then Wick rotate the cylindrical time variables. The corresponding counterpart questions are:
 - Which configurations have convergent s-, t- and u-channel OPE in the sense of functions on the Minkowski cylinder?

³⁶Since such a conformal transformation f is not unique, the definition of this group-valued function depends on how we construct it.

- Can we still classify the OPE convergence properties according to the range of z, \bar{z} and the causal orderings on the Minkowski cylinder?
2. We mainly used the radial coordinates $\rho, \bar{\rho}$ in our analysis. We have seen that by using the q, \bar{q} -variables in 2d, the domain of CFT four-point functions are larger than the domain derived by using the $\rho, \bar{\rho}$ -variables. A natural question is
- For CFTs with only global conformal symmetry, are there any other coordinates which allow us to extend G_4 to some other domains which are not covered by using radial variables?

Our conjecture is that there are no such coordinates.

3. (Probably hard) Our results provide some safe Lorentzian regions where conformal bootstrap approach can be applied. One can use bootstrap equations to analyze the four-point functions at Lorentzian configurations with at least two convergent OPE channels. It is also interesting to play with crossing symmetry at Lorentzian configurations with
- One convergent OPE channel in the sense of functions, another one in the sense of distributions.
 - Two convergent OPE channels in the sense of distributions.³⁷

The above situations are closely related to the topics on analytic functional bootstrap when the functionals touch the boundaries of the regions with convergent OPE [24–27, 70–72].

4. (Hard) There are also Lorentzian configurations with no convergent OPE channels. For these cases we do not know whether the general four-point correlators are genuine functions or not. We may need other techniques to handle these situations. For example, there are questions similar to section 6.2.4:
- One can derive a complex domain \mathcal{D}^{stu} which is the union of the domains of three OPE channels. Then what is \mathcal{D}^{stu} and what is its envelope of holomorphy $H(\mathcal{D}^{stu})$? Does $H(\mathcal{D}^{stu})$ contain more Lorentzian configurations than those provided by the results in this paper?

Once we are able to construct $H(\mathcal{D}^{stu})$, one can ask

- Given a Lorentzian configuration $C_L \in \mathcal{D} \setminus H(\mathcal{D}^{stu})$, can we find a CFT example such that the four-point function is divergent at C_L ?
5. (Hard) One can also consider higher-point correlation functions in CFTs. A natural question is:
- For $n \geq 5$, what is the Lorentzian domain of G_n in the sense of functions?

We leave these questions for future work.

³⁷The similar idea was proposed recently by Gillioz et al, see [69], section 5.

Acknowledgments

JQ thanks Slava Rychkov and Petr Kravchuk for a lot of helpful discussions. This work is a by-product of our collaboration work of a series of papers on distributional properties of four-point functions in CFTs. JQ also thanks Slava Rychkov for the great help in improving the writing of this paper.

JQ thanks Zechuan Zheng, Emilio Trevisani, Dan Mao and Yikun Jiang for helpful discussions and comments.

The work of JQ is supported by the Simons Foundation grant 488655 (Simons Collaboration on the Nonperturbative Bootstrap).

A Why $z(\tau_k, \mathbf{x}_k), \bar{z}(\tau_k, \mathbf{x}_k)$ are not well defined on \mathcal{D} in $d \geq 3$?

A.1 Main idea

Recall that we want to analytically continue the function $g(\tau_k, \mathbf{x}_k)$ to \mathcal{D} by using the compositions (30). In fact, by theorem 3.1 and the fact that \mathcal{D} is simply connected, this would have been possible if analytic functions $z(\tau_k, \mathbf{x}_k), \bar{z}(\tau_k, \mathbf{x}_k)$ existed (see the 2d case in section 3.5).

We are going to show that in $d \geq 3$, there is no analytic function $(z(\tau_k, \mathbf{x}_k), \bar{z}(\tau_k, \mathbf{x}_k))$ on \mathcal{D} which is compatible with (6) and (7). Consequently, some modification of the strategy (30) is needed to construct the analytic continuation of $g(\tau_k, \mathbf{x}_k)$ in $d \geq 3$ (and that's what we did in section 3.4). In this section we do not identify $(z, \bar{z}) \sim (\bar{z}, z)$.

Let us first give the main idea why $z(\tau_k, \mathbf{x}_k), \bar{z}(\tau_k, \mathbf{x}_k)$ are not globally well-defined on \mathcal{D} . This is similar to the reason why the square-root function $f(w) = \sqrt{w}$ is not globally well-defined on \mathbb{C} : there exists a loop of w such that $f(w)$ starts with $f(w_0)$ (w_0 is the start and final point of the loop) but ends with $-f(w_0)$. In $d \geq 3$, there exists a loop γ in \mathcal{D} such that the value $4u - (1 + u - v)^2$ goes around 0 once. Then by (8), we see that $(z(\gamma(s)), \bar{z}(\gamma(s)))$ starts with (z_0, \bar{z}_0) but ends with (\bar{z}_0, z_0) . The construction of such a path γ is given by (167) and (168).³⁸

A.2 Proof

Let Γ be the preimage of Γ_{uv} in \mathcal{D} (i.e. the set of configurations where $4u - (1 + u - v)^2 = 0$, see the definition of Γ_{uv} in (9)). A necessary condition for the existence of such a (z, \bar{z}) function is that

- $(z(\tau_k, \mathbf{x}_k), \bar{z}(\tau_k, \mathbf{x}_k))$ is a continuous function from $\mathcal{D} \setminus \Gamma$ to $\mathbb{C}^2 \setminus \{z = \bar{z}\}$.

It suffices to show that the above condition does not hold in $d \geq 3$.

If the continuous function $(z(\tau_k, \mathbf{x}_k), \bar{z}(\tau_k, \mathbf{x}_k))$ exists, then since (11) is an invertible linear map, the continuous function $\tilde{\alpha}(\tau_k, \mathbf{x}_k) = (w(\tau_k, \mathbf{x}_k), y(\tau_k, \mathbf{x}_k))$ also exists. Then there is the following commutative diagram (the map α is defined by (6), while p is a composition of (11) and (7)):

$$\begin{array}{ccc}
 (w, y) \in \mathbb{C} \times (\mathbb{C} \setminus \{0\}) & \xrightarrow{(11)} & \mathbb{C}^2 \setminus \{z = \bar{z}\} \\
 \tilde{\alpha} \uparrow & \downarrow p & \swarrow (7) \\
 (\epsilon_k + it_k, \mathbf{x}_k) \in \mathcal{D} \setminus \Gamma & \xrightarrow{\alpha} & \mathbb{C}^2 \setminus \Gamma_{uv} \ni (u, v)
 \end{array} \tag{160}$$

³⁸In the proof we will use a formal way to reformulate the idea described here. Readers who got the idea can just go to the construction of the path. We thank Petr Kravchuk for the discussion on this problem.

The map $\tilde{\alpha}$ in (160) satisfies $p \circ \tilde{\alpha} = \alpha$. Since p is a double covering map from $\mathbb{C} \times (\mathbb{C} \setminus \{0\})$ to $\mathbb{C}^2 \setminus \Gamma_{uv}$, recalling the lifting properties of the covering map [41], a sufficient and necessary condition for the existence of $\tilde{\alpha}$ is the following relation of the fundamental groups

$$\alpha_* \left(\pi_1(\mathcal{D} \setminus \Gamma, C_0) \right) \subset p_* \left(\pi_1(\mathbb{C} \times (\mathbb{C} \setminus \{0\}), (w_0, y_0)) \right), \tag{161}$$

where $C_0, (w_0, y_0)$ are base points of the corresponding spaces such that $\alpha(C_0) = p(w_0, y_0)$, and α_*, p_* are the fundamental group homomorphisms induced by α, p .

It remains to show that the condition (161) does not hold in $d \geq 3$. By (10), $\mathbb{C}^2 \setminus \Gamma_{uv}$ is homeomorphic to $\mathbb{C} \times (\mathbb{C} \setminus \{0\})$. So $\mathbb{C}^2 \setminus \Gamma_{uv}$ and $\mathbb{C} \times (\mathbb{C} \setminus \{0\})$ have the same non-trivial fundamental group

$$\pi_1(\mathbb{C} \times (\mathbb{C} \setminus \{0\}), (w_0, y_0)) \simeq \pi_1(\mathbb{C}^2 \setminus \Gamma_{uv}, (u_0, v_0)) \simeq \mathbb{Z}, \tag{162}$$

where (u_0, v_0) is a base point in $\mathbb{C}^2 \setminus \Gamma_{uv}$ such that $p(w_0, y_0) = (u_0, v_0)$. Since p is a double covering map, the group homomorphism

$$p_* : \pi_1(\mathbb{C} \times (\mathbb{C} \setminus \{0\}), (w_0, y_0)) \longrightarrow \pi_1(\mathbb{C}^2 \setminus \Gamma_{uv}, (u_0, v_0)), \tag{163}$$

is not surjective. In fact, by choosing proper basis, the group homomorphism (163) can be written as

$$\begin{aligned} p_* : \mathbb{Z} &\longrightarrow \mathbb{Z}, \\ n &\mapsto 2n. \end{aligned} \tag{164}$$

Now to show that the condition (161) does not hold, it suffices to show that the group homomorphism

$$\alpha_* : \pi_1(\mathcal{D} \setminus \Gamma, C_0) \longrightarrow \pi_1(\mathbb{C}^2 \setminus \Gamma_{uv}, (u_0, v_0)), \tag{165}$$

is surjective. By (10), the generator of $\pi_1(\mathbb{C}^2 \setminus \Gamma_{uv}, (u_0, v_0))$ corresponds to a loop in $\mathbb{C}^2 \setminus \Gamma_{uv}$ such that along this loop, $4u - (1 + u - v)^2$ goes around 0 only once. Let us construct a loop γ in $\mathcal{D} \setminus \Gamma$:

$$\gamma : [0, 1] \longrightarrow \mathcal{D} \setminus \Gamma, \quad \gamma(0) = \gamma(1) = C_0, \tag{166}$$

which induces a loop in $\mathbb{C}^2 \setminus \Gamma_{uv}$ such that $4u - (1 + u - v)^2$ goes around 0 only once.

We pick 4 configurations C_0, C_1, C_2, C_3 in $\mathcal{D} \setminus \Gamma$:

$$\begin{aligned} C_0 : & \quad x_1 = 0, \quad x_2 = (-1, 1, 0, \dots, 0), \quad x_3 = (-2, 0, \dots, 0), \quad x_4 = (-5, 0, \dots, 0). \\ C_1 : & \quad x_1 = (0, -1, 0, \dots, 0), \quad x_2 = (-1 + 3i, -1, 0, \dots, 0), \quad x_3 = (-2, 0, \dots, 0), \\ & \quad x_4 = (-5, 0, \dots, 0). \\ C_2 : & \quad x_1 = 0, \quad x_2 = (-1, -1, 0, \dots, 0), \quad x_3 = (-2, 0, \dots, 0), \\ & \quad x_4 = (-5, 0, \dots, 0). \\ C_3 : & \quad x_1 = (0, 1, 0, \dots, 0), \quad x_2 = (-1, 0, 1, 0, \dots, 0), \quad x_3 = (-2, 0, \dots, 0), \\ & \quad x_4 = (-5, 0, \dots, 0). \end{aligned} \tag{167}$$

We let γ be consisting of four straight lines:

$$\gamma(s) = \begin{cases} (1 - 4s)C_0 + 4sC_1, & 0 \leq s \leq 1/4, \\ (2 - 4s)C_1 + (4s - 1)C_2, & 1/4 \leq s \leq 1/2, \\ (3 - 4s)C_2 + (4s - 2)C_3, & 1/2 \leq s \leq 3/4, \\ (4 - 4s)C_3 + (4s - 3)C_0, & 3/4 \leq s \leq 1. \end{cases} \tag{168}$$

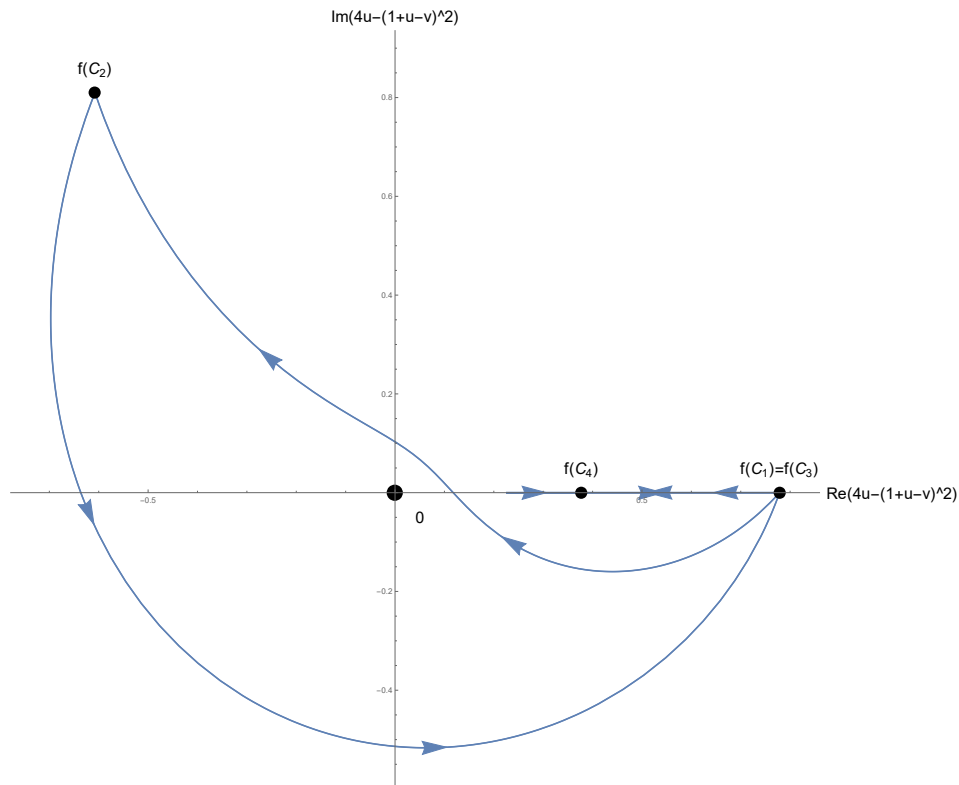


Figure A.1: The curve of $4u - (1 + u - v)^2$ along $\gamma(s)$. We use $f(C_i)$ to denote the value $4u - (1 + u - v)^2$ at the configuration C_i .

Figure A.1 shows the curve of $4u - (1 + u - v)^2$ along the path γ . We see that $4u - (1 + u - v)^2$ is non-zero everywhere, implies that the configurations along γ are always in $\mathcal{D} \setminus \Gamma$ (because the image (u, v) of $\gamma(s)$ is not in Γ_{uv}). Furthermore, $4u - (1 + u - v)^2$ goes around 0 only once. Therefore, fundamental group element $[\gamma] \in \pi_1(\mathcal{D} \setminus \Gamma, C_0)$ is mapped to the generator of $\pi_1(\mathbb{C}^2 \setminus \Gamma_{uv}, (u_0, v_0))$, so (165) is surjective. As a result, the lifted map $\tilde{\alpha}$ does not exist.

We conclude that in $d \geq 3$, there is no analytic function $(z(\tau_k, \mathbf{x}_k), \bar{z}(\tau_k, \mathbf{x}_k))$ on \mathcal{D} .

We also want to remark that in 2d, the analytic function (z, \bar{z}) does exist (see section 3.5). The part of our proof in this section that fails in 2d is the construction of the loop γ in (168). In our construction of C_3 in (167), the third component of x_2 is non-zero. This is where we use the condition $d \geq 3$. In fact, one can show that in 2d, the group homomorphism (165) is not surjective, and the condition (161) holds.

B Connectedness of \mathcal{D}_L^α in $d \geq 3$

In this section we are going to show that in $d \geq 3$, each \mathcal{D}_L^α in (90) is connected.

Observe first of all that all \mathcal{D}_L^α of the same causal type in table 2 have the same connectedness property (this is obvious because they are related by renumbering points), so it suffices to prove the connectedness property for one \mathcal{D}_L^α in each causal type.

Given a \mathcal{D}_L^α , we define $(\mathcal{D}_L^\alpha)_3$ to be the set of all three-point Lorentzian configurations which have the causal ordering of the first three points of the configurations in \mathcal{D}_L^α . Then there is a natural projection from \mathcal{D}_L^α to $(\mathcal{D}_L^\alpha)_3$:

$$\begin{aligned} \pi : \mathcal{D}_L^\alpha &\longrightarrow (\mathcal{D}_L^\alpha)_3, \\ (x_1, x_2, x_3, x_4) &\mapsto (x_1, x_2, x_3). \end{aligned} \tag{169}$$

Then \mathcal{D}_L^α has the following decomposition

$$\mathcal{D}_L^\alpha = \bigcup_{(x_1, x_2, x_3) \in (\mathcal{D}_L^\alpha)_3} \{x_4 \mid (x_1, x_2, x_3, x_4) \in \mathcal{D}_L^\alpha\}. \tag{170}$$

For each causal type in table 2, we want to show that there exists a \mathcal{D}_L^α in this causal type such that

1. For fixed $(x_1, x_2, x_3) \in (\mathcal{D}_L^\alpha)_3$, the set $F_{x_1, x_2, x_3}^\alpha = \{x_4 \mid (x_1, x_2, x_3, x_4) \in \mathcal{D}_L^\alpha\}$ is non-empty and connected.
2. $(\mathcal{D}_L^\alpha)_3$ is connected.

B.1 Step 1

For a fixed three-point configuration (x_1, x_2, x_3) , the set $F_{x_1, x_2, x_3}^\alpha = \{x_4 \mid (x_1, x_2, x_3, x_4) \in \mathcal{D}_L^\alpha\}$ is non-empty and connected if one of the following conditions holds as a consequence of causal ordering imposed by \mathcal{D}_L^α :

1. $x_i \rightarrow x_4$ for $i = 1, 2, 3$.
2. $x_4 \rightarrow x_i$ for $i = 1, 2, 3$.
3. x_4 is space-like separated from all of x_1, x_2, x_3 .

For the first case, F_{x_1, x_2, x_3}^α is given by the intersection of the open forward light-cones of x_1, x_2, x_3 , which is non-empty. Since cones are convex, F_{x_1, x_2, x_3}^α is also convex, thus connected. The connectedness for the second case follows from a similar argument. For the third case, we use the fact that the connectedness property does not change under Poincaré transformations, which allows us to move x_1 to 0 by translation

$$x_k \mapsto x_k - x_1, \quad k = 1, 2, 3, 4, \tag{171}$$

and then move x_2, x_3 onto a 2d subspace by a Lorentz transformation. We enumerate all possible three-point causal orderings

$$a \longrightarrow b \longrightarrow c, \quad \begin{array}{l} a \searrow b \\ \quad \quad c \end{array}, \quad \begin{array}{l} b \searrow a \\ \quad \quad c \end{array}, \quad b \longrightarrow c, \quad \begin{array}{l} a \\ b \\ c \end{array}, \tag{172}$$

and check case by case that in $d \geq 3$ we can always move the extra point x_4 from any position to ∞ , preserving the constraint that x_4 is space-like to a, b, c . This observation implies that F_{x_1, x_2, x_3}^α is connected for the third case.

In table 2, we find a \mathcal{D}_L^α satisfying one of the above conditions for some but not all causal types. That’s why the connectedness of \mathcal{D}_L^α is not so obvious. The exceptional cases are causal type 8, 10 and 11, for which we need to discuss case by case. Without loss of generality we set $a = 1, b = 2, c = 3, d = 4$ (comparing with table 2) in the following discussion.

Type 8. By translations, Lorentz transformations and dilatations we fix the configurations to

$$x_1 = 0, \quad x_2 = (x^0, x^1, 0, \dots, 0), \quad x_3 = (0, 1, 0, \dots, 0). \tag{173}$$

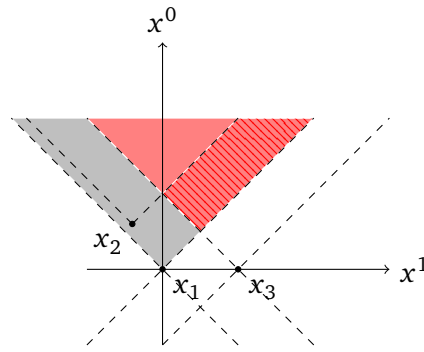


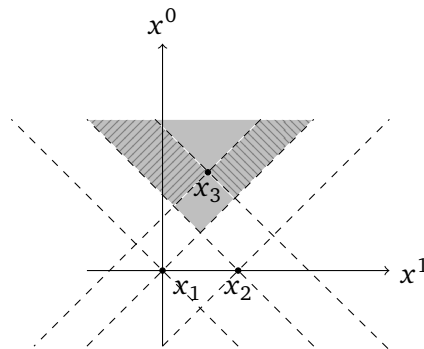
Figure B.1: Type 8

Then x_2 is in the open forward light-cone of x_1 , but out of the light-cones of x_3 (see the grey region in figure B.1), and x_4 is in the intersection of open forward light-cones of x_1 and x_3 (see the red region in figure B.1). Once x_2 is fixed somewhere in the grey region, the space of allowed positions for x_4 is given by the red region minus the forward light-cone of x_2 , so the remaining region for x_4 , which is F_{x_1, x_2, x_3}^α , is the red dashed region in figure B.1. Figure B.1 shows the 2d situation but a similar 3d figure shows that F_{x_1, x_2, x_3}^α is non-empty and connected in 3d, thus also non-empty and connected in higher d (because we can always find a spatial rotation which preserves x_1, x_2, x_3 and maps x_4 to $(x, y, z, 0, \dots, 0)$).

Type 10. By translations, Lorentz transformations and dilatations we fix the configurations to

$$x_1 = 0, \quad x_2 = (0, 1, 0, \dots, 0), \quad x_3 = (x^0, x^1, 0, \dots, 0). \tag{174}$$

Figure B.2: Type 10



The remaining x_3, x_4 pair are in the intersection of the open forward light-cones of x_1, x_2 , i.e. the grey region in figure B.2. Once x_3 is fixed, by the constraint that x_3, x_4 are space-like separated, F_{x_1, x_2, x_3}^α is given by the grey dashed region in figure B.2, which is obviously non-empty. This region is topologically the same as \mathbb{R}^d minus the light-cones of x_3 , thus connected when $d \geq 3$.

Type 11. By translations, Lorentz transformations and dilatations we fix the configurations to

$$x_1 = 0, \quad x_2 = (i, 0, \dots, 0), \quad x_3 = (x^0, x^1, 0, \dots, 0). \tag{175}$$

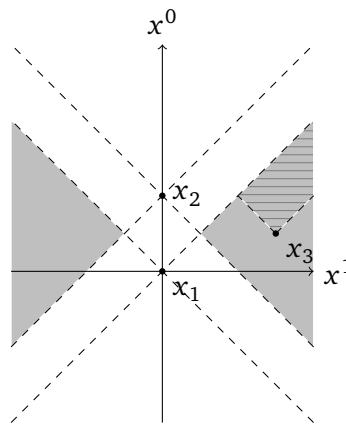


Figure B.3: Type 11

The remaining x_3, x_4 pair are in the grey region in figure B.3. One can see that in $d \geq 3$ the grey region is topologically the same as the triangle slice (see one of the grey triangle in figure B.3) times S^{d-2} , which is connected. Once x_3 is fixed, F_{x_1, x_2, x_3}^α is given by the forward light-cone of x_3 in the grey region (see the grey dashed region in figure B.3), which is connected.

B.2 Step 2

By slightly improving the argument in step 1, we claim that for the representative set \mathcal{D}_L^α (which we chose in step 1) of each causal type in table 2, the map (169) is surjective. In other words, for each three-point configuration in $(\mathcal{D}_L^\alpha)_3$, its preimage in \mathcal{D}_L^α is non-empty.

This claim is true for the cases which satisfy one of the conditions at the beginning of section B.1 because for these cases we can always find an x_4 which is very far away from x_1, x_2 and x_3 . This claim is also true for the exceptional cases because from the figure B.1, B.2 and B.3 we see that the remaining region for x_4 is always non-empty.

Now it remains to show that $(\mathcal{D}_L^\alpha)_3$, which is the set of all three-point configurations with a fixed causal ordering, is connected. For each causal type in (172), we choose

$$x_1 = b, \quad x_2 = c, \quad x_3 = a. \tag{176}$$

Analogously to the four-point case we define a projection

$$\begin{aligned} \pi : (\mathcal{D}_L^\alpha)_3 &\longrightarrow (\mathcal{D}_L^\alpha)_2, \\ (x_1, x_2, x_3) &\mapsto (x_1, x_2). \end{aligned} \tag{177}$$

Then we decompose $(\mathcal{D}_L^\alpha)_3$ into

$$(\mathcal{D}_L^\alpha)_3 = \bigcup_{(x_1, x_2) \in (\mathcal{D}_L^\alpha)_2} \{x_3 \mid (x_1, x_2, x_3) \in (\mathcal{D}_L^\alpha)_3\}. \tag{178}$$

By comparing (172) and (176), we find each $(\mathcal{D}_L^\alpha)_3$ satisfies one of the following conditions:

1. $x_i \rightarrow x_3$ for $i = 1, 2$.
2. $x_3 \rightarrow x_i$ for $i = 1, 2$.
3. x_3 is space-like separated from both of x_1, x_2 .

This observation implies that for each $(\mathcal{D}_L^\alpha)_3$:

- For any fixed $(x_1, x_2) \in (\mathcal{D}_L^\alpha)_2$, the set $\{x_3 \mid (x_1, x_2, x_3) \in (\mathcal{D}_L^\alpha)_3\}$ is connected.
- $(\mathcal{D}_L^\alpha)_2 = \pi((\mathcal{D}_L^\alpha)_3)$ contains all two-point configurations with the corresponding causal ordering.

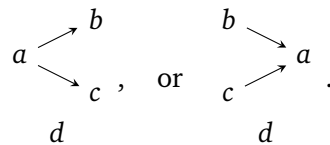
It remains to show that in $d \geq 3$, the set of two-point configurations with a given causal ordering is connected. This is trivial.

C Tables of OPE convergence

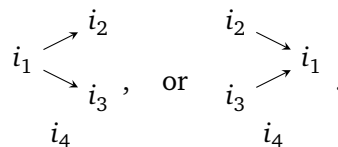
In this appendix we will give 12 tables of the results about convergence properties of three OPE channels: one table for one causal type. For each causal type we will give a template graph with points a, b, c, d . Given a Lorentzian configuration $C_L = (x_1, x_2, x_3, x_4) \in \mathcal{D}_L$, the way to look up the tables is as follows.

1. Compute the causal ordering of C_L , draw the graph of this causal ordering. Find the corresponding type number (say type X) in table 2.
2. Go to the section of causal type X (which is appendix C.X). Compare the causal ordering of C_L with the template causal ordering of causal type X at the beginning of appendix C.X. Match the points i_1, i_2, i_3, i_4 with $(abcd)$. We will get a sequence $(i_1 i_2 i_3 i_4)$.
3. Look up the convergence properties of $(i_1 i_2 i_3 i_4)$ in the table of causal type X.

For example, consider the following template causal ordering



Then $(i_1 i_2 i_3 i_4)$ means



In appendix C.1 we will explain in detail how to make the table of OPE convergence for type 1 causal ordering. The procedure is similar for the other causal types, so we will only give the results for them. Before we start, we would like to introduce some tricks in appendix C.0.1, C.0.2 and C.0.3. They will be helpful in making the tables.

C.0.1 S_4 -action

There is a natural S_4 -action on the space of four-point configurations. Let $\sigma \in S_4$ be a symmetry group element:

$$\sigma = \begin{pmatrix} 1 & 2 & 3 & 4 \\ \sigma(1) & \sigma(2) & \sigma(3) & \sigma(4) \end{pmatrix}. \tag{179}$$

Let $C = (x_1, x_2, x_3, x_4)$ be a four-point configuration such that $x_{ij}^2 \neq 0$ for all x_i, x_j pairs. We define the action

$$\sigma \cdot C = (x'_1, x'_2, x'_3, x'_4), \quad x'_k = x_{\sigma^{-1}(k)}. \tag{180}$$

By computing z, \bar{z} of $\sigma \cdot C$ and comparing with z, \bar{z} of C , we get a natural S_4 -action on z, \bar{z} :

$$\begin{aligned}
 w_\sigma : \mathbb{C} \setminus \{0, 1\} &\longrightarrow \mathbb{C} \setminus \{0, 1\}, \\
 z &\mapsto w_\sigma(z), \\
 \bar{z} &\mapsto w_\sigma(\bar{z}),
 \end{aligned} \tag{181}$$

where $w_\sigma(z), w_\sigma(\bar{z})$ are the variables z, \bar{z} computed from $\sigma \cdot C$. We have the following properties:

- $\{w_\sigma\}_{\sigma \in S_4}$ belong to a set of 6 fractional linear transformation forming a group which is isomorphic to S_3 . The map $\sigma \mapsto w_\sigma$ is a group homomorphism from S_4 to S_3 (i.e. $w_{\sigma_1} \circ w_{\sigma_2} = w_{\sigma_1 \sigma_2}$).
- The S_4 -action on \mathcal{D}_L permutes classes S,T,U among themselves.
- The S_4 -action on \mathcal{D}_L permutes subclasses E_{su}, E_{st}, E_{tu} among themselves.
- The S_4 -action on \mathcal{D}_L preserves the subclass E_{stu} .

Let us denote σ by $[\sigma(1)\sigma(2)\sigma(3)\sigma(4)]$. We summarize the above properties in table 3. Sup-

Table 3: The list of w_σ and the S_4 transformation between classes and subclasses.

σ	$w_\sigma(z)$	S	T	U	E_{su}	E_{st}	E_{tu}	E_{stu}
[1234], [2143], [3412], [4321]	z	S	T	U	E_{su}	E_{st}	E_{tu}	E_{stu}
[2134], [1243], [4312], [3421]	$\frac{z}{z-1}$	S	U	T	E_{st}	E_{su}	E_{tu}	E_{stu}
[3214], [4123], [1432], [2341]	$1-z$	T	S	U	E_{tu}	E_{st}	E_{su}	E_{stu}
[1324], [2413], [3142], [4231]	$\frac{1}{z}$	U	T	S	E_{su}	E_{tu}	E_{st}	E_{stu}
[2314], [1423], [4132], [3241]	$\frac{1}{1-z}$	T	U	S	E_{st}	E_{tu}	E_{su}	E_{stu}
[3124], [4213], [1342], [2431]	$1 - \frac{1}{z}$	U	S	T	E_{tu}	E_{su}	E_{st}	E_{stu}

pose a configuration C_L gives the template causal ordering of a causal type, which means that C_L corresponds to the sequence (1234). For $\sigma = [i_1 i_2 i_3 i_4]$, we get a configuration $C'_L = \sigma \cdot C$ by eq. (180). The causal ordering of C'_L is in the same causal type as C_L . By comparing the causal orderings of C_L and C'_L , we see that the sequence of C'_L is exactly $(i_1 i_2 i_3 i_4)$. Therefore, given a causal type, if we know the class/subclass of the template causal ordering, by looking up table 3 we decide the classes/subclasses of the other causal ordering in the same causal type. Then by looking up table 1, we immediately get a part of the OPE convergence properties for each causal ordering.

By using the above trick, the problem of determining the classes/subclasses of causal orderings belong is reduced to determining the class/subclass of the template causal ordering in each causal type. In appendix C.0.2, we will introduce a trick to determine the classes/subclasses of the template causal orderings.

C.0.2 Lorentzian conformal frame

Our goal in this subsection is to give a systematic way to determine the class/subclass of \mathcal{D}_L^α , where α is a fixed causal ordering.

Recalling lemma 5.1, all configurations in \mathcal{D}_L^α belong to the same class. We can choose a particular configuration $C_L \in \mathcal{D}_L^\alpha$ and compute z, \bar{z} of C_L , then we immediately know the class (not subclass) of \mathcal{D}_L^α .

If \mathcal{D}_L^α belongs to class S/T/U, then we are done. The rest of this subsection is for the case that \mathcal{D}_L^α belongs to class E. If \mathcal{D}_L^α belongs to class E, then according to theorem 5.2, we need to check the OPE convergence properties for the intersection of \mathcal{D}_L^α and each subclass of class E as long as the intersection is non-empty. We will find that only the type 1, 5, 6, 10, 11, 12 causal orderings in table 2 belong to class E.³⁹ In the tables of OPE convergence properties of causal type 5, 10 and 12, we give the results of all subclasses for each causal ordering (see table 9, 14 and 16); while in the tables of causal type 1, 6 and 11, we only give the results of one subclass for each causal ordering (see table 5, 10 and 15). We claim that our tables are complete, based on the following lemma.

Lemma C.1. Given a fixed causal ordering α , if α is in causal type 1/6/11, then \mathcal{D}_L^α only belongs to one of the three subclasses E_{st}, E_{su}, E_{tu} .

The basic tool we use to prove the above lemma is the Lorentzian conformal frame. The Lorentzian conformal frame is similar to the Euclidean conformal frame (12). Given a Lorentzian configuration C_L , its conformal frame configuration C'_L is a Lorentzian configuration which has one of the following forms

$$\begin{aligned} 1. & \quad x'_1 = 0, \quad x'_2 = (ia, b, 0, \dots, 0), \quad x'_3 = (i, 0, \dots, 0), \quad x'_4 = \infty, \\ 2. & \quad x'_1 = 0, \quad x'_2 = (ib, a, 0, \dots, 0), \quad x'_3 = (0, 1, 0, \dots, 0), \quad x'_4 = \infty, \\ 3. & \quad x'_1 = 0, \quad x'_2 = (0, a, b, 0, \dots, 0), \quad x'_3 = (0, 1, 0, \dots, 0), \quad x'_4 = \infty, \end{aligned} \tag{182}$$

where C'_L and C_L are related by a Lorentzian conformal transformation. Computing the cross-ratios from (182), we see that: for the first and second cases $z = a + b, \bar{z} = a - b$; for the third case $z = a + ib, \bar{z} = a - ib$. Analogously to the Euclidean conformal frame, the Lorentzian conformal frame configuration is unique up to a reflection $b \mapsto -b$, which corresponds to interchanging z and \bar{z} .

Let us describe how we map a four-point configuration to the conformal frame by conformal transformations. Let $C_L = (x_1, x_2, x_3, x_4)$ be a Lorentzian configuration. We will go from C_L to C'_L in a few steps, and each step is a conformal transformation. The configuration after the k -th step is denoted by $C_L^{(k)}$.

Step 1. We move x_1 to 0 by translation. The configuration $C_L^{(1)}$ after the first step is given by

$$C_L^{(1)} = (x_1^{(1)}, x_2^{(1)}, x_3^{(1)}, x_4^{(1)}) = (0, x_2 - x_1, x_3 - x_1, x_4 - x_1). \tag{183}$$

This step preserves the causal ordering.

Step 2. We move x_4 to ∞ by special conformal transformation

$$x'^\mu = \frac{x^\mu - x^2 b^\mu}{1 - 2x \cdot b + x^2 b^2}, \quad b^\mu = \frac{(x_4 - x_1)^\mu}{(x_4 - x_1)^2}. \tag{184}$$

$x_1 = 0$ is preserved by special conformal transformation. This step may change the causal ordering. Under general conformal transformations, x_{ij}^2 transforms as

$$\begin{aligned} (x'_i - x'_j)^2 &= \Omega(x_i)\Omega(x_j)(x_i - x_j)^2, \\ (ds'^2 &= \Omega(x)^2 ds^2), \end{aligned} \tag{185}$$

³⁹This can be easily done by choosing one particular configuration and compute z, \bar{z} for each template causal ordering, and by the fact that the S_4 -action preserves class E (as discussed in appendix C.0.1).

and for special conformal transformation (184), the scaling factor at $x_k^{(1)} = x_k - x_1$ is given by

$$\Omega(x_k^{(1)}) = \frac{(x_4 - x_1)^2}{(x_4 - x_k)^2}, \quad k = 1, 2, 3, 4. \tag{186}$$

Let $C_L^{(2)} = (x_1^{(2)}, x_2^{(2)}, x_3^{(2)}, x_4^{(2)})$ be the configuration after step 2. For any configuration C_L in \mathcal{D}_L (where the light-cone singularities are excluded), by (185) and (186) we have

$$(x_i^{(2)} - x_j^{(2)})^2 \neq 0, \quad i, j = 1, 2, 3. \tag{187}$$

Furthermore, the sign of $(x_i^{(2)} - x_j^{(2)})^2$ is determined by the causal ordering of C_L . So we know if each $x_i^{(2)}, x_j^{(2)}$ pair of $C_L^{(2)}$ is space-like or time-like. The information we do not know a priori from (185) and (186) is the causal orderings of time-like $x_i^{(2)}, x_j^{(2)}$ pairs (who is in the future of whom).⁴⁰

Step 3. We move x_3 to its final position by some composition of Lorentz transformations, dilatations and time reversal θ_L (these conformal transformations preserve $x_1 = 0$ and $x_4 = \infty$). Lorentz transformations and dilatations preserve causal orderings, and time reversal only reverse causal orderings (i.e. x_i, x_j pairs change from time-like to time-like, or from space-like to space-like). There are two possibilities after step 2: $x_3^{(2)}$ could be space-like or time-like to $x_1^{(2)}$. If $x_1^{(2)}, x_3^{(2)}$ are time-like, then $x_3^{(3)}$ is put at $(i, 0, \dots, 0)$. If $x_1^{(2)}, x_3^{(2)}$ are space-like, then $x_3^{(3)}$ is put at $(0, 1, 0, \dots, 0)$. Therefore, $C_L^{(3)}$ is in one of the following forms:

1. $x_1^{(3)} = 0, x_3^{(3)} = (i, 0, \dots, 0), x_4^{(3)} = \infty$.
2. $x_1^{(3)} = 0, x_3^{(3)} = (0, 1, 0, \dots, 0), x_4^{(3)} = \infty$.

Step 4. We move x_2 to somewhere in the (01)-plane or (12)-plane by Lorentz transformations in the little group of $x_3^{(3)}$. If $x_3^{(3)} = (i, 0, \dots, 0)$, then we move x_2 to the (01)-plane by rotation, i.e. $x_2^{(4)} = (ia, b, 0, \dots, 0)$. If $x_3^{(3)} = (0, 1, 0, \dots, 0)$, then we move x_2 onto the (01)-plane or the (12)-plane, determined as follows:

- If $x_2^{(3)} = (i\beta_1, a, \beta_2, \dots, \beta_{d-1})$ with $(\beta_1)^2 \geq (\beta_2)^2 + \dots + (\beta_{d-1})^2$, then x_2 is put in the (01)-plane, i.e. $x_2^{(4)} = (ib, a, 0, \dots, 0)$ and $b^2 = (\beta_1)^2 - (\beta_2)^2 - \dots - (\beta_{d-1})^2$.
- If $x_2^{(3)} = (i\beta_1, a, \beta_2, \dots, \beta_{d-1})$ with $(\beta_1)^2 \leq (\beta_2)^2 + \dots + (\beta_{d-1})^2$, then x_2 is put in the (01)-plane, i.e. $x_2^{(4)} = (0, a, b, 0, \dots, 0)$ and $b^2 = (\beta_2)^2 + \dots + (\beta_{d-1})^2 - (\beta_1)^2$.

In the end, $C'_L = C_L^{(4)}$ has one of the forms in eq. (182). Moreover, the above discussion provides us with the following fact:

- the sign of $(x'_{ij})^2$ of C'_L is going to be the same for all configurations $C_L \in \mathcal{D}_L^\alpha$ in each causal ordering α .

Now back to our question. Suppose \mathcal{D}_L^α is in class E. Let $C'_L = (x'_1, x'_2, x'_3, x'_4)$ be the conformal frame configuration of $C_L \in \mathcal{D}_L^\alpha$. Comparing the range of the (a, b) pair in (182) with the range of the (z, \bar{z}) pair in class E (see section 5.1) and using the above fact, we see that there are only two possibilities for C'_L :

⁴⁰Of course for any particular configuration we can just compute $C_L^{(2)}$ and then determine its causal ordering.

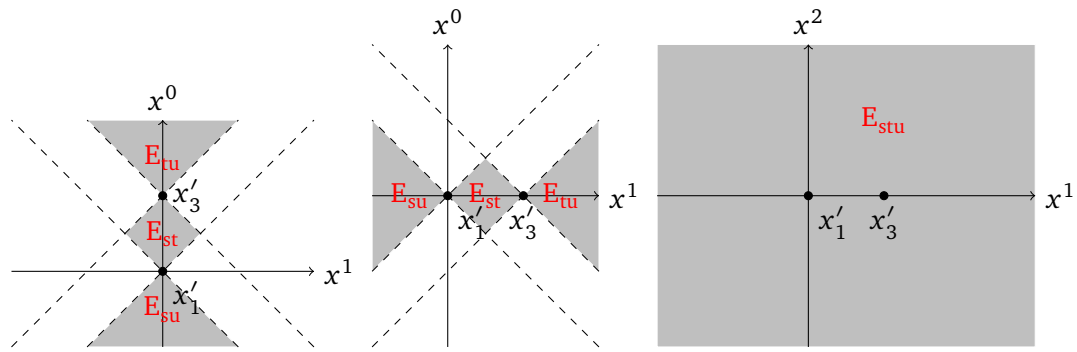


Figure C.1: The conformal frame configurations realized by configurations in class E.

1. $(x'_{13})^2, (x'_{12})^2, (x'_{23})^2 < 0$ for all $C_L \in \mathcal{D}_L^\alpha$. All possible C'_L are given by the grey region in the first picture of figure C.1. In this case z, \bar{z} are real, so we have

$$\mathcal{D}_L^\alpha = (\mathcal{D}_L^\alpha \cap E_{st}) \sqcup (\mathcal{D}_L^\alpha \cap E_{su}) \sqcup (\mathcal{D}_L^\alpha \cap E_{tu}). \tag{188}$$

Because the z, \bar{z} ranges corresponding to E_{st}, E_{su}, E_{tu} are disconnected from each other in figure C.1 and because \mathcal{D}_L^α is connected in $d \geq 3$, only one of the above intersections is non-empty. We conclude that such \mathcal{D}_L^α only belongs to one of the three subclasses E_{st}, E_{su}, E_{tu} . This conclusion remains valid also in 2d, because 2d configurations can be embedded into higher d.

2. $(x'_{13})^2, (x'_{12})^2, (x'_{23})^2 > 0$ for all $C_L \in \mathcal{D}_L^\alpha$. All possible conformal frame configurations are given by the grey region in the second and third pictures of figure C.1. In this case we have

$$\mathcal{D}_L^\alpha = (\mathcal{D}_L^\alpha \cap E_{st}) \sqcup (\mathcal{D}_L^\alpha \cap E_{su}) \sqcup (\mathcal{D}_L^\alpha \cap E_{tu}) \sqcup (\mathcal{D}_L^\alpha \cap E_{stu}), \tag{189}$$

which means that the configurations in \mathcal{D}_L^α may appear in all subclasses.

To see which of these possibilities is realized, it is enough to know the sign of $(x'_{13})^2$. To finish the proof of lemma C.1, it remains to check that $(x'_{13})^2 < 0$ for all type 1, 6, 11 causal orderings (so that possibility 1 is realized for C'_L). Since all causal orderings of a fixed causal type can be realized by permuting the indices of the template causal ordering and such S_4 -action permutes subclasses E_{st}, E_{su}, E_{tu} among themselves (see section C.0.1), it suffices to check that $(x'_{13})^2 < 0$ for the template causal orderings of causal type 1, 6, 11. Moreover, since we are only interested in the sign of $(x'_{13})^2$, we can use the following formula:

$$\text{Sign}((x'_{13})^2) = \text{Sign}(x_{13}^2 x_{14}^2 x_{34}^2). \tag{190}$$

(190) follows from (185), (186) and the fact that step 3,4 (of constructing the conformal frame) preserve the sign of $(x_{ij}^{(k)})^2$. Now let us do the check.

Type 1. The template causal ordering is given by

$$1 \rightarrow 2 \rightarrow 3 \rightarrow 4, \tag{191}$$

which gives $x_{13}^2, x_{14}^2, x_{34}^2 < 0$, hence $(x'_{13})^2 < 0$.

Type 6. The template causal ordering is given by

$$1 \rightarrow \begin{matrix} 2 & \rightarrow & 3 \\ & 4 & \end{matrix}, \tag{192}$$

which gives $x_{13}^2 < 0$ and $x_{14}^2, x_{34}^2 > 0$, hence $(x'_{13})^2 < 0$.

Type 11. The template causal ordering is given by

$$\begin{aligned} 1 &\longrightarrow 2 \\ 3 &\longrightarrow 4 \end{aligned} \tag{193}$$

which gives $x_{13}^2, x_{14}^2 > 0$ and $x_{34}^2 < 0$, hence $(x'_{13})^2 < 0$.

So we finished the proof of lemma C.1. As a consistency check one can also compute the sign of $(x'_{13})^2$ for type 5,10,12 causal orderings and find that $(x'_{13})^2 > 0$ for these cases.

For type 1, 6, 11 causal orderings, to determine the subclasses, it remains to determine the subclass of one particular configuration of the template causal ordering in each type, then determine the subclasses of other causal orderings by looking up table 3.

We would like to remark that Lorentzian conformal frame is just a way to figure out the range of z, \bar{z} . There is no claim that correlation functions at C_L, C'_L agree. As mentioned in section 6.3.3, the global conformal invariance does not hold in a general Lorentzian CFT.

C.0.3 Symmetry of the graph

Usually, we go from one causal ordering to another by permuting the indices. For example, given the causal ordering $1 \rightarrow 2 \rightarrow 3 \rightarrow 4$, by permuting 1, 4 we get another causal ordering $4 \rightarrow 2 \rightarrow 3 \rightarrow 1$.

However, a causal ordering may have a non-trivial little group.⁴¹ For example, consider the following causal ordering

$$a \longrightarrow b \begin{cases} \nearrow c \\ \searrow d \end{cases} . \tag{194}$$

The causal ordering (194) does not change if we interchange c and d , so it has a non-trivial little group \mathbb{Z}_2 .

The little group is unique up to an isomorphism for all causal orderings in the same causal type. Let G be the little group of one causal type and let $|G|$ be the order of G . Then the total number of causal orderings in this type is given by $24/|G|$. So in the table of each causal type, we will only list $24/|G|$ sequences $(i_1 i_2 i_3 i_4)$. Below the tables, we will point out the sequences which give the same causal ordering.

C.1 Type 1

The type 1 causal ordering is given by

$$a \rightarrow b \rightarrow c \rightarrow d . \tag{195}$$

We let (195) be the template causal ordering, then the causal ordering $i_1 \rightarrow i_2 \rightarrow i_3 \rightarrow i_4$ is labelled by the sequence $(i_1 i_2 i_3 i_4)$. Any permutation of the indices in (195) will change the causal ordering, so the little group of the type 1 causal orderings is trivial. We have to list 24 causal orderings in the table.

Under time reversal θ_L , $a \rightarrow b \rightarrow c \rightarrow d$ is mapped to $d \rightarrow c \rightarrow b \rightarrow a$, which is equivalent to the permutation $\theta_L : a \leftrightarrow d, b \leftrightarrow c$. This action is causal-type specific. In addition, we have θ_E action which is always given by $\theta_E : 1 \leftrightarrow 4, 2 \leftrightarrow 3$ (see eq. (98)). Using $\mathbb{Z}_2 \times \mathbb{Z}_2$ generated by these permutations, we divide 24 type 1 causal orderings into 8 orbits:

⁴¹By little group of a causal ordering, we mean the permutations of the indices which do not change this causal ordering.

1. (1234), (4321).
2. (1243), (4312), (3421), (2134).
3. (1324), (4231).
4. (1423), (3241), (4132), (2314).
5. (1342), (2431), (4213), (3124).
6. (1432), (2341), (4123), (3214).
7. (2143), (3412).
8. (2413), (3142).

As discussed in section 5.4, all the causal orderings in each orbit have the same convergent OPE channels.

Let us consider (1234), or equivalently the causal ordering $1 \rightarrow 2 \rightarrow 3 \rightarrow 4$. We first pick a particular configuration and compute z, \bar{z} . Here we choose

$$x_1 = 0, x_2 = (i, 0, \dots, 0), x_3 = (2i, 0, \dots, 0), x_4 = (3i, 0, \dots, 0), \tag{196}$$

and get $z = \bar{z} = \frac{1}{4}$, which is in the range corresponding to subclass E_{st} . By lemma C.1, the whole (1234) is in subclass E_{st} .

All other $(i_1 i_2 i_3 i_4)$ causal orderings can be obtained by applying permutation $\sigma = [i_1 i_2 i_3 i_4]$ to the template ordering (1234). Using table 3, we can easily determine the subclasses of all other $(i_1 i_2 i_3 i_4)$ sequences (look at the column having E_{st} on top). Then by looking up table 1, we get some OPE convergence properties of type 1 causal orderings, which are summarized in table 4. It remains to complete the rest of table 4. For this we choose a representative

Table 4: The classes/subclasses of type 1 causal orderings

causal ordering	class/subclass	s-channel	t-channel	u-channel
(1234), (4321)	E_{st}	✓		✗
(1243), (3421), (4312), (2134)	E_{su}	✓	✗	
(1324), (4231)	E_{tu}	✗		
(1423), (3241), (4132), (2314)	E_{tu}	✗		
(1342), (2431), (4213), (3124)	E_{su}	✓	✗	
(1432), (2341), (4123), (3214)	E_{st}	✓		✗
(2143), (3412)	E_{st}	✓		✗
(2413), (3142)	E_{tu}	✗		

configuration for each orbit of causal orderings and choose a path to compute the curves of z, \bar{z} , then decide the convergence properties of t- and u-channel expansions. In practice this is done numerically, by plotting the curves of z, \bar{z} and staring at the plots to determine N_t, N_u (as in examples in section 5.6). The final results of OPE convergence properties in the three channels are shown in table 5, where we use red to indicate the new marks.

Table 5: OPE convergence properties of type 1 causal orderings

causal ordering	class/subclass	s-channel	t-channel	u-channel
(1234), (4321)	E_{st}	✓	✓	✗
(2143), (3412)	E_{st}	✓	✗	✗
(1432), (2341), (4123), (3214)	E_{st}	✓	✓	✗
(1324), (4231)	E_{tu}	✗	✓	✗
(2413), (3142)	E_{tu}	✗	✗	✗
(1423), (3241), (4132), (2314)	E_{tu}	✗	✓	✗
(1342), (2431), (4213), (3124)	E_{su}	✓	✗	✗
(1243), (3421), (4312), (2134)	E_{su}	✓	✗	✗

C.2 Type 2

The type 2 causal ordering is given by

$$a \rightarrow b \begin{cases} \nearrow c \\ \searrow d \end{cases}, \quad \begin{cases} c \\ d \end{cases} \rightarrow b \rightarrow a. \quad (197)$$

We choose a particular configuration for (1234):

$$x_1 = 0, x_2 = (i, 0, \dots, 0), x_3 = (2i, 0.5, 0, \dots, 0), x_4 = (2i, -0.5, 0, \dots, 0), \quad (198)$$

and get $z = -\frac{8}{5}$, $\bar{z} = \frac{4}{9}$, which is in the range corresponding to class S. So we conclude that (1234) is in class S. The remaining steps are the same as appendix C.1. The results of OPE convergence properties in the three channels are shown in table 6. There are only 12 causal orderings because $(i_1 i_2 i_3 i_4)$ and $(i_1 i_2 i_4 i_3)$ are the same causal ordering (the little group is \mathbb{Z}_2).

Table 6: OPE convergence properties of type 2 causal orderings

causal ordering	class/subclass	s-channel	t-channel	u-channel
(1234), (4321)	S	✓	✗	✗
(1324), (4231)	U	✗	✗	✗
(1423), (4132)	T	✗	✓	✗
(2134), (3421)	S	✓	✗	✗
(3124), (2431)	U	✗	✗	✗
(2314), (3241)	T	✗	✓	✗

C.3 Type 3

The type 3 causal ordering is given by

$$a \begin{cases} \rightarrow b \\ \searrow d \end{cases} \rightarrow c, \quad c \rightarrow b \begin{cases} \rightarrow a \\ \nearrow d \end{cases}. \quad (199)$$

We choose a particular configuration for (1234):

$$x_1 = 0, x_2 = (i, 0, \dots, 0), x_3 = (2i, 0, \dots, 0), x_4 = (1.5i, 1, 0, \dots, 0), \quad (200)$$

and get $z = \frac{1}{6}$, $\bar{z} = \frac{3}{2}$, which is in the range corresponding to class T. So we conclude that (1234) is in class T. The results of OPE convergence properties in the three channels are shown in table 7.

Table 7: OPE convergence properties of type 3 causal orderings

causal ordering	class/subclass	s-channel	t-channel	u-channel
(1234), (4321)	T	✗	✓	✗
(1243), (4312)	U	✗	✗	✓
(1324), (4231)	T	✗	✓	✗
(1342), (4213)	S	✓	✗	✗
(1423), (4132)	U	✗	✗	✓
(1432), (4123)	S	✓	✗	✗
(2134), (3421)	U	✗	✗	✗
(2143), (3412)	T	✗	✗	✗
(2314), (3241)	U	✗	✗	✗
(2341), (3214)	S	✓	✗	✗
(2413), (3142)	T	✗	✗	✗
(2431), (3124)	S	✓	✗	✗

C.4 Type 4

The type 4 causal ordering is given by

$$\begin{array}{c}
 & & b & & \\
 & \nearrow & & \searrow & \\
 a & & & & d \\
 & \searrow & & \nearrow & \\
 & & c & &
 \end{array} . \quad (201)$$

We choose a particular configuration for (1234):

$$x_1 = 0, x_2 = (i, 0.5, 0, \dots, 0), x_3 = (i, -0.5, 0, \dots, 0), x_4 = (2i, 0, \dots, 0), \quad (202)$$

and get $z = \frac{1}{9}$, $\bar{z} = 9$, which is in the range corresponding to class T. So we conclude that (1234) is in class T. The results of OPE convergence properties in the three channels are shown in table 8. Here we use the fact that $(i_1 i_2 i_3 i_4)$ and $(i_1 i_3 i_2 i_4)$ are the same causal ordering (the little group is \mathbb{Z}_2).

C.5 Type 5

The type 5 causal ordering is given by

$$\begin{array}{c}
 & & b & & \\
 & \nearrow & & \searrow & \\
 a & & & & \\
 & \searrow & & \nearrow & \\
 & & c & & \\
 & & & & d
 \end{array} , \quad
 \begin{array}{c}
 b & & \\
 \nearrow & & \searrow \\
 c & & a \\
 \nearrow & & \searrow \\
 d & &
 \end{array} . \quad (203)$$

Table 8: OPE convergence properties of type 4 causal orderings

causal ordering	class/subclass	s-channel	t-channel	u-channel
(1234), (4321)	T	✗	✓	✗
(1243), (4312), (2134), (3421)	U	✗	✗	✗
(1342), (4213), (2341), (3214)	S	✓	✗	✗
(2143), (3412)	T	✗	✗	✗

We choose a particular configuration for (1234):

$$x_1 = 0, x_2 = (i, 0.5, 0, \dots, 0), x_3 = (i, 0, \dots, 0), x_4 = (i, -0.5, \dots, 0), \quad (204)$$

and get $z = \frac{1}{4}$, $\bar{z} = \frac{3}{4}$, which is in the range corresponding to subclass E_{st} . So (1234) is in class E. We would like to find a particular configuration in each subclass of class E. The little group of this causal type is S_3 , which corresponds to permutations among b, c, d in (203). By looking up table 3, we see that permuting x_2, x_3 in (204) gives E_{tu} and permuting x_3, x_4 gives E_{su} . To realize E_{stu} we choose the following configuration in (1234):

$$x_1 = 0, x_2 = (i, 0.5, 0, \dots, 0), x_3 = (i, -0.5, 0, \dots, 0), x_4 = (i, 0, 0.5, 0, \dots, 0), \quad (205)$$

and get $z = i$, $\bar{z} = -i$, which is indeed in the range corresponding to subclass E_{stu} . So we conclude that the configurations of (1234) do appear in all subclasses of class E in $d \geq 3$, while they only appear in subclasses E_{st}, E_{su}, E_{tu} in 2d.⁴²

The results of OPE convergence properties in the three channels are shown in table 9. Here we use the fact that for $(i_1 i_2 i_3 i_4)$, any permutation of 2, 3, 4 does not change the causal ordering (the little group is S_3).

Table 9: OPE convergence properties of type 5 causal orderings

causal ordering	class/subclass	s-channel	t-channel	u-channel
(1234), (4321)	E_{st}	✓	✓	✗
	E_{su}	✓	✗	✓
	E_{tu}	✗	✓	✓
	E_{stu}	✓	✓	✓
(2134), (3124)	E_{st}	✓	✗	✗
	E_{su}	✓	✗	✗
	E_{tu}	✗	✗	✗
	E_{stu}	✓	✗	✗

C.6 Type 6

The type 6 causal ordering is given by

$$a \longrightarrow b \longrightarrow c \\ \qquad \qquad \qquad d \qquad \qquad \qquad . \quad (206)$$

⁴²We used two dimensions in (204) and three dimensions in (205). On the other hand, as mentioned at the end of section 5.3.2, subclass E_{stu} does not exist in 2d because z, \bar{z} can only be real.

We choose a particular configuration for (1234):

$$x_1 = 0, x_2 = (i, 0, \dots, 0), x_3 = (2i, 0, \dots, 0), x_4 = (i, 2, \dots, 0), \tag{207}$$

and get $z = \frac{1}{4}, \bar{z} = \frac{3}{4}$, which is in the range corresponding to subclass E_{st} . By lemma C.1, the whole (1234) is in subclass E_{st} . The results of OPE convergence properties in the three channels are shown in table 10.

Table 10: OPE convergence properties of type 6 causal orderings

causal ordering	class/subclass	s-channel	t-channel	u-channel
(1234), (4321), (3214), (2341)	E_{st}	✓	✓	✗
(1243), (4312), (4213), (1342)	E_{su}	✓	✗	✓
(1324), (4231), (2314), (3241)	E_{tu}	✗	✓	✗
(1423), (4132), (2413), (3142)	E_{tu}	✗	✗	✓
(1432), (4123), (3412), (2143)	E_{st}	✓	✗	✗
(2134), (3421), (3124), (2431)	E_{su}	✓	✗	✗

C.7 Type 7

The type 7 causal ordering is given by

$$\begin{array}{ccc}
 & b & b \\
 a & \nearrow & \searrow \\
 & c & a \\
 & d & d
 \end{array}
 , \quad
 \begin{array}{ccc}
 & b & \\
 & \searrow & \\
 c & \nearrow & a \\
 & d &
 \end{array}
 . \tag{208}$$

We choose a particular configuration for (1234):

$$x_1 = 0, x_2 = (i, 0.5, 0, \dots, 0), x_3 = (i, -0.5, 0, \dots, 0), x_4 = (0, 2, 0, \dots, 0), \tag{209}$$

and get $z = \frac{7}{15}, \bar{z} = 9$, which is in the range corresponding to class T. So we conclude that (1234) is in class T. The results of OPE convergence properties in the three channels are shown in table 11. Here we use the fact that $(i_1 i_2 i_3 i_4)$ and $(i_1 i_3 i_2 i_4)$ are the same causal ordering (the little group is \mathbb{Z}_2).

Table 11: OPE convergence properties of type 7 causal orderings

causal ordering	class/subclass	s-channel	t-channel	u-channel
(1234), (4321)	T	✗	✓	✗
(1243), (4312)	U	✗	✗	✓
(1342), (4213)	S	✓	✗	✗
(2134), (3421)	U	✗	✗	✗
(2143), (3412)	T	✗	✗	✗
(2341), (3124)	S	✓	✗	✗

C.8 Type 8

The type 8 causal ordering is given by



We choose a particular configuration for (1234):

$$x_1 = 0, \quad x_2 = (i, -0.5, 0, \dots, 0), \quad x_3 = (0, 1, 0, \dots, 0), \quad x_4 = (i, 0.5, 0, \dots, 0), \quad (211)$$

and get $z = \frac{1}{4}$, $\bar{z} = \frac{9}{4}$, which is in the range corresponding to class T. So we conclude that (1234) is in class T. The results of OPE convergence properties in the three channels are shown in table 12.

Table 12: OPE convergence properties of type 8 causal orderings

causal ordering	class/subclass	s-channel	t-channel	u-channel
(1234), (4321)	T	✗	✗	✗
(1243), (4312), (3421), (2134)	U	✗	✗	✓
(1342), (4213), (2431), (3124)	S	✓	✗	✗
(2143), (3412)	T	✗	✗	✗
(1324), (4231)	T	✗	✗	✗
(1432), (4123), (2341), (3214)	S	✓	✗	✗
(1423), (4132), (3241), (2314)	U	✗	✗	✗
(2413), (3142)	T	✗	✗	✗

C.9 Type 9

The type 9 causal ordering is given by



We choose a particular configuration for (1234):

$$x_1 = 0, \quad x_2 = (i, 0, \dots, 0), \quad x_3 = (0, 2, 0, \dots, 0), \quad x_4 = (0, 3, 0, \dots, 0), \quad (213)$$

and get $z = -\frac{1}{8}$, $\bar{z} = \frac{1}{4}$, which is in the range corresponding to class S. So we conclude that (1234) is in class S. The results of OPE convergence properties in the three channels are shown in table 13. Here we use the fact that $(i_1 i_2 i_3 i_4)$ and $(i_1 i_2 i_4 i_3)$ are the same causal ordering (the little group is \mathbb{Z}_2).

C.10 Type 10

The type 10 causal ordering is given by



Table 13: OPE convergence properties of type 9 causal orderings

causal ordering	class/subclass	s-channel	t-channel	u-channel
(1234), (4312), (2134), (3412)	S	✓	✗	✗
(1324), (4213), (3124), (2413)	U	✗	✗	✓
(1423), (4123)	T	✗	✓	✗
(2314), (3214)	T	✗	✓	✗

We choose a particular configuration for (1234):

$$x_1 = 0, x_2 = (0, 1, 0, \dots, 0), x_3 = (2i, 0, \dots, 0), x_4 = (2i, 1, \dots, 0), \tag{215}$$

and get $z = \bar{z} = \frac{1}{4}$, which is in the range corresponding to subclass E_{st} . So (1234) is in class E. We would like to find a particular configuration in each subclass of class E. The little group of this causal type is $\mathbb{Z}_2 \times \mathbb{Z}_2$, which is generated by $a \leftrightarrow b$ and $c \leftrightarrow d$ in (214). By looking up table 3, we see that by acting with the little group on configuration (215), we can get E_{su} , but we cannot get E_{tu} . The underlying fact is that the 2d configurations of (1234) do not appear in E_{tu} (it is obvious that 2d configurations do not appear in E_{stu}). Let us show this fact. In 2d Minkowski space we can use the light-cone coordinates:

$$z_k = t_k + \mathbf{x}_k, \quad \bar{z}_k = t_k - \mathbf{x}_k, \quad (x_k = (it_k, \mathbf{x}_k)). \tag{216}$$

The causal ordering (214) implies

$$\begin{aligned} z_3, z_4 > z_1, z_2, \quad \bar{z}_3, \bar{z}_4 > \bar{z}_1, \bar{z}_2, \\ (z_1 - z_2)(\bar{z}_1 - \bar{z}_2) < 0, \quad (z_3 - z_4)(\bar{z}_3 - \bar{z}_4) < 0. \end{aligned} \tag{217}$$

Since the little group $\mathbb{Z}_2 \times \mathbb{Z}_2$ of (1234) preserves E_{tu} (see table 3), by the $\mathbb{Z}_2 \times \mathbb{Z}_2$ -action, it suffices to show that E_{tu} configurations do not exist when

$$\begin{aligned} z_3, z_4 > z_1, z_2, \quad \bar{z}_3, \bar{z}_4 > \bar{z}_1, \bar{z}_2, \\ z_1 - z_2 < 0, \quad \bar{z}_1 - \bar{z}_2 > 0, \\ z_3 - z_4 < 0, \quad \bar{z}_3 - \bar{z}_4 > 0. \end{aligned} \tag{218}$$

In this case the computation is straightforward:

$$\begin{aligned} z &= \frac{(z_2 - z_1)(z_4 - z_3)}{(z_3 - z_1)(z_4 - z_2)} < \frac{(z_3 - z_1)(z_4 - z_2)}{(z_3 - z_1)(z_4 - z_2)} = 1, \\ \bar{z} &= \frac{(\bar{z}_1 - \bar{z}_2)(\bar{z}_3 - \bar{z}_4)}{(\bar{z}_3 - \bar{z}_1)(\bar{z}_4 - \bar{z}_2)} < \frac{(\bar{z}_4 - \bar{z}_2)(\bar{z}_3 - \bar{z}_1)}{(\bar{z}_3 - \bar{z}_1)(\bar{z}_4 - \bar{z}_2)} = 1. \end{aligned} \tag{219}$$

So we conclude that the 2d configurations in (1234) have $z, \bar{z} < 1$, i.e. (1234) does not intersect with subclass E_{tu} in 2d. To find a E_{tu} configuration in (1234) we need to construct it in $d \geq 3$. We choose the 3d configuration (114) and get $z \approx 1.1$, $\bar{z} \approx 6.3$, which is in the range corresponding to subclass E_{tu} .

To realize E_{stu} we choose the following configuration in (1234):

$$x_1 = 0, x_2 = (0, 0.5, 0, \dots, 0), x_3 = (2i, 0, 0.5, 0, \dots, 0), x_4 = (i, 0.5, 0, \dots, 0), \tag{220}$$

and get $z \approx 0.33 + 0.24i$, $\bar{z} = 0.33 - 0.24i$, which is in the range corresponding to subclass E_{stu} . So we conclude that the configurations of (1234) do appear in all subclasses of class E in $d \geq 3$, while they only appear in subclasses E_{st}, E_{su} in 2d.

The results of OPE convergence properties in the three channels are shown in table 14: Here we use the fact $(i_1 i_2 i_3 i_4), (i_2 i_1 i_3 i_4), (i_1 i_2 i_4 i_3)$ and $(i_2 i_1 i_4 i_3)$ are the same causal ordering (the little group is $\mathbb{Z}_2 \times \mathbb{Z}_2$).

Table 14: OPE convergence properties of type 10 causal orderings

causal ordering	class/subclass	s-channel	t-channel	u-channel
(1234), (3412)	E_{st}	✓	✗	✗
	E_{su}	✓	✗	✗
	E_{tu}	✗	✗	✗
	E_{stu}	✓	✗	✗
(1324), (2413)	E_{st}	✓	✗	✗
	E_{su}	✓	✗	✗
	E_{tu}	✗	✗	✗
	E_{stu}	✓	✗	✗
(1423), (2314)	E_{st}	✓	✓	✗
	E_{su}	✓	✗	✓
	E_{tu}	✗	✓	✓
	E_{stu}	✓	✓	✓

C.11 Type 11

The type 11 causal ordering is given by

$$\begin{aligned} a &\rightarrow b \\ c &\rightarrow d \end{aligned} \quad (221)$$

We choose a particular configuration for (1234):

$$x_1 = 0, \quad x_2 = (i, 0, \dots, 0), \quad x_3 = (0, 2, \dots, 0), \quad x_4 = (i, 2, \dots, 0), \quad (222)$$

and get $z = \bar{z} = \frac{1}{4}$, which is in the range corresponding to subclass E_{st} . By lemma C.1, the whole (1234) is in subclass E_{st} . The results of OPE convergence properties in the three channels are shown in table 15. Here we use the fact that $(i_1 i_2 i_3 i_4)$ and $(i_3 i_4 i_1 i_2)$ are the same causal

Table 15: OPE convergence properties of type 11 causal orderings

causal ordering	class/subclass	s-channel	t-channel	u-channel
(1234), (2143)	E_{st}	✓	✗	✗
(1243), (2134)	E_{su}	✓	✗	✓
(1324), (3142)	E_{tu}	✗	✗	✓
(1342), (3124)	E_{su}	✓	✗	✓
(1423), (3241)	E_{tu}	✗	✓	✗
(1432), (2341)	E_{st}	✓	✓	✗

ordering (the little group is \mathbb{Z}_2).

C.12 Type 12

The type 12 causal ordering is given by

$$a \quad b \quad c \quad d. \quad (223)$$

One can show that this causal type belongs to class E. In fact this is the “Euclidean” case (that’s why this class is called class E), and there is no need to check numerically for this type. Suppose we have a totally space-like separated configuration (x_1, x_2, x_3, x_4) , where $x_k = (it_k, \mathbf{x}_k)$. We can reach this configuration via the path

$$x_k(s) = \begin{cases} ((1 - 2s)\epsilon_k, 2s\mathbf{x}_k) & s \in [0, 1/2], \\ ((2s - 1)it_k, \mathbf{x}_k) & s \in [1/2, 1]. \end{cases} \quad (224)$$

Along the path all the x_i, x_j pairs are space-like separated. As a result, the totally space-like separated configurations always have $N_t = N_u = 0$ (as long as N_t, N_u are well-defined). On the other hand, there is no doubt that all subclasses of class E can be realized in $d \geq 3$.⁴³ We summarize the OPE convergence properties of this type in table 16. Here we use the fact that there is only 1 causal ordering in this type (the little group is S_4).

Table 16: OPE convergence properties of type 12 causal orderings

causal ordering	class/subclass	s-channel	t-channel	u-channel
(1234)	E_{st}	✓	✓	✗
	E_{su}	✓	✗	✓
	E_{tu}	✗	✓	✓
	E_{stu}	✓	✓	✓

References

- [1] R. Jost, *The general theory of quantized fields*, Am. Math. Soc. **4**, 79 (1965), doi:[10.1002/zamm.19660460139](https://doi.org/10.1002/zamm.19660460139).
- [2] K. Osterwalder and R. Schrader, *Axioms for Euclidean Green’s functions*, Commun. Math. Phys. **31**, 83 (1973), doi:[10.1007/BF01645738](https://doi.org/10.1007/BF01645738).
- [3] V. Glaser, *On the equivalence of the Euclidean and Wightman formulation of field theory*, Commun. Math. Phys. **37**, 257 (1974), doi:[10.1007/BF01645941](https://doi.org/10.1007/BF01645941).
- [4] K. Osterwalder and R. Schrader, *Axioms for Euclidean Green’s functions II*, Commun. Math. Phys. **42**, 281 (1975), doi:[10.1007/BF01608978](https://doi.org/10.1007/BF01608978).
- [5] R. F. Streater and A. S. Wightman, *PCT, spin and statistics, and all that*, Addison-Wesley, Redwood City, ISBN 9780201094107 (1989), doi:[10.1515/9781400884230](https://doi.org/10.1515/9781400884230).
- [6] R. Jost, *A remark on the c.t.p. theorem*, Helv. Phys. Acta **30**, 409 (1957), doi:[10.5169/seals-112824](https://doi.org/10.5169/seals-112824).
- [7] D. Ruelle, *Analyticity of wightman functions at completely space-like points*, Helv. Phys. Acta **32**, 135 (1959), doi:[10.5169/seals-113000](https://doi.org/10.5169/seals-113000).
- [8] K. Dietz, *Light-cone singularities in quantum field theory*, Nuov. Cim. A **18**, 1 (1973), doi:[10.1007/BF02820833](https://doi.org/10.1007/BF02820833).

⁴³One can realize one of the three subclasses E_{st}, E_{su}, E_{tu} in 2d, and then realize the other two subclasses by S_4 -action. For subclass E_{stu} , one can put four points in the hyperplane with $t = 0$.

- [9] D. Pappadopulo, S. Rychkov, J. Espin and R. Rattazzi, *Operator product expansion convergence in conformal field theory*, Phys. Rev. D **86**, 105043 (2012), doi:[10.1103/PhysRevD.86.105043](https://doi.org/10.1103/PhysRevD.86.105043).
- [10] A. A. Belavin, A. M. Polyakov and A. B. Zamolodchikov, *Infinite conformal symmetry in two-dimensional quantum field theory*, Nucl. Phys. B **241**, 333 (1984), doi:[10.1016/0550-3213\(84\)90052-X](https://doi.org/10.1016/0550-3213(84)90052-X).
- [11] A. B. Zamolodchikov, *Conformal symmetry in two-dimensional space: Recursion representation of conformal block*, Theor. Math. Phys. **73**, 1088 (1987), doi:[10.1007/BF01022967](https://doi.org/10.1007/BF01022967).
- [12] J. Maldacena, D. Simmons-Duffin and A. Zhiboedov, *Looking for a bulk point*, J. High Energy Phys. **01**, 013 (2017), doi:[10.1007/JHEP01\(2017\)013](https://doi.org/10.1007/JHEP01(2017)013).
- [13] M. Hogervorst and S. Rychkov, *Radial coordinates for conformal blocks*, Phys. Rev. D **87**, 106004 (2013), doi:[10.1103/PhysRevD.87.106004](https://doi.org/10.1103/PhysRevD.87.106004).
- [14] P. Di Francesco, P. Mathieu and D. Sénéchal, *Conformal field theory*, Springer, New York, US, ISBN 9781461274759 (1997), doi:[10.1007/978-1-4612-2256-9](https://doi.org/10.1007/978-1-4612-2256-9).
- [15] D. Poland, S. Rychkov and A. Vichi, *The conformal bootstrap: Theory, numerical techniques, and applications*, Rev. Mod. Phys. **91**, 015002 (2019), doi:[10.1103/RevModPhys.91.015002](https://doi.org/10.1103/RevModPhys.91.015002).
- [16] S. El-Showk, M. F. Paulos, D. Poland, S. Rychkov, D. Simmons-Duffin and A. Vichi, *Solving the 3D Ising model with the conformal bootstrap*, Phys. Rev. D **86**, 025022 (2012), doi:[10.1103/PhysRevD.86.025022](https://doi.org/10.1103/PhysRevD.86.025022).
- [17] S. El-Showk, M. F. Paulos, D. Poland, S. Rychkov, D. Simmons-Duffin and A. Vichi, *Solving the 3D Ising model with the conformal bootstrap II. c -minimization and precise critical exponents*, J. Stat. Phys. **157**, 869 (2014), doi:[10.1007/s10955-014-1042-7](https://doi.org/10.1007/s10955-014-1042-7).
- [18] F. Kos, D. Poland and D. Simmons-Duffin, *Bootstrapping mixed correlators in the 3D Ising model*, J. High Energy Phys. **11**, 109 (2014), doi:[10.1007/JHEP11\(2014\)109](https://doi.org/10.1007/JHEP11(2014)109).
- [19] D. Simmons-Duffin, *A semidefinite program solver for the conformal bootstrap*, J. High Energy Phys. **06**, 174 (2015), doi:[10.1007/JHEP06\(2015\)174](https://doi.org/10.1007/JHEP06(2015)174).
- [20] F. Kos, D. Poland, D. Simmons-Duffin and A. Vichi, *Precision islands in the Ising and $O(N)$ models*, J. High Energy Phys. **08**, 036 (2016), doi:[10.1007/JHEP08\(2016\)036](https://doi.org/10.1007/JHEP08(2016)036).
- [21] F. Kos, D. Poland and D. Simmons-Duffin, *Bootstrapping the $O(N)$ vector models*, J. High Energy Phys. **06**, 091 (2014), doi:[10.1007/JHEP06\(2014\)091](https://doi.org/10.1007/JHEP06(2014)091).
- [22] F. Kos, D. Poland, D. Simmons-Duffin and A. Vichi, *Bootstrapping the $O(N)$ archipelago*, J. High Energy Phys. **11**, 106 (2015), doi:[10.1007/JHEP11\(2015\)106](https://doi.org/10.1007/JHEP11(2015)106).
- [23] S. M. Chester, W. Landry, J. Liu, D. Poland, D. Simmons-Duffin, N. Su and A. Vichi, *Carving out OPE space and precise $O(2)$ model critical exponents*, J. High Energy Phys. **06**, 142 (2020), doi:[10.1007/JHEP06\(2020\)142](https://doi.org/10.1007/JHEP06(2020)142).
- [24] D. Mazáč, *Analytic bounds and emergence of AdS_2 physics from the conformal bootstrap*, J. High Energy Phys. **04**, 146 (2017), doi:[10.1007/JHEP04\(2017\)146](https://doi.org/10.1007/JHEP04(2017)146).
- [25] D. Mazáč and M. F. Paulos, *The analytic functional bootstrap. Part I: 1D CFTs and 2D S -matrices*, J. High Energy Phys. **02**, 162 (2019), doi:[10.1007/JHEP02\(2019\)162](https://doi.org/10.1007/JHEP02(2019)162).

- [26] D. Mazáč and M. F. Paulos, *The analytic functional bootstrap. Part II. Natural bases for the crossing equation*, J. High Energy Phys. **02**, 163 (2019), doi:[10.1007/JHEP02\(2019\)163](https://doi.org/10.1007/JHEP02(2019)163).
- [27] M. F. Paulos, *Analytic functional bootstrap for CFTs in $d > 1$* , J. High Energy Phys. **04**, 093 (2020), doi:[10.1007/JHEP04\(2020\)093](https://doi.org/10.1007/JHEP04(2020)093).
- [28] Z. Komargodski and A. Zhiboedov, *Convexity and liberation at large spin*, J. High Energy Phys. **11**, 140 (2013), doi:[10.1007/JHEP11\(2013\)140](https://doi.org/10.1007/JHEP11(2013)140).
- [29] A. L. Fitzpatrick, J. Kaplan, D. Poland and D. Simmons-Duffin, *The analytic bootstrap and AdS superhorizon locality*, J. High Energy Phys. **12**, 004 (2013), doi:[10.1007/JHEP12\(2013\)004](https://doi.org/10.1007/JHEP12(2013)004).
- [30] T. Hartman, S. Jain and S. Kundu, *Causality constraints in conformal field theory*, J. High Energy Phys. **05**, 099 (2016), doi:[10.1007/JHEP05\(2016\)099](https://doi.org/10.1007/JHEP05(2016)099).
- [31] T. Hartman, S. Jain and S. Kundu, *A new spin on causality constraints*, J. High Energy Phys. **10**, 141 (2016), doi:[10.1007/JHEP10\(2016\)141](https://doi.org/10.1007/JHEP10(2016)141).
- [32] T. Hartman, S. Kundu and A. Tajdini, *Averaged null energy condition from causality*, J. High Energy Phys. **07**, 066 (2017), doi:[10.1007/JHEP07\(2017\)066](https://doi.org/10.1007/JHEP07(2017)066).
- [33] S. Caron-Huot, *Analyticity in spin in conformal theories*, J. High Energy Phys. **09**, 078 (2017), doi:[10.1007/JHEP09\(2017\)078](https://doi.org/10.1007/JHEP09(2017)078).
- [34] D. Simmons-Duffin, D. Stanford and E. Witten, *A spacetime derivation of the Lorentzian OPE inversion formula*, J. High Energy Phys. **07**, 085 (2018), doi:[10.1007/JHEP07\(2018\)085](https://doi.org/10.1007/JHEP07(2018)085).
- [35] G. Mack, *Convergence of operator product expansions on the vacuum in conformal invariant quantum field theory*, Commun. Math. Phys. **53**, 155 (1977), doi:[10.1007/BF01609130](https://doi.org/10.1007/BF01609130).
- [36] P. Kravchuk, J. Qiao and S. Rychkov, *Distributions in CFT. Part I. Cross-ratio space*, J. High Energy Phys. **05**, 137 (2020), doi:[10.1007/JHEP05\(2020\)137](https://doi.org/10.1007/JHEP05(2020)137).
- [37] P. Kravchuk, J. Qiao and S. Rychkov, *Distributions in CFT. Part II. Minkowski space*, J. High Energy Phys. **08**, 094 (2021), doi:[10.1007/JHEP08\(2021\)094](https://doi.org/10.1007/JHEP08(2021)094).
- [38] P. Kravchuk, J. Qiao and S. Rychkov, *Distributions in CFT III. Lorentzian cylinder*, in preparation.
- [39] S. Rychkov, *EPFL lectures on conformal field theory in $D \geq 3$ dimensions*, Springer International Publishing, Cham, ISBN 9783319436258 (2017), doi:[10.1007/978-3-319-43626-5](https://doi.org/10.1007/978-3-319-43626-5).
- [40] D. Simmons-Duffin, *The conformal bootstrap*, World Scientific, Singapore, ISBN 9789813149441 (2016), doi:[10.1142/9789813149441_0001](https://doi.org/10.1142/9789813149441_0001).
- [41] J. R. Munkres, *Topology; a first course*, Prentice-Hall, Hoboken, New Jersey, US, ISBN 9780139254956 (1974).
- [42] S. Ferrara, A. F. Grillo and R. Gatto, *Tensor representations of conformal algebra and conformally covariant operator product expansion*, Ann. Phys. **76**, 161 (1973), doi:[10.1016/0003-4916\(73\)90446-6](https://doi.org/10.1016/0003-4916(73)90446-6).
- [43] A. M. Polyakov, *Non-Hamiltonian approach to conformal quantum field theory*, Sov. J. Exp. Theor. Phys. **39**, 10 (1974).

- [44] T. H. Go, H. A. Kastrup and D. H. Mayer, *Properties of dilatations and conformal transformations in Minkowski space*, Rept. Math. Phys. **6**, 395 (1974), doi:[10.1016/S0034-4877\(74\)80006-6](https://doi.org/10.1016/S0034-4877(74)80006-6).
- [45] H. Lehmann, K. Symanzik and W. Zimmermann, *Zur formulierung quantisierter feldtheorien*, Nuovo Cim. **1**, 205 (1955), doi:[10.1007/BF02731765](https://doi.org/10.1007/BF02731765).
- [46] M. E. Peskin and D. V. Schroeder, *An introduction to quantum field theory*, Addison-Wesley, Reading, Pennsylvania, US, ISBN 9780201503975 (1995), doi:[10.1201/9780429503559](https://doi.org/10.1201/9780429503559).
- [47] L. V. Keldysh, *Diagram technique for nonequilibrium processes*, Zh. Eksp. Teor. Fiz. **47**, 1515 (1964).
- [48] A. Kitaev, *Hidden correlations in the Hawking radiation and thermal noise*, (2015), <http://online.itp.ucsb.edu/online/joint98/kitaev/>.
- [49] J. Maldacena, S. H. Shenker and D. Stanford, *A bound on chaos*, J. High Energy Phys. **08**, 106 (2016), doi:[10.1007/JHEP08\(2016\)106](https://doi.org/10.1007/JHEP08(2016)106).
- [50] I. L. Aleiner, L. Faoro and L. B. Ioffe, *Microscopic model of quantum butterfly effect: Out-of-time-order correlators and traveling combustion waves*, Ann. Phys. **375**, 378 (2016), doi:[10.1016/j.aop.2016.09.006](https://doi.org/10.1016/j.aop.2016.09.006).
- [51] D. Bagrets, A. Altland and A. Kamenev, *Power-law out of time order correlation functions in the SYK model*, Nucl. Phys. B **921**, 727 (2017), doi:[10.1016/j.nuclphysb.2017.06.012](https://doi.org/10.1016/j.nuclphysb.2017.06.012).
- [52] M. Gärttner, J. G. Bohnet, A. Safavi-Naini, M. L. Wall, J. J. Bollinger and A. Maria Rey, *Measuring out-of-time-order correlations and multiple quantum spectra in a trapped-ion quantum magnet*, Nat. Phys. **13**, 781 (2017), doi:[10.1038/nphys4119](https://doi.org/10.1038/nphys4119).
- [53] R. Fan, P. Zhang, H. Shen and H. Zhai, *Out-of-time-order correlation for many-body localization*, Sci. Bull. **62**, 707 (2017), doi:[10.1016/j.scib.2017.04.011](https://doi.org/10.1016/j.scib.2017.04.011).
- [54] F. Haehl, R. Loganayagam, P. Narayan and M. Rangamani, *Classification of out-of-time-order correlators*, SciPost Phys. **6**, 001 (2019), doi:[10.21468/SciPostPhys.6.1.001](https://doi.org/10.21468/SciPostPhys.6.1.001).
- [55] L. Cornalba, *Eikonal methods in AdS/CFT: Regge theory and multi-reggeon exchange*, [arXiv:0710.5480](https://arxiv.org/abs/0710.5480).
- [56] L. Cornalba, M. S. Costa and J. Penedones, *Eikonal methods in AdS/CFT: BFKL Pomeron at weak coupling*, J. High Energy Phys. **06**, 048 (2008), doi:[10.1088/1126-6708/2008/06/048](https://doi.org/10.1088/1126-6708/2008/06/048).
- [57] M. S. Costa, V. Goncalves and J. Penedones, *Conformal Regge theory*, J. High Energy Phys. **12**, 091 (2012), doi:[10.1007/JHEP12\(2012\)091](https://doi.org/10.1007/JHEP12(2012)091).
- [58] M. Lüscher and G. Mack, *Global conformal invariance in quantum field theory*, Commun. Math. Phys. **41**, 203 (1975), doi:[10.1007/BF01608988](https://doi.org/10.1007/BF01608988).
- [59] O. Aharony, S. S. Gubser, J. Maldacena, H. Ooguri and Y. Oz, *Large N field theories, string theory and gravity*, Phys. Rep. **323**, 183 (2000), doi:[10.1016/S0370-1573\(99\)00083-6](https://doi.org/10.1016/S0370-1573(99)00083-6).
- [60] I. Segal, *Causally oriented manifolds and groups*, Bull. Amer. Math. Soc. **77**, 958 (1971), doi:[10.1090/S0002-9904-1971-12815-X](https://doi.org/10.1090/S0002-9904-1971-12815-X).

- [61] I. T. Todorov, *Conformal invariant quantum field theory with anomalous dimensions*, Tech. Rep. CERN-TH-1697, CERN, Geneva, (1973) <https://cds.cern.ch/record/967138/files/CM-P00060449.pdf>.
- [62] N. N. Bogolyubov, A. A. Logunov, A. I. Oksak and I. T. Todorov, *General principles of quantum field theory (Mathematical physics and applied mathematics, 10)*, Springer, Berlin, Germany, ISBN 9780792305408 (1989).
- [63] G. E. Šilov and I. M. Gelfand, *Generalized functions. 1. Properties and operations*, Academic Press, Cambridge, Massachusetts, US, ISBN 9780122795015 (1964), doi:[10.1090/chel/377](https://doi.org/10.1090/chel/377)
- [64] D. Hall and A. S. Wightman, *A theorem on invariant analytic functions with applications to relativistic quantum field theory*, Det K. Dan. Vidensk. Selsk. (1957).
- [65] V. S. Vladimirov, *Methods of the theory of functions of several complex variables*, MIT Press, Cambridge, Massachusetts, US, ISBN 9780262220095 (1966).
- [66] G. Kařllén, *The analyticity domain of the four point function*, Nucl. Phys. **25**, 568 (1961), doi:[10.1016/0029-5582\(61\)90184-5](https://doi.org/10.1016/0029-5582(61)90184-5).
- [67] P. Kravchuk and D. Simmons-Duffin, *Counting conformal correlators*, J. High Energy Phys. **02**, 096 (2018), doi:[10.1007/JHEP02\(2018\)096](https://doi.org/10.1007/JHEP02(2018)096).
- [68] D. Karateev, P. Kravchuk, M. Serone and A. Vichi, *Fermion conformal bootstrap in 4d*, J. High Energy Phys. **06**, 088 (2019), doi:[10.1007/JHEP06\(2019\)088](https://doi.org/10.1007/JHEP06(2019)088).
- [69] M. Gillioz, X. Lu, M. A. Luty and G. Mikaberidze, *Convergent momentum-space OPE and bootstrap equations in conformal field theory*, J. High Energy Phys. **03**, 102 (2020), doi:[10.1007/JHEP03\(2020\)102](https://doi.org/10.1007/JHEP03(2020)102).
- [70] A. Kaviraj and M. F. Paulos, *The functional bootstrap for boundary CFT*, J. High Energy Phys. **04**, 135 (2020), doi:[10.1007/JHEP04\(2020\)135](https://doi.org/10.1007/JHEP04(2020)135).
- [71] D. Mazáč, L. Rastelli and X. Zhou, *An analytic approach to BCFTd*, J. High Energy Phys. **12**, 004 (2019), doi:[10.1007/JHEP12\(2019\)004](https://doi.org/10.1007/JHEP12(2019)004).
- [72] D. Mazáč, L. Rastelli and X. Zhou, *A basis of analytic functionals for CFTs in general dimension*, J. High Energy Phys. **08**, 140 (2021), doi:[10.1007/JHEP08\(2021\)140](https://doi.org/10.1007/JHEP08(2021)140).